The Use of Vestibular Models in Flight Simulator Motion Washout Systems: An Experimental Evaluation

by

Robert Bryan Sullivan

B.S., Aero. Engr., Texas A & M Univ.
(1983)

Submitted to the Department of Aeronautics
and Astronautics in partial fulfillment
of the requirements for
the Degree of

Master of Science in Aeronautics and Astronautics

at the
Massachusetts Institute of Technology
May, 1985

Signature of Author _____
Department of Aeronautics and Astronautics
May 10, 1985

Certified by _____
Professor Steven R. Bussolari
Thesis Supervisor

Accepted by _____
Professor Harold Y. Wachman, Chairman
Departmental Graduate Committee
Department of Aeronautics and Astronautics

The Use of Vestibular Models in Flight Simulator Motion Washout Systems: An Experimental Evaluation

by

Robert Bryan Sullivan

Submitted to the Department of Aeronautics and Astronautics on May 10, 1985 in partial fulfillment of the requirements for the Degree of Master of Science in Aeronautics and Astronautics

ABSTRACT

In an attempt to improve the fidelity of motion in flight simulators, a motion control system that accounts for the dynamics of the human vestibular (motion sensing) system has been implemented on the NASA Ames Vertical Motion Simulator (VMS). The motion control system, called the Optimal Washout System (OWS), minimizes the vector difference between the sensory outputs of the vestibular systems of a pilot in the modeled aircraft and of the pilot in the simulator. This is accomplished by minimizing the error in the outputs of mathematical models of the otolith organs (linear acceleration detectors) of the two pilots and the error in the outputs of mathematical models of the semicircular canal organs (angular acceleration sensors) of the two pilots. The OWS controls the motion of the simulator cab by minimizing a weighted quadratic cost function of otolith error, semicircular canal error, and simulator cab displacement.

A set of experiments was performed on the VMS to evaluate the performance of the OWS and to determine valid measures of simulator motion fidelity. During the experiments, four experimental test pilots compared the OWS system to the motion control system normally used on the VMS. Three versions of each washout system were tried. To compare the motion characteristics of each system, the pilots flew a generic thrust vectored hovering vehicle and performed the following tasks: (1) four trials of a formation flight tracking task with a sum-of-sines disturbance on the lead aircraft, (2) three dash quick stop maneuvers, and (3) several sinusoidal pitching maneuvers from a stationary hover at 1, 2, and 4 cycles per second. Tracking performance during formation flight was recorded. Cooper-Harper handling quality ratings (HQR) and simulator motion quality ratings were given by the pilot subjects.

Pilot comments and ratings indicate that the OWS is a reasonable control system for simulator motion; however, some refinement is necessary before operational use. The data from the test also indicates that performance in the tracking task is not necessarily a good measure of washout motion, due to corruption by learning effects and large

variations in performance among trials and pilots. Similarly, describing functions calculated from the stick inputs of the pilot during the tracking task are not necessarily good indicators of motion fidelity. The performance variability among trials and the lack of performance differences among washouts makes the describing functions difficult to interpret. Cooper-Harper handling quality ratings recorded for each washout were analyzed and appear to be reasonable indicators of simulator motion fidelity. The motion quality ratings also appear useful in determining the strengths and deficiencies of the motion washouts.

Thesis Supervisor: Dr. Steven Bussolari
Assistant Professor of Aeronautics and Astronautics

Acknowledgements

I would like to thank Steve Bussolari for his guidance and patience throughout this research. I will always be grateful for the knowledge I have gained through my relationship with him, both as a friend and an advisor.

A special thanks to John Stewart and Dick Bray of NASA Ames for their helpful wisdom and for allowing us to use the Ames simulation facilities. I also appreciate the assistance of Bill Chung as well as Lee and Tueng in helping us implement our software on the VMS. Another thanks goes to the NASA Ames test pilots for their patience and professionalism during the experiments. This research was supported by the NASA Ames Research Center Grant NAG 2-12, Visual Vestibular Interaction and Its Application to Flight Simulation.

Also, I will be eternally grateful to the following people: my mother and father for having me in the first place; my grandmother for the nice cookies, the cooks in the following restaurants: Baker House, Lobdell, Storey's, TT the Bear's, Latino, Legal Seafood, George & Nicks's, Kebabish (?), the DeliHaus, and many others far too numerous to mention; the farmers and fishermen across this fine nation of ours for growing and/or catching all this food, as well as those diligent people in the food processing industry; Mohammed Massoumnia for sharing my interest in the timely procurement of food; Bob Renshaw for his German chocolate; Sherry Modestino for procuring occasional food; Steve Bussolari for not complaining too much about my cooking during our stay in California; Crystal Williams for her unique philosophy on life and for letting me pull her arms out; Marilyn Williams for typing the * on the bottom of Table 4-2; Alan Natapoff for his advice on statistics and for the fine piano lessons; Mark Shelhamer for many things, none of which I can remember; Jim Shelhamer for reminding me that not all Shelhamers are extremely abnormal; Dan Merfeld for telling me about his experiences at the airport and telling me about his experiences at the airport and telling ...; Remy Malan for his hours of unfailing encouragement; Bob Kenyon for my many new names; Bob McCoy for showing me the true joy of Air Force life; all of these Bob's for convincing me not to use my first name; Anthony Arrott for convincing me not to get a Ph.D.; Amy Thompson for giving me new insight into female psychology; Fariba Zarinetchi for her faith in my endeavors and all the chickens; Jennifer Wiseman for being tall; Anne LaVin for listening to my stories with such avid interest; Kathy Misovec for doing my work for me; Linda Robeck for being left-eye dominant; the MVL volleyball team for showing me the importance of winning, and the MIT housing office for my interesting array of roommates.

Finally, I would like to thank Sherry Modestino for writing my acknowledgements and would like to add a sincere thanks to Sherry, Marilyn, Dan, Mohammed, and Mark for your continuing friendship.

Table of Contents

1. Introduction

1.0 Motivation for Research

The increased use of flight simulators for pilot training and certification is a result of the large cost associated with operating and maintaining flight vehicles and the need to practice maneuvers that are too dangerous to perform in the actual aircraft (i.e.-engine out on takeoff). However, to adequately train pilots in the simulator, it is necessary to provide them with a realistic cockpit environment including visual inputs and motion sensations. Both of these sensory input systems add a significant cost to the price of the simulator; however, with time, the cost of the visual systems is decreasing while the cost of motion systems remains approximately constant. Therefore, for given size contraints of the motion system, it is desirable to maximize the sensory inputs generated by the motion system. This thesis deals with this optimization of the motion system.

Because flight simulators have limited motion excursions, the simulator cannot exactly replicate the motions of an aircraft; consequently, the accelerations of the aircraft are transformed so that only the high frequency components are used to drive the simulator motion base. This technique of filtering the aircraft motion to produce simulated motion is valid since the human vestibular system, composed of organs that detect linear and angular accelerations, is most sensitive to high frequency motion [Young, et al 73]. The filtering system, or simulator drive logic, described in this thesis utilizes the dynamics of

the vestibular organs in an attempt to improve the simulator motion characteristics. Referred to as the Optimal Washout System (OWS), it operates by minimizing the error between the output of mathematical models of the vestibular systems of the aircraft pilot and the simulator pilot.

1.1 Current Filtering Techniques

Various experimenters have developed and tested a number of acceleration filtering systems or "washouts". The term "washout" refers to the technique of giving the pilot the initial acceleration of a maneuver and then slowly attenuating the simulator motion before the limit of simulator travel is reached. Some of the representative filtering systems include the crossfeed washout [Sinacori, et al 77], the adaptive gain washout [Reidell, Hoffman 78], the parabolic limiting signal compressor [Sinacori 73] and the human dynamic orientation model washout [Fuller 77]. The crossfeed washout, the adaptive gain washout, and the parabolic limiting signal compressor are typical of many current washout routines, each designed mainly by intuition and less by scientific information about human perception of motion. The crossfeed washout (Figure 1-1) uses second order high-pass filters with cross-coupling between linear acceleration and angular rate to minimize undesired accelerations in the plane of the maneuver. The adaptive gain washout (Figure 1-2) calculates the proper motion gain based on the terms of a cost equation. The parabolic signal compressor (Figure 1-3) calculates the proper simulator acceleration based on the aircraft acceleration and the current position and velocity of the simulator cab. The final filtering system, the orientation model washout (Figure 1-4),

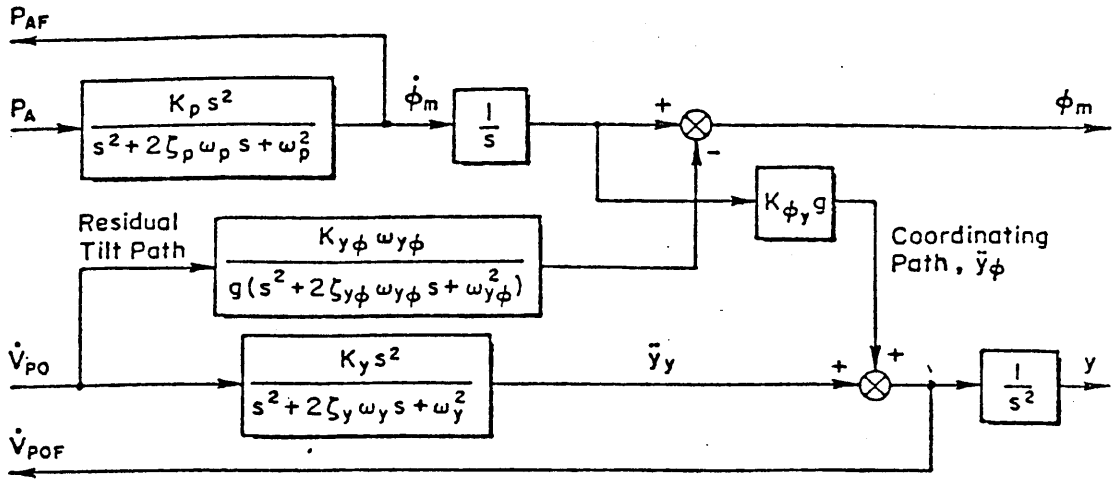

Figure 1-1. Crossfeed Washout [Sinacori, et al 77]

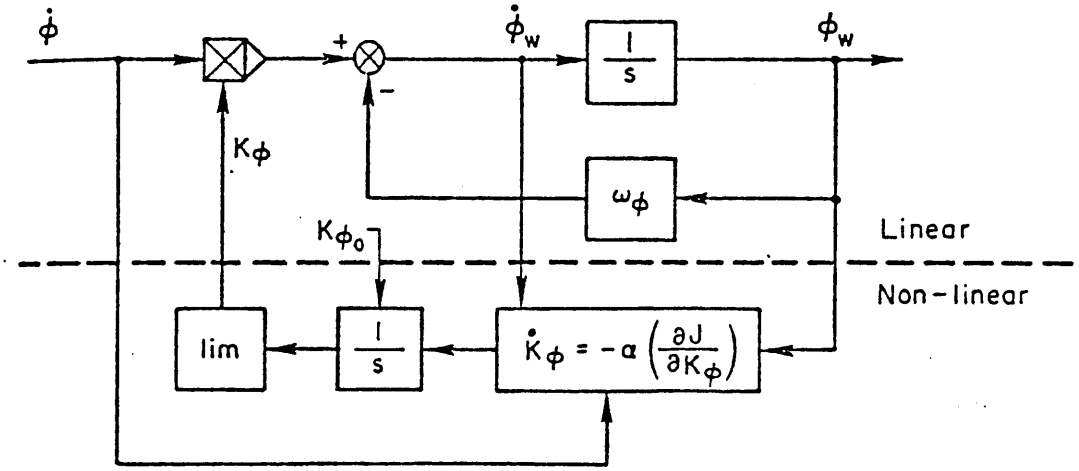

$$\dot{\phi}_\omega = K_\phi \dot{\phi} - \omega_\phi \phi_\omega$$

$$\dot{K}_\phi = -\alpha(\partial J/\partial K_\phi)$$

$$J = 1/2\left[(\dot{\phi}-\dot{\phi}_\omega)^2 + b_\phi \phi_\omega^2 + b_{K_\phi}(K_\phi - K_{\phi_0})^2\right]$$

Figure 1-2 Adaptive Gain Washout [Reidel, Hoffman 78]

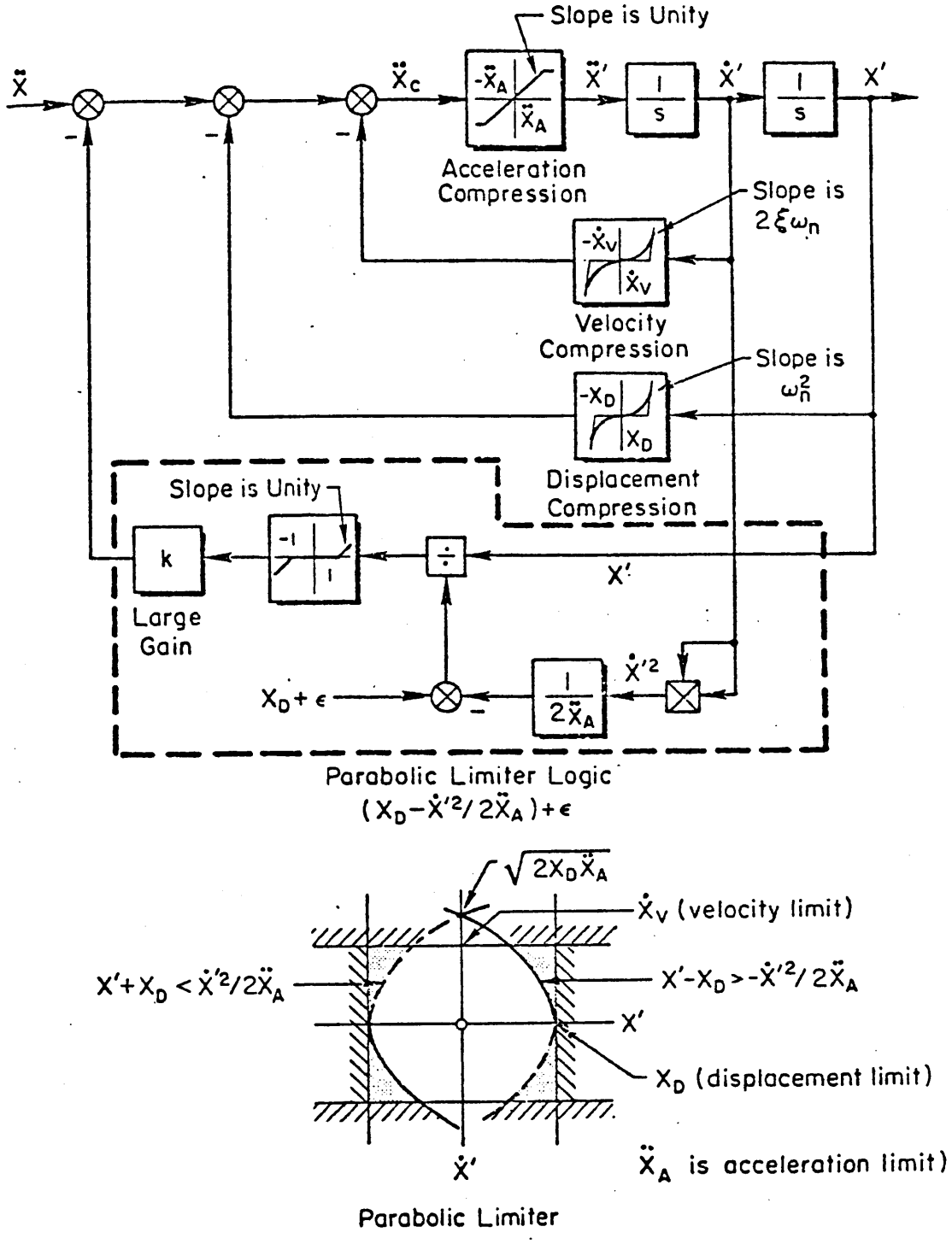

Figure 1-3. Parabolic Limiting Signal Compressor
[Sinacori 73]

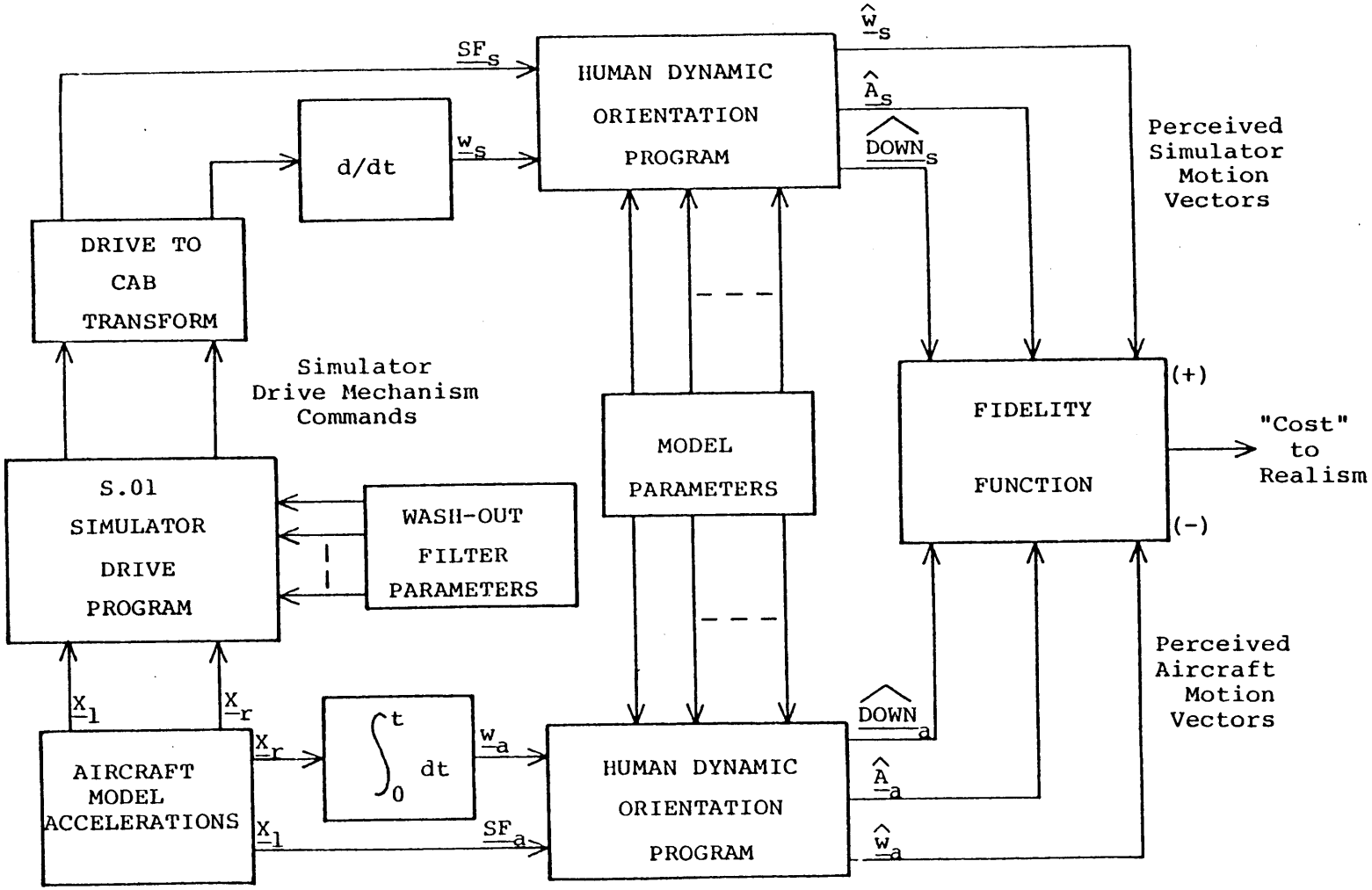

Figure 1-4. Human Dynamic Orientation Model Washout
[Fuller 77]

is an outgrowth of work by Ormsby [Ormsby 74] and is similar to the Optimal Washout System in that it uses models of the vestibular system. The orientation model washout, however, uses these vestibular models to match the simulator pilot's perception of "down" with that of the actual aircraft pilot, while the OWS matches the output of models of the neural firing rates of the organs in the vestibular system.

1.2 Development of the Optimal Control Washout

In 1980, Sivan, Ish-Shalom, and Huang [Sivan, Ish Shalom, Huang 82] completed the development of the optimal washout control system, following which, Ish-Shalom implemented the washout on a three degree of freedom Link GAT-1 flight simulator [Ish- Shalom 82]. Unfortunately, due to limitations in the simulator's motion capability, the tests were not conclusive. Therefore, the purpose of the current research was to implement the control system on a flight simulator with sufficient motion capability that the characteristics of the OWS could be observed. The NASA Ames Vertical Motion Simulator (VMS) was selected for this task. To evaluate the performance of the optimal washout system, experimental comparisons were made with an existing washout of the crossfeed type. To quantify the pilots' perceptions of motion with each washout, various motion evaluation procedures and rating scales were utilized.

1.3 Description of Thesis

Chapter 2 of this document details the formulation of the Optimal Washout System and includes a description of the human vestibular system. Various assumptions used in the developement of the washout

system are highlighted.

Chapter 3 explains the experimental procedures used to compare the operation of the Optimal Washout System to that of the NASA Ames washout system. The design methodology for each of six washouts used in the experiment is discussed and the dynamic characteristics of the washouts are compared. A discussion of the test procedures follows, along with a description of the techniques for pilot subjective evaluation of the washouts.

The experimental results are then presented in Chapter 4 and the data analysis techniques described. The relationship between pilot performance in a tracking task is compared to subjective ratings of the aircraft handling qualities and to ratings of the washout system fidelity.

Chapter 5 summarizes the findings of the experiment and describes recommendations for future work.

2. Optimal Washout System Formulation

2.0 Introduction

In an attempt to improve the fidelity of motion in flight simulators, a washout system has been designed that explicitly utilizes the dynamics of the human vestibular (motion sensing) organs. The washout system observes the surge linear acceleration and pitch angular velocity of the mathematical aircraft model and calculates the imaginary aircraft pilot's vestibular states (otolith and semicircular canal physiological outputs) in terms of normalized units. The washout system then determines what surge linear acceleration and pitch angular velocity to command to the simulator to minimize the error between the vestibular states of the simulator pilot and the imaginary aircraft pilot (Figure 2-1). This error is a vector composed of the difference in neural firing rates of the otoliths of the two pilots and the difference in firing rates of the semicircular canals of the two pilots. If this was the only task of the washout, the controller would command simulator motions such that the simulator pilot's vestibular states exactly match those of the imaginary aircraft pilot; consequently, the travel of the simulator cab would closely match the trajectory of the aircraft. Since, however, the simulator does not have unlimited travel, the controller must constrain the motion of the simulator to within the hardware limits of the facility while simultaneously minimizing the error between the aircraft pilot's and the simulator pilot's vestibular systems. This tradeoff between vestibular error and cab displacement is

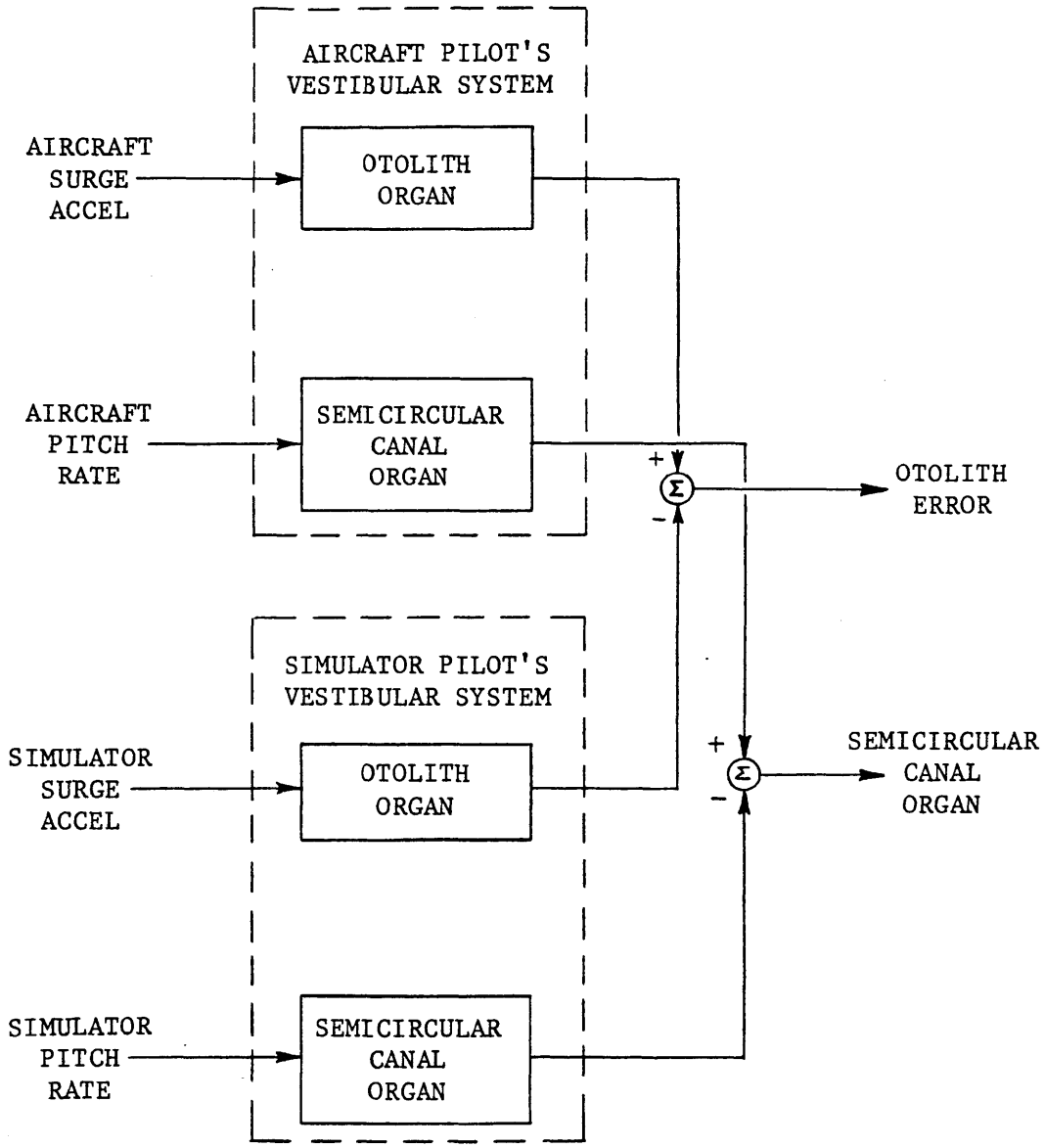

Figure 2-1. Vestibular System Output Error

best solved by optimal control techniques.

Prior to applying optimization techniques, this problem must be cast into linear control system form. In order to do this, the following assumptions have been made:

- -The utility and acceptability of flight simulator motion is improved by minimizing the expected value of the mean squared error between the aircraft pilot's and the simulator pilot's vestibular systems. This criterion is assumed independent of the motion cues provided by the simulator's visual system.

- -The pilot's vestibular system can be modeled as a linear, time-invariant system. This neglects any threshold or saturation effects.

- -The pilot's perception of motion is assumed to be linearly related to the firing rate of the vestibular system organs, i.e.- the higher the firing rate, the greater the sensation of motion.

- -In determining his spatial orientation, the pilot uses proprioceptive cues to a much lesser extent than vestibular cues.

- -Aircraft motions resulting from pilot inputs and external disturbances generally cannot be predicted; therefore aircraft motions can be modeled as random processes.

2.1 Vestibular System Description

The vestibular system is the pilot's primary means of motion detection in the absence of visual cues. The vestibular system, located near the iinner ear, consists of the semicircular canals, that detect angular motion, and the otoliths, that detect linear accelerations and the force due to gravity. By understanding the structure and dynamics

of these organs, a mathematical model can be developed to approximate the physiological outputs of the vestibular system and thereby obtain a greater understanding of the motion perception process.

2.1.1 Semicircular Canal Structure

Two sets of semicircular canals are located in the head near the inner ear, each set consisting of three approximately orthogonal rings that eminate from a central bulb called the ampulla. The rings are filled with fluid which tends to remain inertially fixed as the ring rotates with the head; however, the fluid is forced to rotate with the ring due to a gelatinous plug called the crista ampullaris. The inertial force of the fluid causes a deflection of the crista, though the visco-elastic properties of the crista cause this deflection to eventually decay even under steady state rotation. Hair cells imbedded in the crista measure the deflection of the crista and trigger nerve signals that are sent to the brain for determination of angular motion. Figure 2-2a and 2-2b illustrate the structure of the semicircular canals and the crista ampullaris.

2.1.2 Semicircular Canal Model

The semicircular canals can be modeled as a damped torsional pendulum [Young 74] that relates an angular velocity input to crista defletion (Figure 2-3). In the model, "d" represents the deflection of the crista and "θ" represents the angular motion input to the system. This is a valuable model in understanding the dynamics of the semicircular canals; however, for the purposes of the washout system, the model is extended one step in the perceptual process. It is assumed

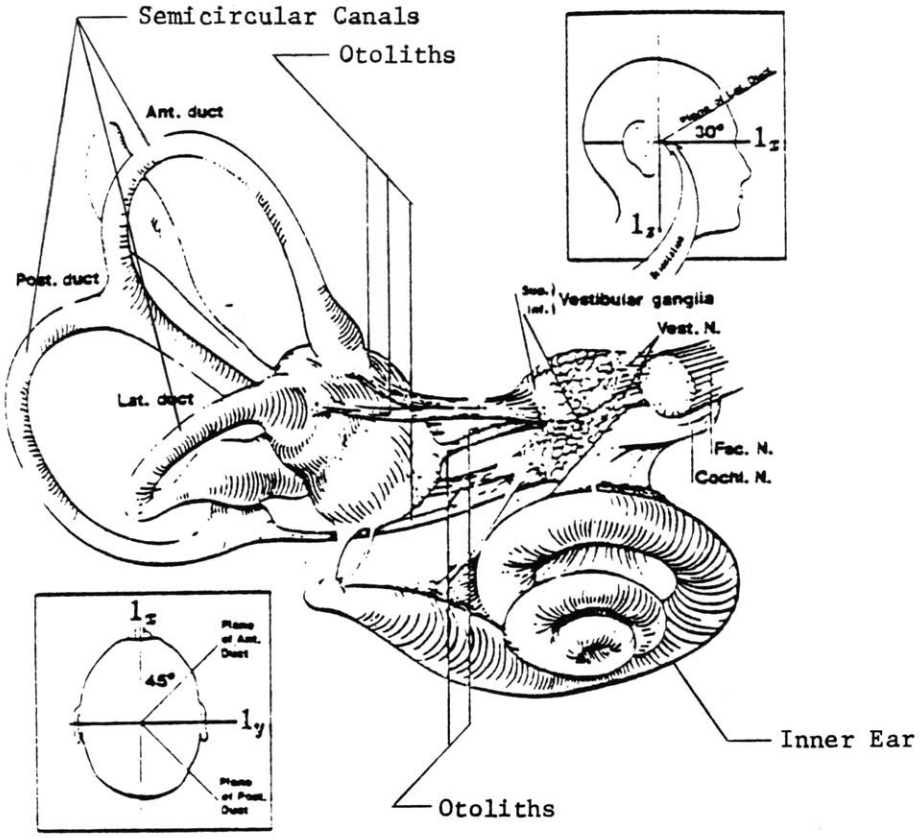

Figure 2-2A Semicircular Canal Location

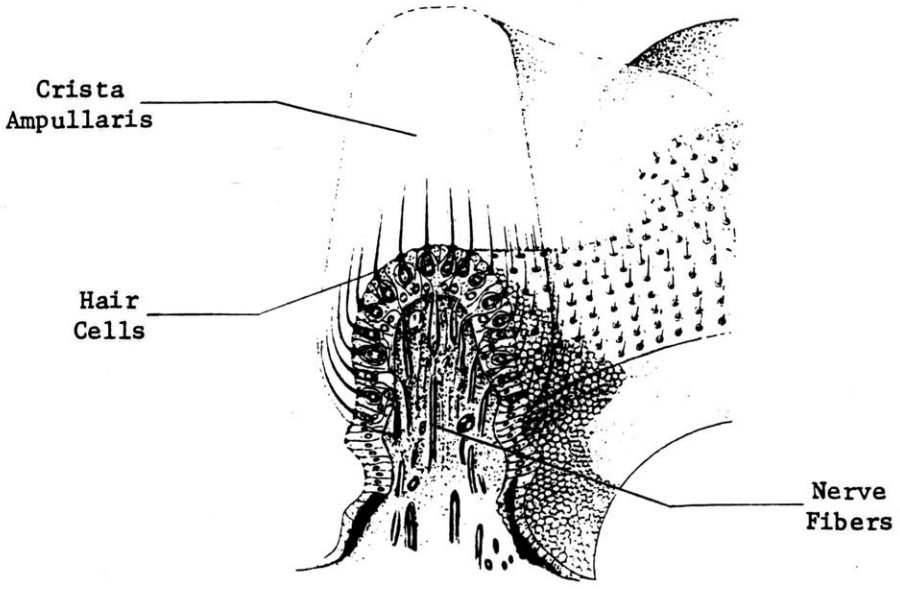

Figure 2-2B. Crista Ampullaris

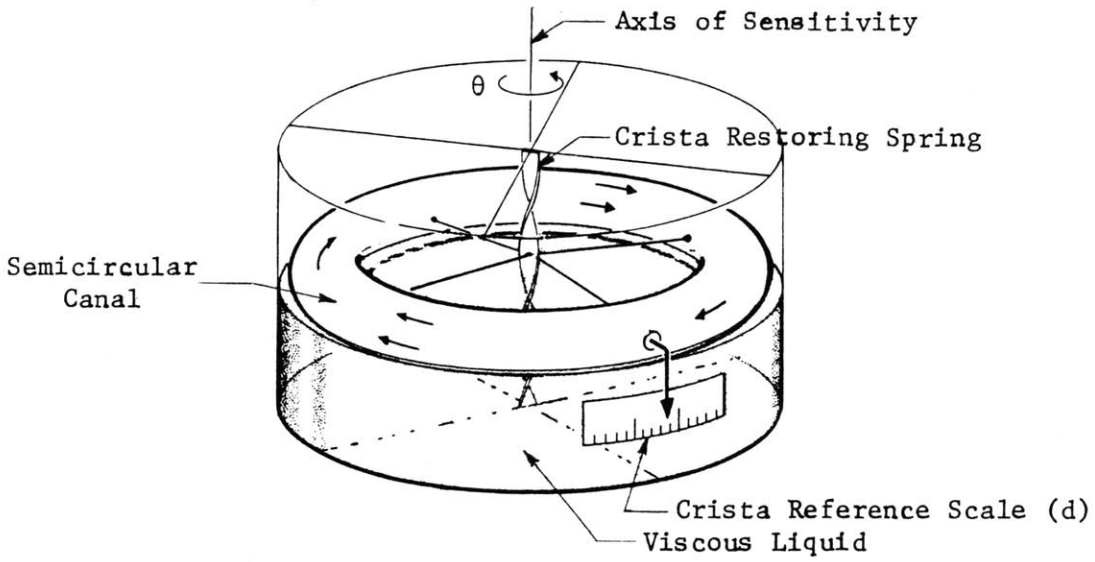

Figure 2-3. Torsional Pendulum Model of Semicircular Canal

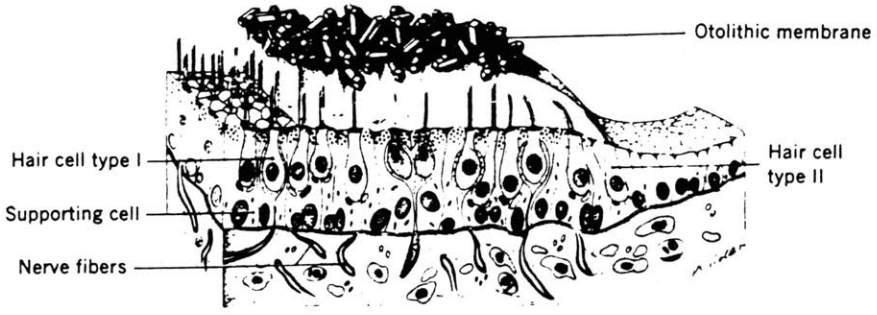

Figure 2-4. Otolith Organ Structure

that the neural firing rate of the nerve cells in the crista is a better predictor of motion perception than is the deflection of the crista; therefore, the following model is used [Shalom 82].

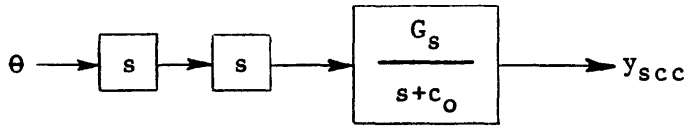

where y_{scc} is the normalized firing rate in threshold units, i.e.- $y_{scc}=1$ when the subject is being accelerated at a threshold level. The G_s and c_o are determined from Hosman's work [Hosman 78] which states that the threshold of angular acceleration is 1.45 deg/sec^2 at a frequency of 0.94 rad/sec ; consequently, $G_s=37.746$ and $c_o=0.169$.

2.1.3 Otolith Structure

The otoliths are small bony cavities, adjacent to the semicircular canals, whose inside surfaces are covered with a gelatinous layer that is coated with small calcite deposits. When the organ is accelerated, the calcite deposits tend to remain inertially fixed, thereby causing a shear in the gelatinous layer. As with the semicircular canals, the shear deflection is detected by hair cells that trigger nerve signals that are then processed by the brain. The structure of the otolith is shown in Figure 2-4.

2.1.4 Otolith Modeling

The otolith organ can be modeled as overdamped spring-mass-damper system with the visco-elastic gelatinous layer determining the damping

and stiffness of the system. However, as with the semicircular canals, the model is then extended one step in the perceptual process. The normalized firing rate of the nerves at the base of the hair cells is calculated instead of the deflection of the gelatinous layer [Shalom 82].

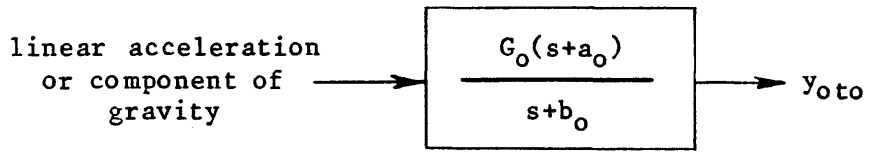

where y_{oto} is the normalized firing rate in threshold units, G_o=1.62 sec^2/ft, a_o=0.076 rad/sec and b_o=0.19 rad/sec. The values of a_o and b_o are taken from Zacharias's work [Zacharias 78]. The value of G_o is determined from Hosman's work [Hosman 78] which states that the threshold of linear acceleration is 0.47 m/sec^2 at a frequency of 0.0 rad/sec (ramp acceleration). Actually, throughout the work presented here, the incorrect value of 0.66 was used for G_o which was calculated using an acceleration of 0.47 m/sec^2 at a frequency of 0.94 rad/sec. This should be corrected for future experiments.

2.2 Problem Formulation

The otolith and semicircular canal models form the basis of the optimal control washout. They are combined to form a vestibular system model for both the imaginary aircraft pilot and the simulator pilot. These vestibular system models are then combined with a mathematical model of the simulator motion base system, and an aircraft maneuver shaping filter. During the operation of the washout, the difference in the outputs of the two vestibular subsystems is minimized by commanding

the proper inputs to the simulator motion base hardware. A mathematical model of the hardware, the motion base subsytem, monitors these inputs and updates the calculated position and velocity of the simulator cab. With this knowledge, the washout can restrain the displacement of the cab to within the travel limits of the motion base. The shaping filter operates on white noise to produce a spectrum of maneuvers similar to that of the aircraft being simulated. It is assumed that the summation of an infinite number of aircraft maneuvers would produce a spectrum similar to that generated by a low pass filter. The break frequency of the filter is a function of the types of maneuvers being performed and the type of aircraft being flown [Ish-Shalom 82]. The shaping filter is used only during the washout design process and it informs the controller of the expected frequency components of the maneuvers to be performed in the simulator.

2.2.1 Vestibular Subsystem Description

The vestibular system models use as inputs, the linear accelerations and angular velocities illustrated in Figure 2-5. Note that as the pilot pitches the aircraft, a component of the gravity vector couples into the longitudinal acceleration vector in the aircraft body axis. This component has a magnitude of g*SIN(θ), but by making small angle assumptions, the coupling, called g-tilt, can be modeled as shown in Figure 2-6. G-tilt is exploited in many washout systems to give the pilot the sensation of constant acceleration in the plane of the tilting. For example, if a takeoff is being simulated, the simulator cannot provide the required long duration linear acceleration; however, by slowly pitching the pilot to a constant nose-up attitude, a

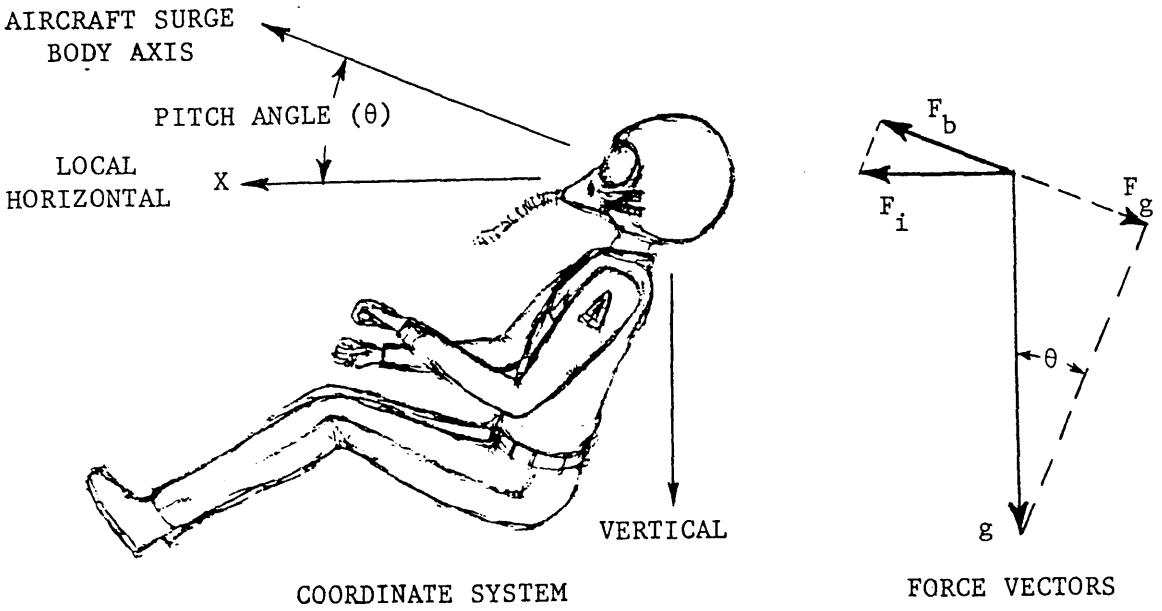

Figure 2-5. Coupling of g Vector

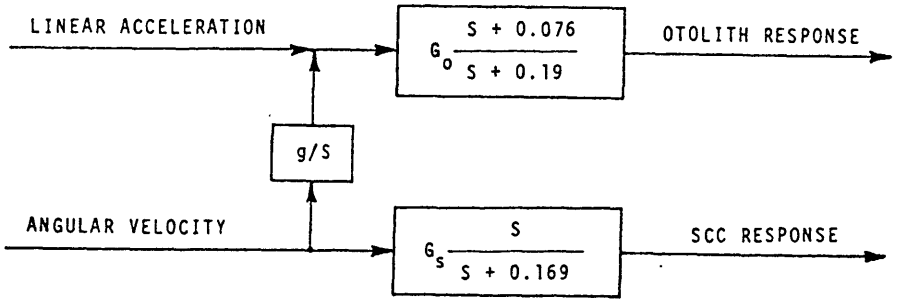

Figure 2-6. Coupled Otolith and Semicircular Canal Models

component of the g vector causes the pilot to feel a constant surge acceleration.

The combined vestibular model is then cast into state space form for the imaginary aircraft pilot and for the simulator pilot, as shown in equations 2.1 through 2.4 .

Aircraft Pilot's Vestibular System:

$$\dot{\underline{x}}_a(t)=A_a\underline{x}_a(t)+B_a\underline{u}_a(t) \qquad (2.1)$$

$$\underline{y}_a(t)=C_a\underline{x}_a(t)+D_a\underline{u}_a(t) \qquad (2.2)$$

where:

$$\underline{x}_a=\begin{bmatrix} * \text{ aircraft pilot's otolith state} \\ * \text{ aircraft pitch angle (integral of pitch rate)} \\ * \text{ aircraft pilot's semicircular canal state} \end{bmatrix}$$

$$\underline{u}_a=\begin{bmatrix} * \text{ aircraft linear surge acceleration} \\ * \text{ aircraft pitch rate} \end{bmatrix}$$

$$\underline{y}_a=\begin{bmatrix} * \text{ aircraft pilot's normalized otolith firing rate} \\ * \text{ aircraft pilot's normalized semicircular canal firing rate} \end{bmatrix}$$

g= acceleration due to gravity

$$A_a=\begin{bmatrix} -b_o & \pm G_o g(a_o-b_o) & 0.0 \\ 0.0 & 0.0 & 0.0 \\ 0.0 & 0.0 & -c_o \end{bmatrix} \quad B_a=\begin{bmatrix} G_o(a_o-b_o) & 0.0 \\ 0.0 & 1.0 \\ 0.0 & -G_s c_o \end{bmatrix}$$

$$C_a=\begin{bmatrix} -1.0 & \mp G_o g & 0.0 \\ 0.0 & 0.0 & -1.0 \end{bmatrix} \quad D_a=\begin{bmatrix} -G_o & 0.0 \\ 0.0 & -G_s \end{bmatrix}$$

where the upper sign is for the pitch-surge case and the lower sign is for the roll-sway case. This sign convention results from the fact that with a positive aircraft pitch rate (pitch up), with no coordinating

linear acceleration, the pilot feels he is accelerating in the positive x direction; however, a positive aircraft roll rate (roll right), with no coordinating linear acceleration, causes the pilot to feel he is accelerating in the negative y direction.

Simulator Pilot's Vestibular System:

$$\dot{\underline{x}}_s(t)=A_s\underline{x}_s(t)+B_s\underline{u}_s(t) \qquad (2.3)$$

$$\underline{y}_s(t)=C_s\underline{x}_s(t)+D_s\underline{u}_s(t) \qquad (2.4)$$

where:

$$\underline{x}_s=\begin{bmatrix} * \text{ simulator pilot's otolith state} \\ * \text{ simulator pitch angle (integral of pitch rate)} \\ * \text{ simulator pilot's semicircular canal state} \end{bmatrix}$$

$$\underline{u}_s=\begin{bmatrix} * \text{ commanded simulator linear surge acceleration} \\ * \text{ commanded simulator pitch rate} \end{bmatrix}$$

$$\underline{y}_s=\begin{bmatrix} * \text{ simulator pilot's normalized otolith firing rate} \\ * \text{ simulator pilot's normalized semicircular canal firing rate} \end{bmatrix}$$

g= acceleration due to gravity

$$A_s=\begin{bmatrix} -b_o & \pm G_o g(a_o-b_o) & 0.0 \\ 0.0 & 0.0 & 0.0 \\ 0.0 & 0.0 & -c_o \end{bmatrix} \quad B_s=\begin{bmatrix} G_o(a_o-b_o) & 0.0 \\ 0.0 & 1.0 \\ 0.0 & -G_s c_o \end{bmatrix}$$

$$C_s=\begin{bmatrix} 1.0 & \pm G_o g & 0.0 \\ 0.0 & 0.0 & 1.0 \end{bmatrix} \quad D_s=\begin{bmatrix} G_o & 0.0 \\ 0.0 & G_s \end{bmatrix}$$

where the upper sign is for the pitch-surge case and the lower sign is for the roll-sway case. This sign convention follows from the same reasoning as with the aircraft pilot's vestibular subsystem.

2.2.2 Motion Base Subsystem Description

The third subsystem, the simulator motion base system, determines the position and velocity states of the simulator cab. The washout controller monitors these states and issues commands to keep the simulator within the limits of allowable travel. For simplicity, during the validation phase of this program, the simulator has been assumed to have no dynamics and hence acts simply as a double integrator, as shown in equations 2.5 and 2.6 . For future tests, the simulator dynamics can be more accurately modeled as a low pass filter.

$$\dot{\underline{x}}_{mb}(t)=A_{mb}\underline{x}_{mb}(t)+B_{mb}\underline{u}_s(t) \qquad (2.5)$$

$$\underline{y}_{mb}(t)=C_{mb}\underline{x}_{mb}(t)+D_{mb}\underline{u}_s(t) \qquad (2.6)$$

where:

$$\underline{x}_{mb}=\begin{bmatrix} * \text{ simulator motion base displacement} \\ * \text{ simulator motion base velocity} \end{bmatrix}$$

$$\underline{u}_s=\begin{bmatrix} * \text{ commanded simulator linear surge acceleration} \\ * \text{ commanded simulator pitch rate} \end{bmatrix}$$

$$A_{mb}=\begin{bmatrix} 0.0 & 1.0 \\ 0.0 & 0.0 \end{bmatrix} \qquad B_{mb}=\begin{bmatrix} 0.0 & 0.0 \\ 1.0 & 0.0 \end{bmatrix}$$

$$C_{mb}=\begin{bmatrix} 1.0 & 0.0 \\ 0.0 & 1.0 \end{bmatrix} \qquad D_{mb}=\begin{bmatrix} G_o & 0.0 \\ 0.0 & G_s \end{bmatrix}$$

To further improve the operation of the washout system, the cab position, velocity, and pitch angle states could be updated with actual hardware measurements passed through a Kalman Filter. This technique could be used to reduce unmodeled simulator dynamics if sufficient control authority is available.

2.2.3 Shaping Filter Subsytem

The final subsystem acts is a shaping filter that operates on white noise to produce a spectrum of maneuvers similar to that of the aircraft being simulated. The system contains two low pass filters with b_1 being the break frequency of the aircraft's longitudinal acceleration spectrum and b_2 being the break frequency of the aircraft's pitch rate spectrum. Values for b_1 and b_2 are found by performing a Fourier analysis on typical aircraft maneuvers. For the recent OWS experiments, the Fourier analysis was performed on a simulated pilot dash-quick stop maneuver; b_1 was found to be 0.20 and b_2 was found to be 0.26 .

The state equations for the shaping filter are as follows:

$$\dot{\underline{x}}_n(t)=A_n x_n(t)+B_n(t) \tag{2.7}$$

$$\underline{u}_a(t)=C_n x_n(t) \tag{2.8}$$

where:

$$\underline{x}_n=\begin{bmatrix} * \text{ aircraft linear acceleration noise state} \\ * \text{ aircraft pitch rate noise state} \end{bmatrix}$$

$$n(t)=\begin{bmatrix} * \text{ aircraft linear acceleration driving noise} \\ * \text{ aircraft pitch rate driving noise} \end{bmatrix}$$

$$\underline{u}_a=\begin{bmatrix} * \text{ aircraft linear acceleration} \\ * \text{ aircraft pitch rate} \end{bmatrix}$$

$$A_n=\begin{bmatrix} -b_1 & 0 \\ 0 & -b_2 \end{bmatrix} \quad B_n=\begin{bmatrix} b_1 & 0 \\ 0 & b_2 \end{bmatrix} \quad C_n=\begin{bmatrix} 1 & 0 \\ 0 & 1 \end{bmatrix}$$

2.2.4 Combined System Description

The aircraft pilot's vestibular subsystem, the simulator pilot's

vestibular subsystem, the simulator motion base subsystem, and the shaping filter are then combined as shown in Figure 2-7 and equations 2.9 and 2.10 .

Combined System Equations

$$\underline{\dot{x}}(t)=A^*\underline{x}(t)+B^*\underline{u}_s(t)+H^*\underline{n}(t) \qquad (2.9)$$

$$\underline{y}(t)=C^*\underline{x}(t)+D^*\underline{u}_s(t) \qquad (2.10)$$

where:

$$\underline{x}=\begin{bmatrix}\underline{x}_a\\ \underline{x}_s\\ \underline{x}_{mb}\\ \underline{x}_n\end{bmatrix} \qquad \underline{y}=\begin{bmatrix}* \text{ otolith error}\\ * \text{ semicircular canal error}\\ * \text{ simulator displacement}\\ * \text{ simulator velocity}\end{bmatrix}$$

$$A^*=\begin{bmatrix}A_a & 0 & 0 & B_aC_n\\ 0 & A_s & 0 & 0\\ 0 & 0 & A_{mb} & 0\\ 0 & 0 & 0 & A_n\end{bmatrix} \qquad B^*=\begin{bmatrix}0\\ B_s\\ B_{mb}\\ B_c\end{bmatrix} \qquad H^*=\begin{bmatrix}0\\ 0\\ 0\\ B_n\end{bmatrix}$$

$$C^*=\begin{bmatrix}C_a & C_s & 0 & D_aC_n\\ 0 & 0 & C_{mb} & 0\end{bmatrix} \qquad D^*=\begin{bmatrix}D_s\\ 0\end{bmatrix}$$

$$B_c=\begin{bmatrix}1X10\text{-}5 & 0\\ 0 & 1X10\text{-}5\end{bmatrix}$$

Although B_c should contain four elements equal to zero, the finite values shown above were chosen to speed convergence of the numerical Ricatti Equation solver during the calculation of the feedback gains.

The feedback gains of the combined system are generated to minimize the expected value of the following cost equation:

$$J=E[\underline{x}^TR\underline{x}+\underline{u}^TQ\underline{u}] \qquad (2.11)$$

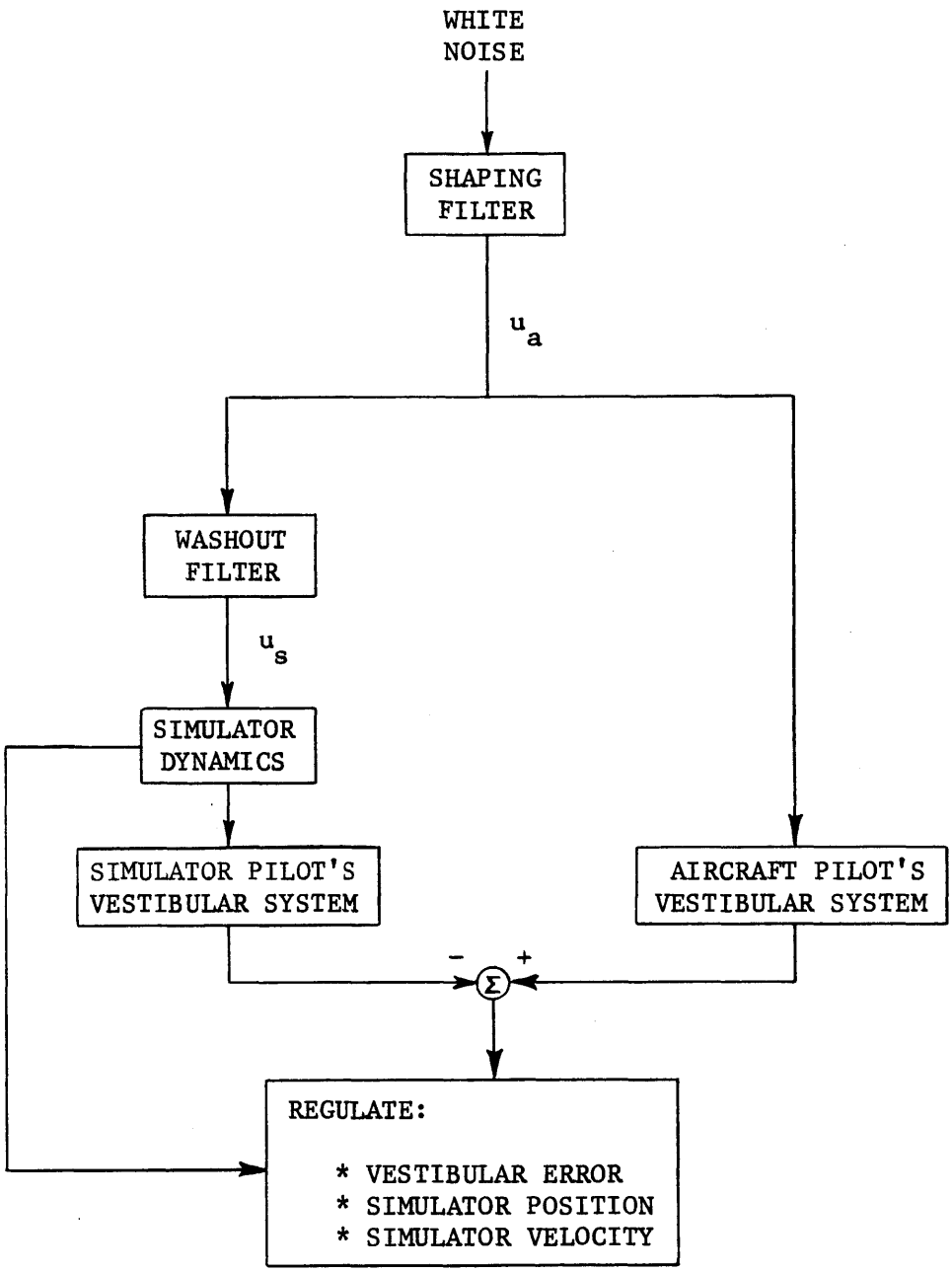

Figure 2-7. Optimal Washout System Architecture

$$J=E[q_1*(\text{otolith error})^2+$$
$$+q_2*(\text{semicircular canal error})^2+$$
$$+q_3*(\text{simulator displacement})^2+$$
$$+q_4*(\text{simulator velocity})^2+$$
$$+r_1*(\text{commanded simulator surge acceleration})^2+$$
$$+r_2*(\text{commanded simulator pitch rate})^2] \quad (2.12)$$

where q_1, q_2, q_3, q_4, r_1, r_2 are weighting factors selected by the designer.

Writing the cost equation in more standard form:

$$J=E[\underline{y}_{vest}^T Q_v \underline{y}_{vest}+p(\underline{u}_s^T R \underline{u}_s+\underline{y}_{mb}^T R_d \underline{y}_{mb})] \quad (2.13)$$

where:

$$\underline{y}_{vest}=\begin{bmatrix} * \text{ otolith error} \\ * \text{ semicircular canal error} \end{bmatrix}$$

$$\underline{y}_{mb}=\begin{bmatrix} * \text{ simulator displacement} \\ * \text{ simulator velocity} \end{bmatrix}$$

$$Q_v=\begin{bmatrix} q_1 & 0 \\ 0 & q_2 \end{bmatrix} \quad R=\begin{bmatrix} r_1 & 0 \\ 0 & r_2 \end{bmatrix} \quad R_d=\begin{bmatrix} q_3 & 0 \\ 0 & q_4 \end{bmatrix}$$

Now by concatenating the y vectors:

$$J=E[\underline{y}^T Q \underline{y}+p\underline{u}_s^T R \underline{u}_s] \quad (2.14)$$

where:

$$Q=\begin{bmatrix} q_1 & 0 & 0 & 0 \\ 0 & q_2 & 0 & 0 \\ 0 & 0 & pq_3 & 0 \\ 0 & 0 & 0 & pq_4 \end{bmatrix} \quad R=\begin{bmatrix} r_1 & 0 \\ 0 & r_2 \end{bmatrix}$$

In terms of the system formulation, this becomes:

$$J=E[\underline{x}^T R_1 \underline{x}+2\underline{x}^T R_{12} \underline{u}_s+\underline{u}_s^T R_2 \underline{u}_s] \quad (2.15)$$

where:

$$R_1=C^{*T}QC^* \qquad R_{12}=C^{*T}QD^* \qquad R_2=pR+D^{*T}QD^* \tag{2.16}$$

The matrices A^*, B^*, C^*, D^*, H^*, R_1, R_{12}, and R_2 are substituted into a Linear Quadratic Gaussian algorithm which solves the steady state Riccati Equation and produces a 2x10 feedback matrix F. This matrix is used to calculate the inertial axis simulator commands through the equation:

$$\underline{u}_s=-F\underline{x} \tag{2.17}$$

where F can be partitioned:

$$\underline{u}_s=\begin{bmatrix}-F_a & -F_s & -F_{mb} & -F_n\end{bmatrix}\begin{bmatrix}\underline{x}_a\\ \underline{x}_s\\ \underline{x}_{mb}\\ \underline{x}_n\end{bmatrix} \tag{2.18}$$

$$\underline{u}_s=-F_a\underline{x}_a-F_s\underline{x}_s-F_{mb}\underline{x}_{mb}-F_n\underline{x}_n \tag{2.19}$$

Note that $\underline{x}_n=\underline{u}_a$ and the states, $\underline{x}(t)$, are updated through the equation:

$$\dot{\underline{x}}(t)=A^*\underline{x}(t)+B^*\underline{u}_s(t) \tag{2.20}$$

Equations 2.19 and 2.20 are implemented in software to produce the washout system. The system is shown in block diagram form in Figure 2-8. Note that in this figure, an additional block has been included which represents the simulator displacement limiting logic on the Ames VMS simulator. This non-linear limiting logic system uses the current cab position, velocity, and acceleration to predict if the cab will hit the end of the simulator track. If no impact is predicted, the simulator simply uses the acceleration commanded by the linear washout system. If an impact is predicted, the limiting logic commands

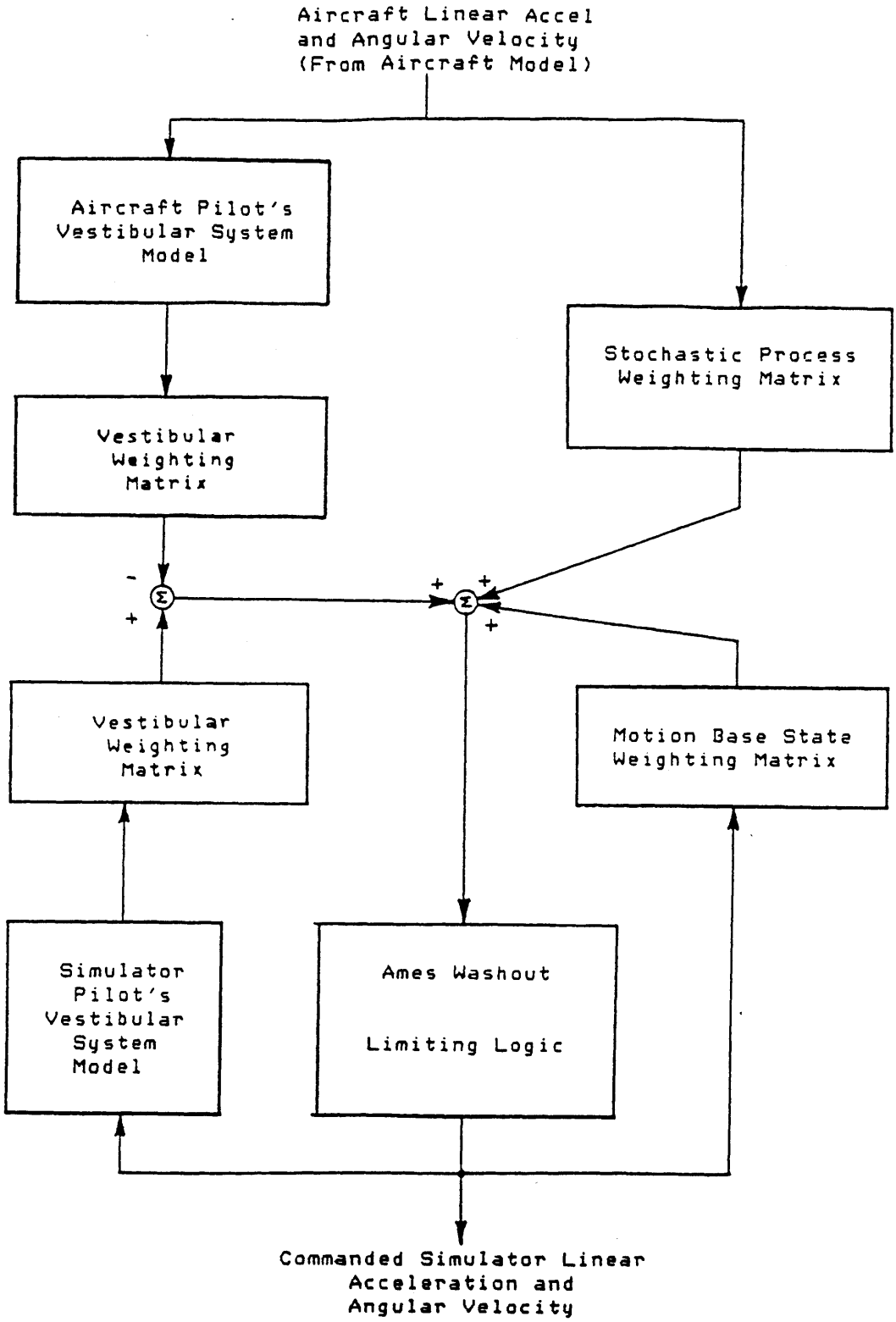

Figure 2-8. Incorporation of Limiting Logic into OWS

accelerations to brake the cab before a limit is reached. As seen in Figure 2-8, the commanded acceleration output of the limiting logic is fed back to update the simulator pilot's vestibular model states and the simulator motion base subsystem states; thereby keeping the model states synchronized with the states of the actual systems.

2.3 Transfer Function Matrix Computation

Using equations 2.1, 2.3, and 2.5, the transfer functions of each subsystem can be written as follows.

$$X_a(s)=(sI-A_a)^{-1}B_aU_a(s) \tag{2.21}$$

$$X_s(s)=(sI-A_s)^{-1}B_sU_s(s) \tag{2.22}$$

$$X_{mb}(s)=(sI-A_{mb})^{-1}B_{mb}U_s(s) \tag{2.23}$$

but from equation 2.19:

$$U_s(s)=-F_aX_a(s)-F_sX_s(s)-F_{mb}X_{mb}(s)-F_nX_n(s) \tag{2.24}$$

Substituting equations 2.21, 2.22, and 2.23 into 2.24 yields:

$$U_s(s)=-F_a(sI-A_a)^{-1}B_aU_a(s)-F_s(sI-A_s)^{-1}B_sU_s(s)- \\ -F_{mb}(sI-A_{mb})^{-1}B_{mb}U_s(s)-F_nX_n(s) \tag{2.25}$$

Now from equation 2.25, if $C_n=I$, then $U_a(s)=X_n(s)$; therefore, equation 2.25 becomes:

$$U_s(s)=[I+F_s(sI-A_s)^{-1}B_s+F_{mb}(sI-A_{mb})^{-1}B_{mb}]^{-1} \\ *[-F_a(sI-A_a)^{-1}B_a-F_n]U_a(s) \tag{2.26}$$

This equation produces a 2x2 matrix with each element being an eighth order order transfer function.

3. Experimental Procedures

3.0 Description of Ames Vertical Motion Simulator Facility

In order to evaluate the performance of the Optimal Washout System, a series of tests was conducted on the NASA Ames Vertical Motion Simulator (VMS) (see Figure 3-1). This facility, designed primarily for helicopter simulations, has a vertical travel capability of $\pm$23 ft and a horizontal travel capability of $\pm$15 ft. The simulator cab can be rotated 90 degrees about a vertical axis to allow the horizontal track to be used for surge accelerations or sway accelerations. For the experiments described here, the cab was aligned with the surge axis.

The VMS facility is supported by three computer systems: a Sigma-8, a PDP 11/34, and a visual scene generator. The Sigma-8 accepts pilot control inputs through a set of analog-to-digital converters and uses these inputs to update the aircraft model states. The angular rates and linear accelerations from the aircraft model are then sent to the motion washout program, implemented on the PDP 11/34, that commands the proper linear accelerations and angular rates to the simulator motion base. The visual scene computer then updates the pilot's external view based on the current aircraft position and attitude. Because a finite amount of time is required to cycle through these computations and to store the desired data, an iteration step size is selected. For the tests described here, this step size was set at 34 milliseconds.

3.1 Description of Washouts

Six washouts were evaluated in this study: three "high fidelity"

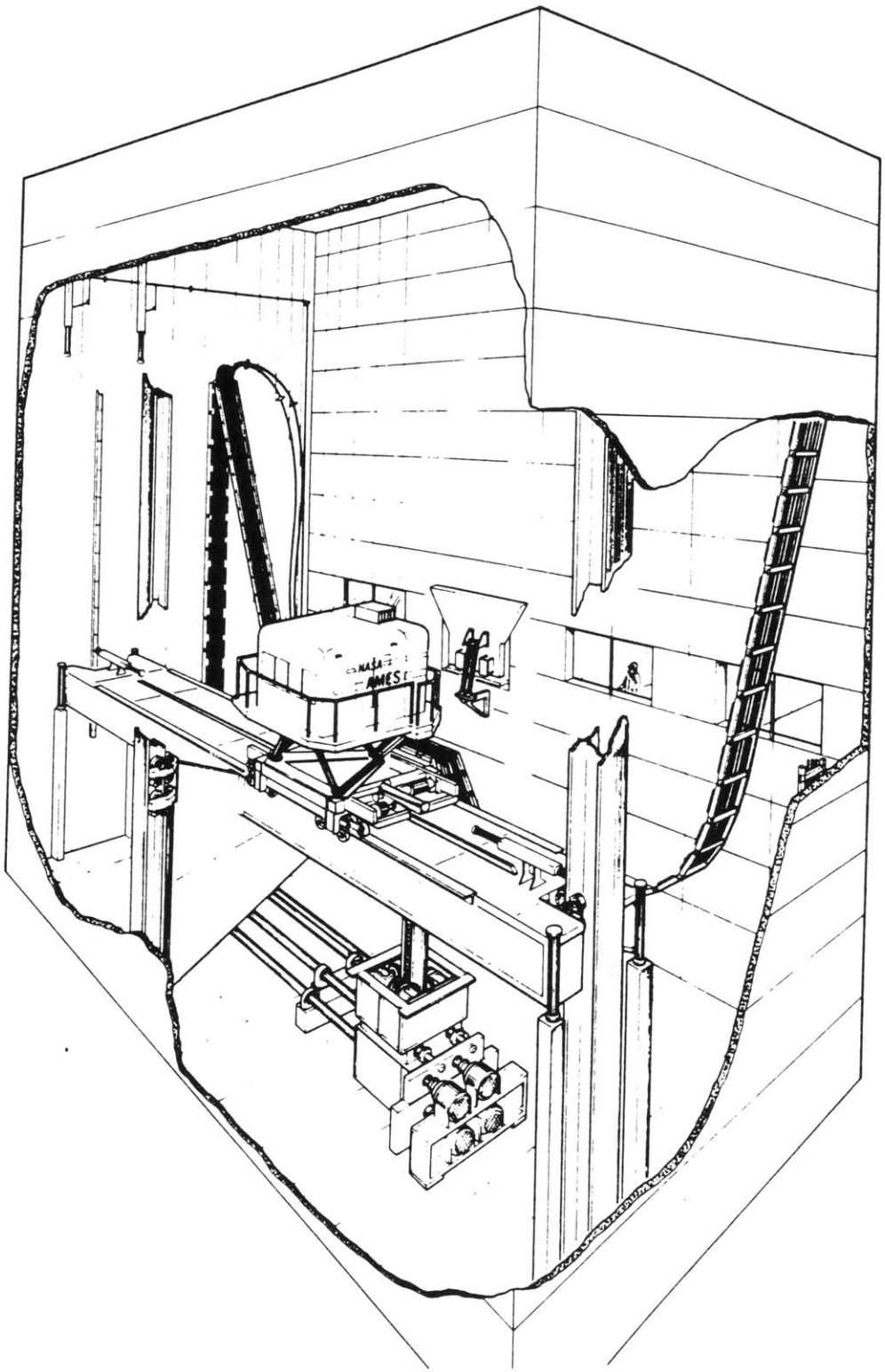

Figure 3-1. NASA Ames Vertical Motion Simulator

washouts and three "low fidelity" washouts. For the maneuvers being performed, the three high fidelity washouts (Ames Nominal, OWS Nominal, and OWS High Otolith Weighting) were designed to utilize most of the motion base's ± 15 ft horizontal travel capacity. The three low fidelity washouts (Ames Decreased Gain, Ames Increased Omega, and OWS Decreased Gain) were designed to utilize approximately half the horizontal travel. The purpose of these last three washouts was to simulate a motion base of lesser capability.

The Ames washout structure is shown in block diagram form in Figure 3-2; the parameter values for each of the Ames washouts are listed in Table 3-1. With knowledge of the aircraft being simulated and the maneuvers being performed, Richard Bray, the designer of Ames washout system, selected the parameter values for the Ames Nominal washout. The two other Ames washouts were designed to test the effects of decreased washout filter gain and increased filter break frequency. By decreasing the filter gain, the amplitude of accelerations commanded to the simulator are reduced at all frequencies. By increasing the break frequency of the filter, the low frequency motion is attenuated while less motion attenuation occurs at higher frequencies.

The maneuvers performed in the experiment were approximately coordinated, meaning that as the aircraft pitched forward, the pilot felt no net surge acceleration in the body axis. Although the aircraft is accelerating forward in the inertial surge axis, the body axis component of this acceleration is countered by the body axis component of the acceleration due to gravity (Figure 3-3). Because of this

Angular Drive:

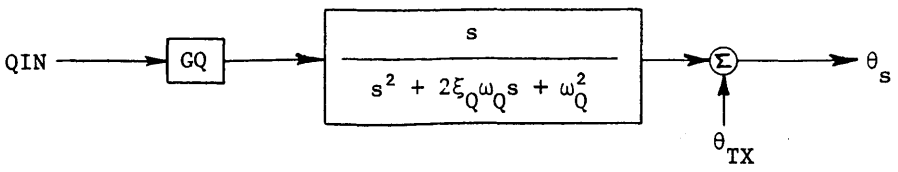

Low Frequency Tilt:

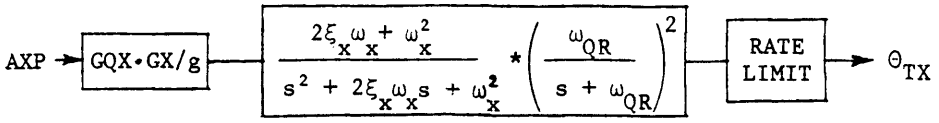

Linear Drives:

$$XIN = AXP + \ddot{Z}_s\Theta_s$$

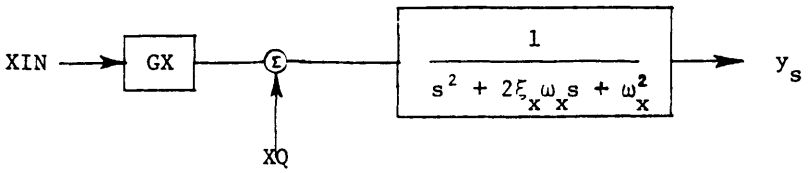

X-Θ Coordination:

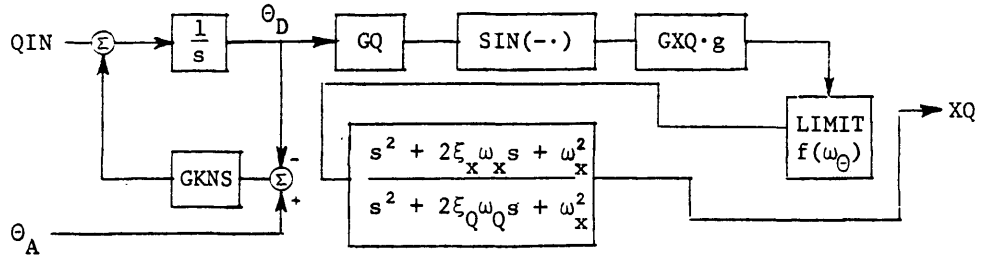

AXP = PILOT SENSED ACCELERATION (BODY AXIS)

XIN = PILOT SENSED ACCELERATION (INERTIAL AXIS)

$\ddot{Z}_s$ = SIMULATOR VERTICAL ACCELERATION

QIN = AIRCRAFT PITCH RATE (INERTIAL AXIS)

θ_A = AIRCRAFT PITCH ANGLE

θ_s = SIMULATOR PITCH ANGLE (BODY AXIS)

y_s = SIMULATOR DISPLACEMENT

Figure 3-2. NASA Ames Motion Washout Architecture

Table 3-1. Parameters for Ames Washouts

	NOMINAL	DECREASED GAIN	INCREASED OMEGA
GQ	0.6	0.3	0.6
ξ_Q	0.7	0.7	0.7
ω_Q	0.4	0.6	0.6
GQX	1.0	1.0	1.0
GX	1.0	1.0	1.0
ξ_X	0.7	0.7	0.7
ω_X	0.7	0.7	0.7
ω_{QR}	4.0	4.0	4.0
GKNS	0.1	0.1	0.1
GXQ	0.6	0.6	0.6

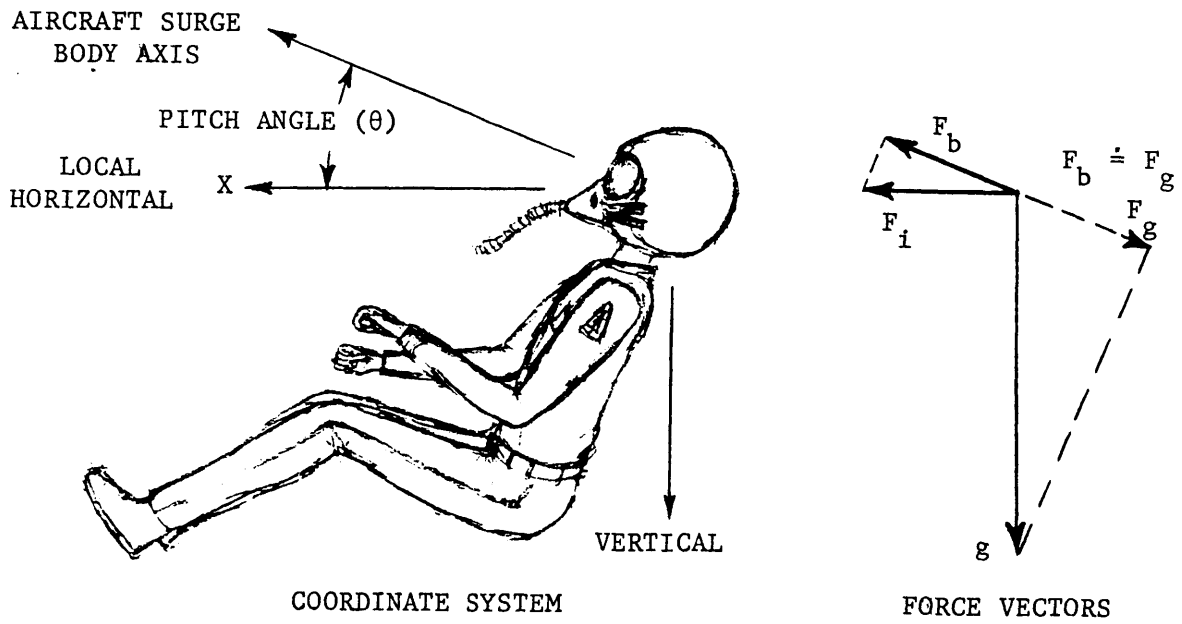

Figure 3-3. Forces on the Pilot

effect, the surge acceleration sensed by the pilot, AXP (Figure 3-2), is approximately equal to zero; furthermore, since the simulator vertical acceleration is typically close to zero, XIN (Figure 3-2) is also approximately equal to zero. As a result, little motion is commanded by the low frequency tilt and linear drive channels of the Ames washout; the primary motion results from the X-θ coordination channel. Therefore, to control the amount of simulator motion commanded, the gain and break frequency of the simulator pitch rate filter were varied in the Ames washouts.

The Ames Increased Omega washout was designed by increasing the break frequency of the pitch rate filter, thereby decreasing the amount of low frequency pitch rate, and consequently, the amount of low frequency surge acceleration commanded to the simulator motion base. To evaluate the effects of reduced amplitude surge acceleration, the Ames Decreased Gain washout was then designed to utilize half the simulator travel. This was accomplished by reducing the pitch rate gain by one-half. Unfortunately, due to an error in implementation, the Decreased Gain washout also had an increased pitch rate break frequency; consequently, this washout is of lower fidelity than originally designed.

The three optimal control washouts were designed to minimize the cost functional:

$$
\begin{aligned}
J=E[&q1*(\text{otolith error})^2+\\
&+q2*(\text{semicircular canal error})^2+\\
&+q3*(\text{simulator displacement})^2+\\
&+q4*(\text{simulator velocity})^2+\\
&+r1*(\text{commanded simulator surge acceleration})^2+\\
&+r2*(\text{commanded simulator pitch rate})^2]
\end{aligned}
$$

The values of the cost functional weighting parameters are listed in Table 3-2. The OWS Nominal washout was designed by choosing the parameter weights presumed to produce the best motion characteristics. By increasing the cost on the motion base displacement term in the cost functional, the OWS Decreased Gain washout was generated. It utilizes approximately half the horizontal travel of the simulator. For this washout and the OWS Nominal washout, the weighting on otolith error was equivalent to the weighting on semicircular canal error. The final washout, the OWS High Otolith Weighting washout, was designed with a higher cost on the otolith error than on the semicircular canal error; therefore, relative to the other OWS washouts, it reduces otolith error at the expense of semicircular canal error. All OWS washouts were designed, for typical maneuvers, to limit the maximum cab velocity below the Ames hardware limits of 6 ft/sec^2.

Table 3-2. Cost Weightings for the OWS

	NOMINAL	DECREASED GAIN	HIGH OTOLITH WEIGHTING
OTOLITH ERROR WEIGHT	0.707	0.707	1.4
SIMULATOR DISPLACEMENT WEIGHT	0.707	0.707	0.707
SIMULATOR VELOCITY WEIGHT	3×10^{-2}	5×10^{-2}	1×10^{-2}
SIMULATOR ACCELERATION WEIGHT	4×10^{-2}	4×10^{-2}	8×10^{-2}
SIMULATOR PITCH RATE WEIGHT	1×10^{-4}	1×10^{-4}	1×10^{-4}

During the tests, the Optimal Washout System was implemented on the Sigma-8 computer and, for safety reasons, the Ames washout was left operational on the PDP 11/34 even when the OWS was utilized. This arrangement allowed the Ames limiting logic to remain active at all times. To remove the dynamics of the Ames washout filters from the system when the OWS was being tested, the proper gains, damping ratios, and natural frequencies were selected in the Ames surge acceleration filter and pitch rate filter to cause them to simply act as a unitary gain elements (see Figure 3-2 and Table 3-3). The gain of the X-θ coordinating channel and the gain of the low frequency pitch tilt channel were set equal to zero such that no cross-coupling dynamics occurred when the OWS was operational. Since the OWS was not set up to control the remaining axes (roll-sway, yaw, and heave), the Ames washout in these axes was used as it normally would be in typical VMS operations.

To compare the characteristics of the washouts, Bode plots of each are presented in Figures 3-4 through 3-9. In each plot, the upper left transfer function (A_{11}) filters the aircraft linear acceleration to generate a component of simulator linear acceleration; the upper right block (A_{12}) generates the other component from aircraft pitch rate. Similarly, A_{21} and A_{22} are used to generate the simulator pitch rate based on aircraft linear acceleration and pitch rate.

$$\begin{bmatrix} \text{Simulator Surge Accel (inertial axis)} \\ \text{Sim Pitch Rate} \end{bmatrix} = \begin{bmatrix} A_{11} & A_{12} \\ A_{21} & A_{22} \end{bmatrix} \begin{bmatrix} \text{Aircraft Surge Accel (inertial axis)} \\ \text{Aircraft Pitch Rate} \end{bmatrix}$$

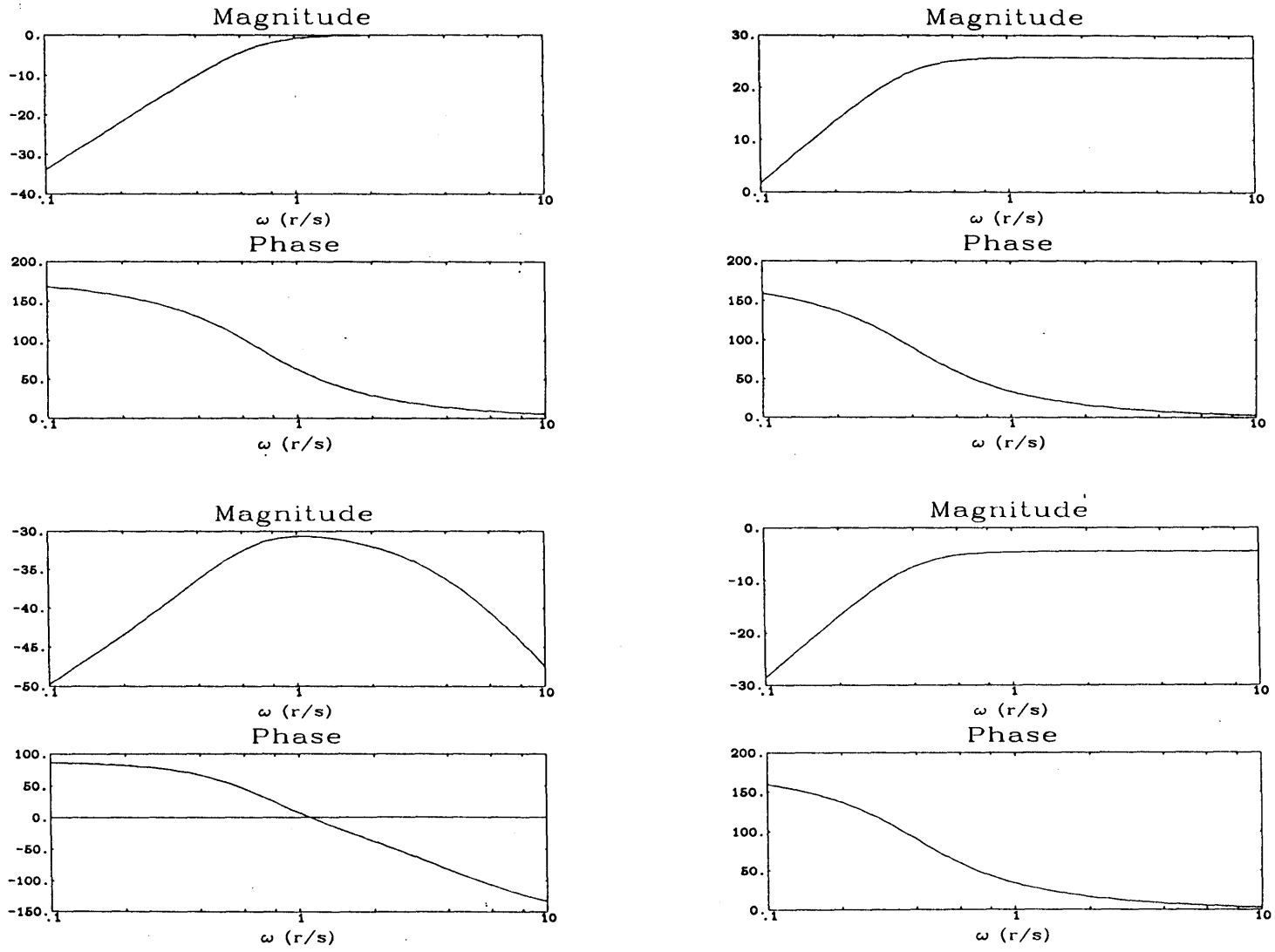

Figure 3-4. Bode Plot Matrix of the Ames Nominal Washout

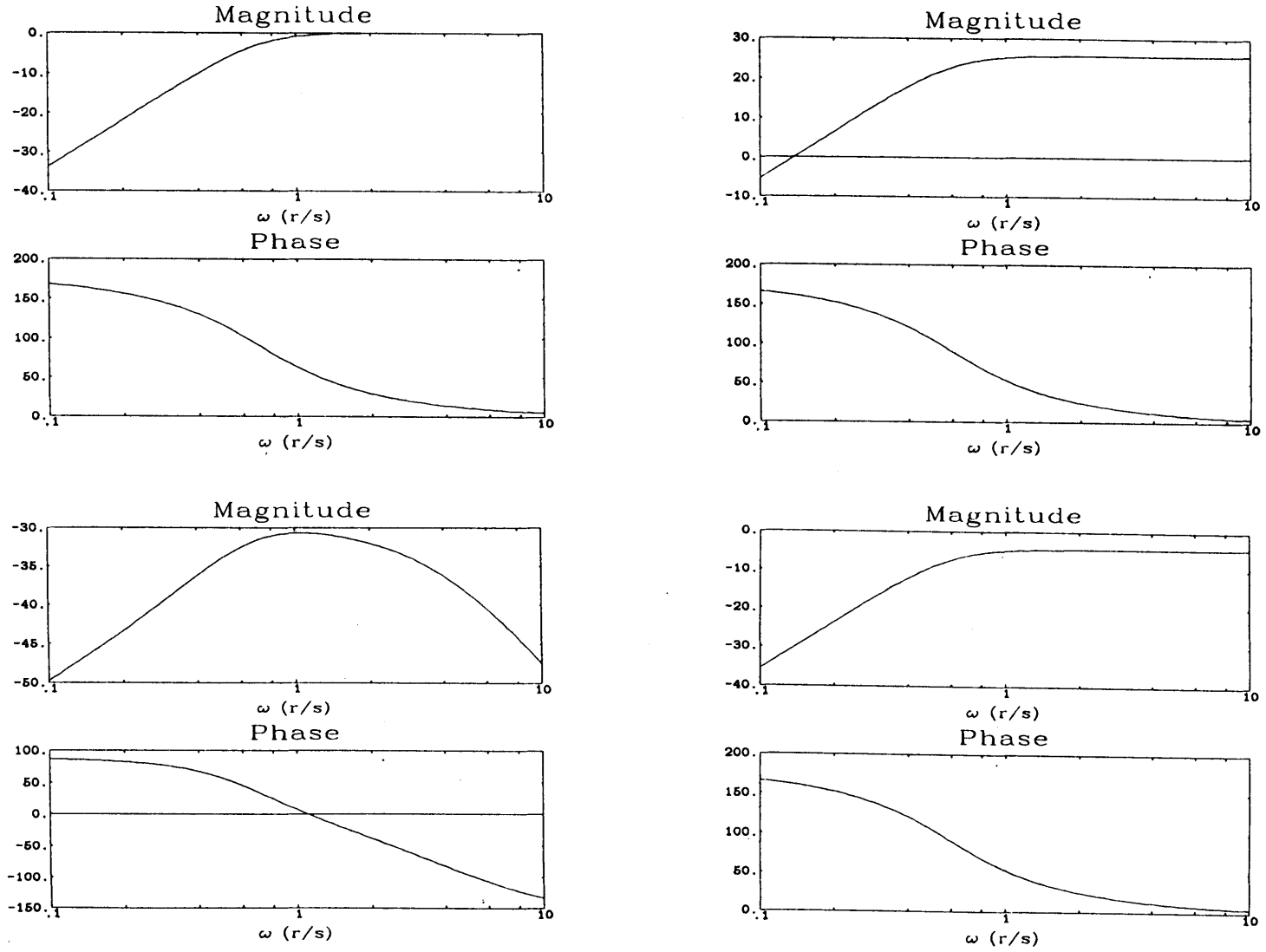

Figure 3-5. Bode Plot Matrix of the Ames Decreased Gain Washout

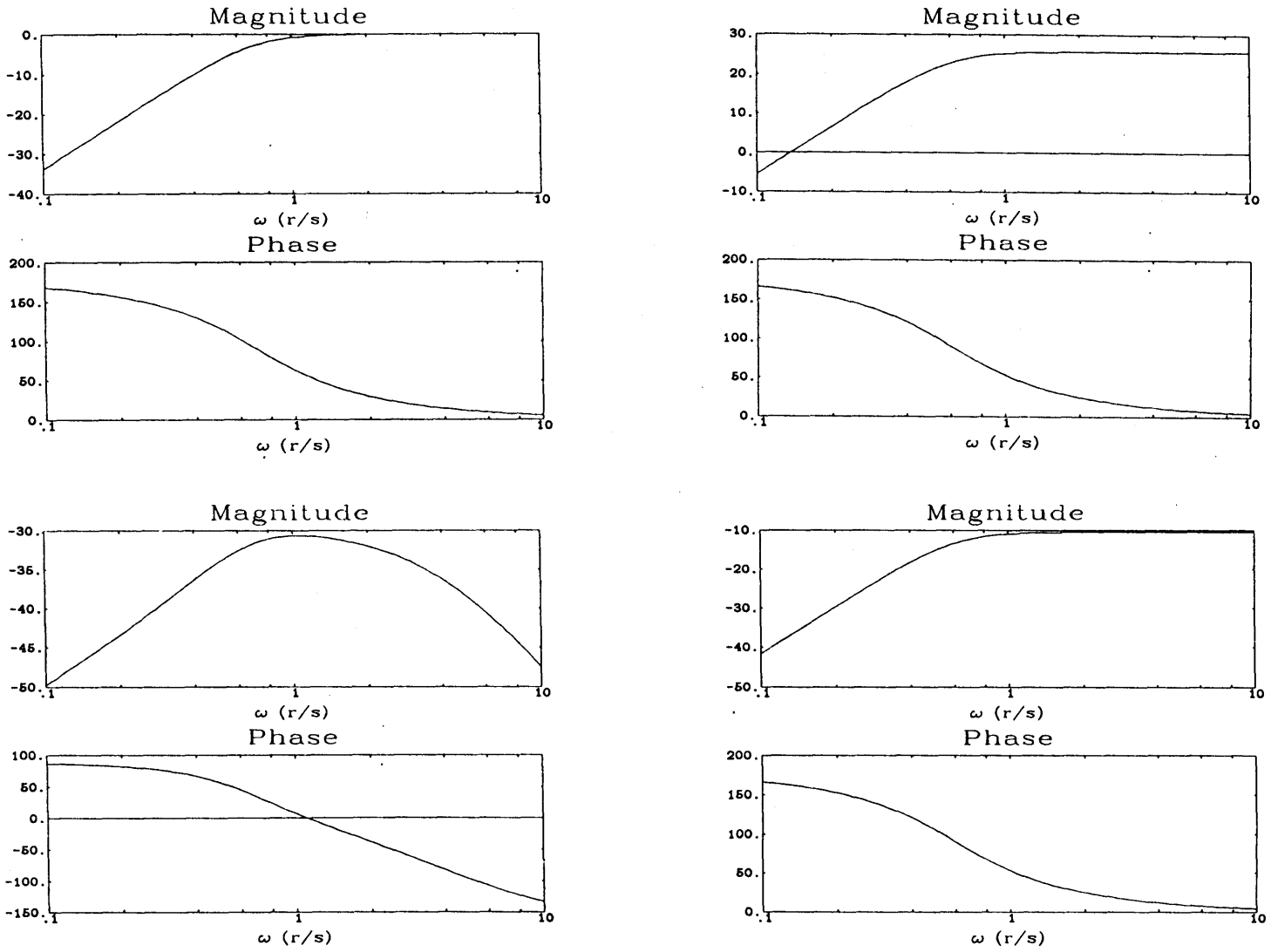

Figure 3-6. Bode Plot Matrix of the Ames Increased Omega Washout

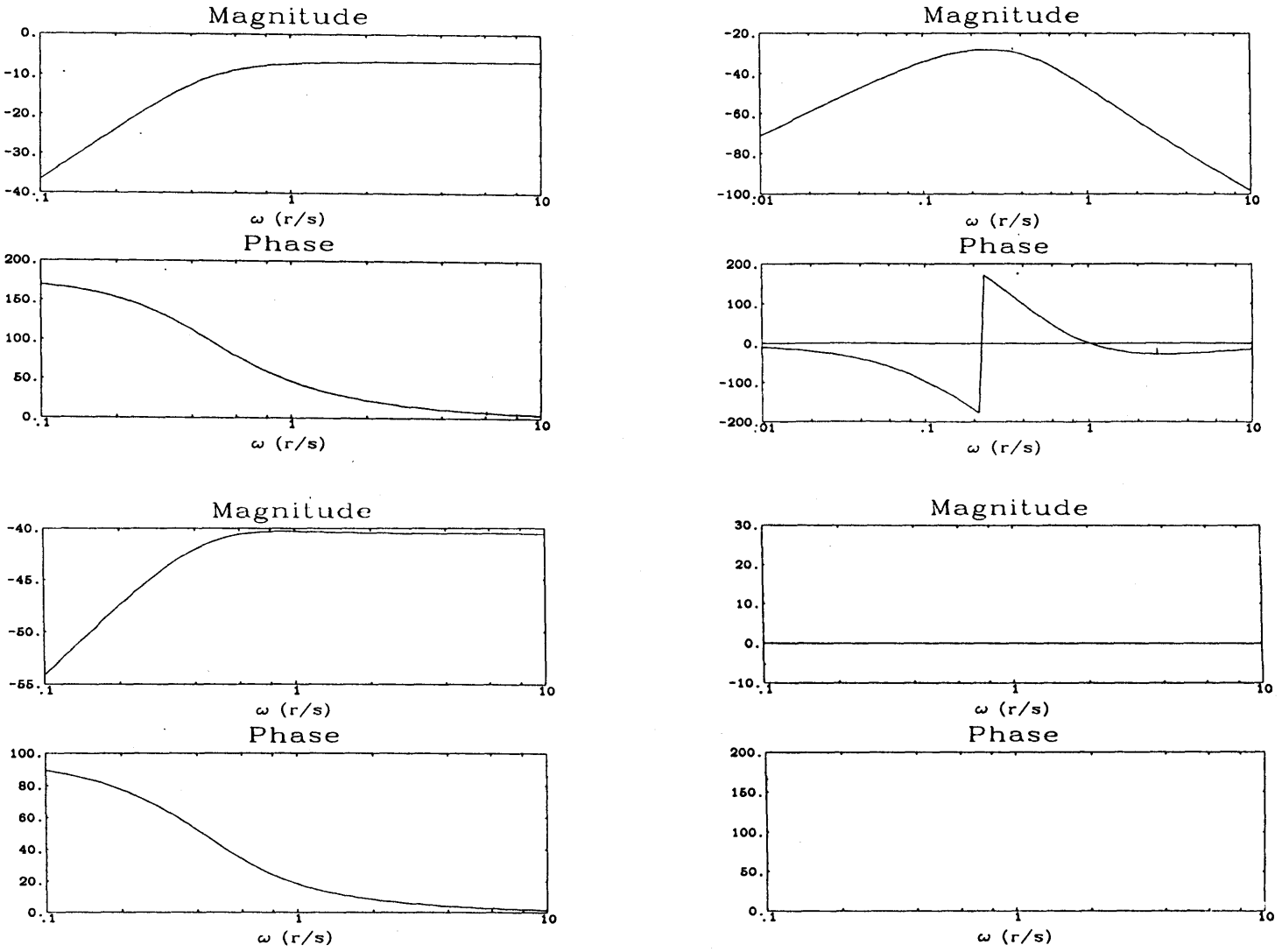

Figure 3-7. Bode Plot Matrix of the OWS Nominal Washout

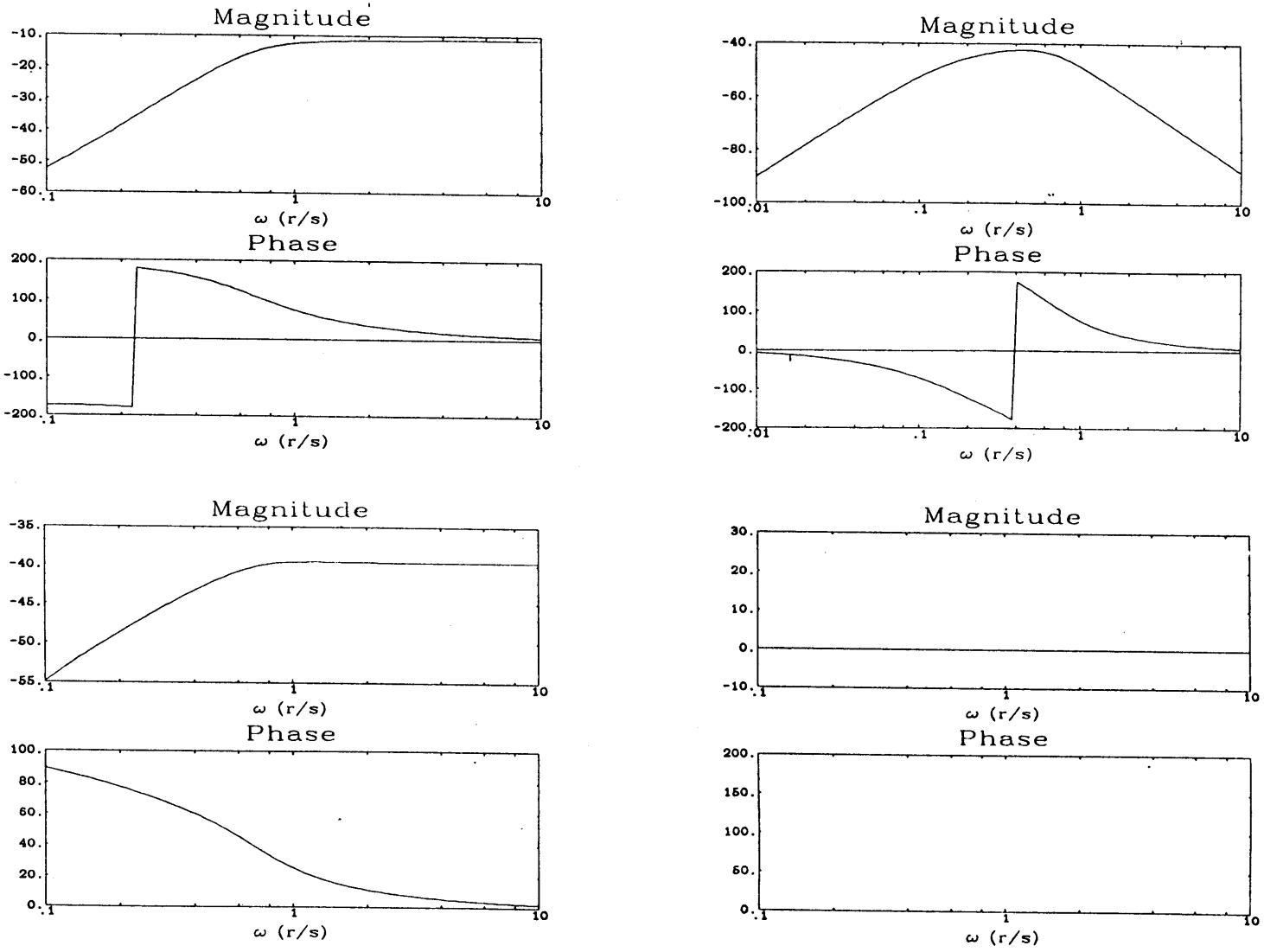

Figure 3-8. Bode Plot Matrix of the OWS Decreased Gain Washout

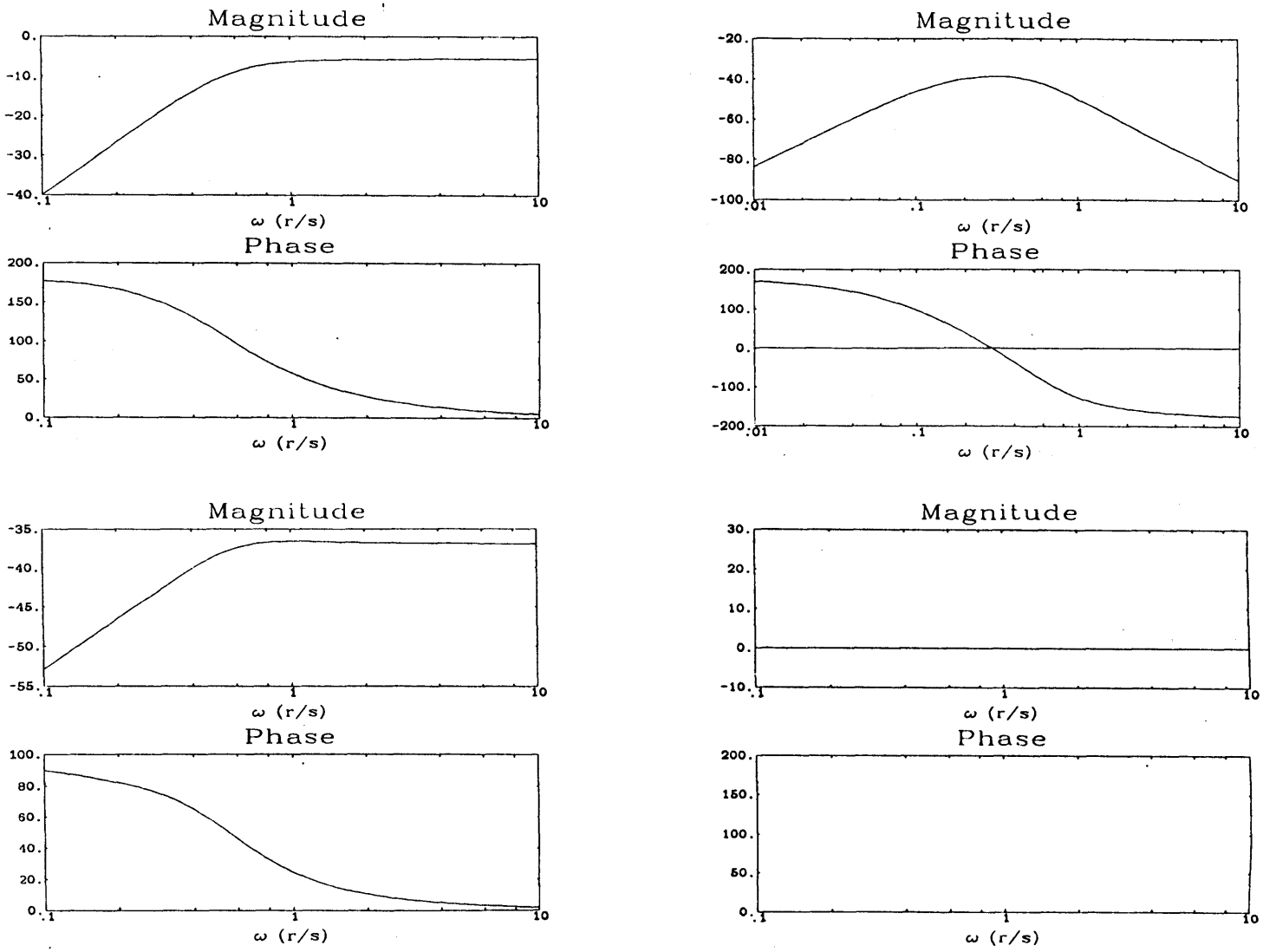

Figure 3-9. Bode Plot Matrix of the OWS High Otolith Weighting Washout

Table 3-3. Parameters to Nullify the Dynamics of the Ames Washout

GQ	1.0
ω_Q	0.0
GQX	0.0
GX	1.0
ω_X	0.0
GXQ	0.0
VWOL	1000.0 ft/sec
VWOF	1000.0 ft/sec

Note: Two sets of motion parameters are actually used by the washout routine. One set is used when the speed of the aircraft is below the value of VWOL, the other set is used when the speed is above VWOF. When the OWS system was operational, VWOL and VWOF were set higher than the maximum speed of the aircraft so that the parameters in this table were always used by the washout.

Because of non-linear elements in the Ames washouts, the gain levels shown in the A_{21} blocks of the Ames washouts cannot be directly compared to those of the OWS washouts, though the dynamics should be comparable. This block of the OWS washouts filter out only the low frequencies, but the Ames washouts filter out both high and low frequencies; consequently, with the Ames washouts, aircraft step linear acceleration inputs (e.g.-application of brakes) do not cause perceptible simulator step pitch accelerations.

To evaluate the washout performance with actual pilot inputs, a dash-quick stop maneuver has been executed on each of the washouts; the cab trajectories and vestibular responses are plotted in Figures 3-10 through 3-15 and the summed squared otolith and semicircular canal errors are listed in Table 3-4. Note that the same pilot inputs (Figures 3-16) are used for each washout case. It is interesting that

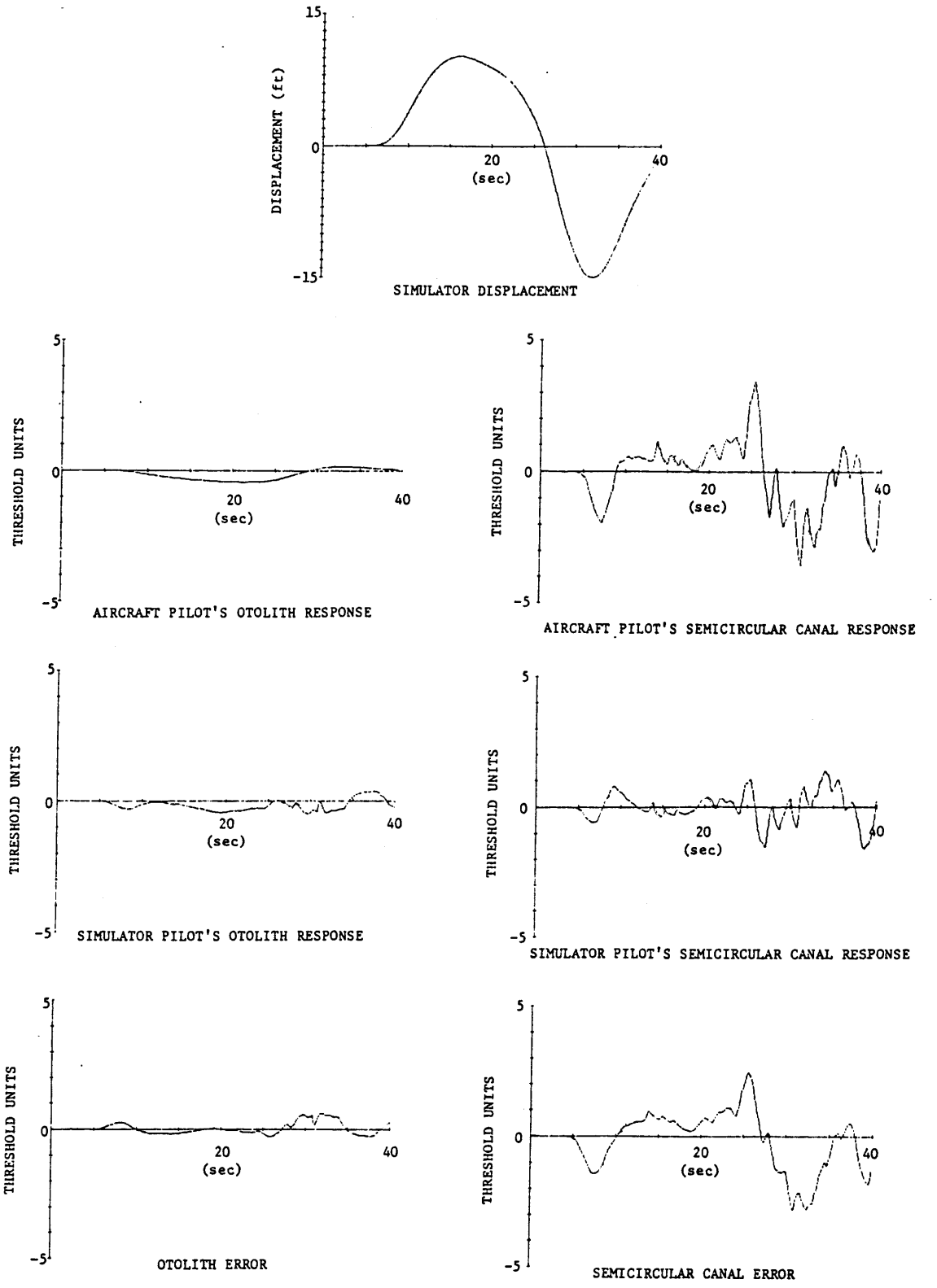

Figure 3-10. Time Response of the Ames Nominal Washout

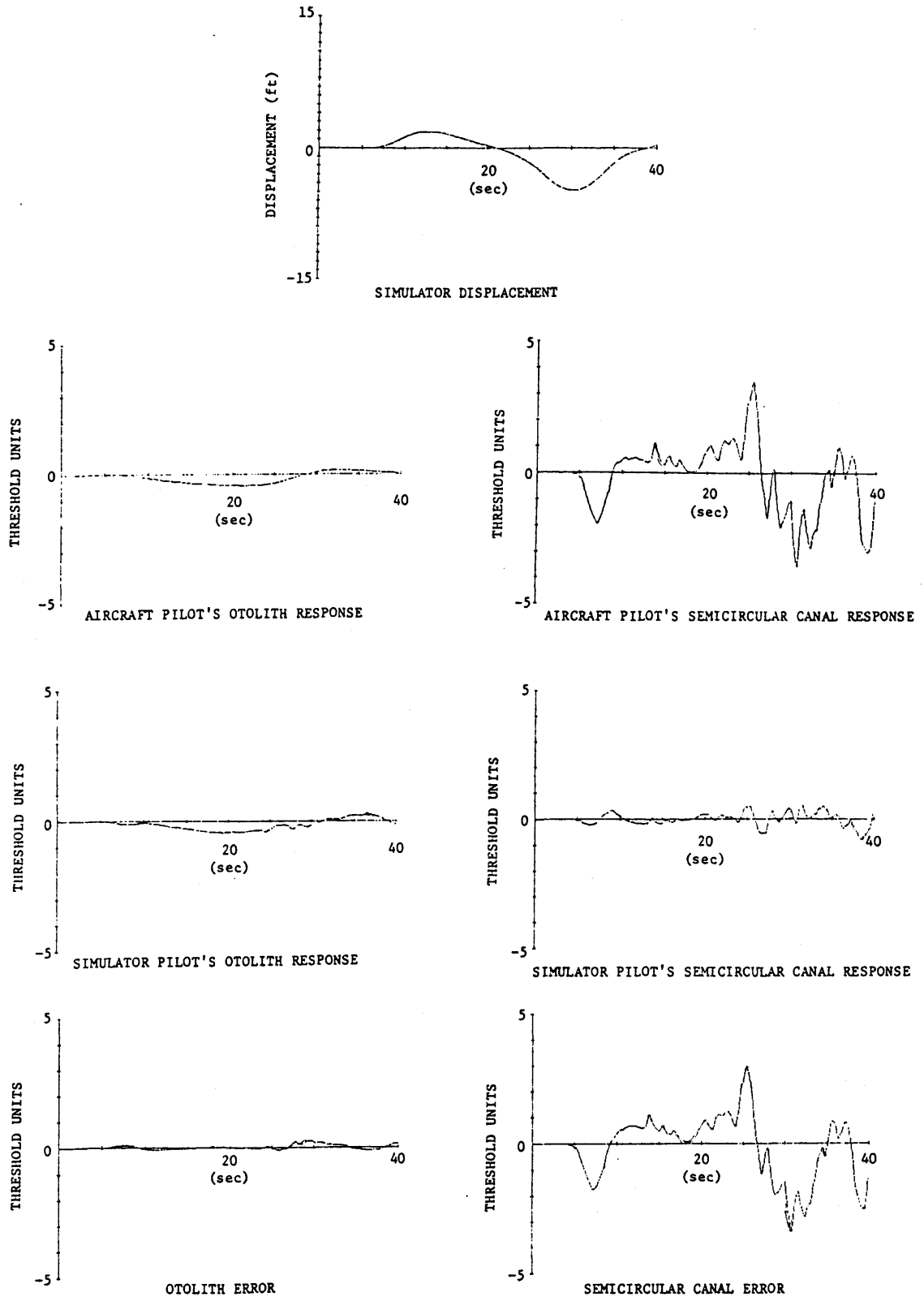

Figure 3-11. Time Response of the Ames Decreased Gain Washout

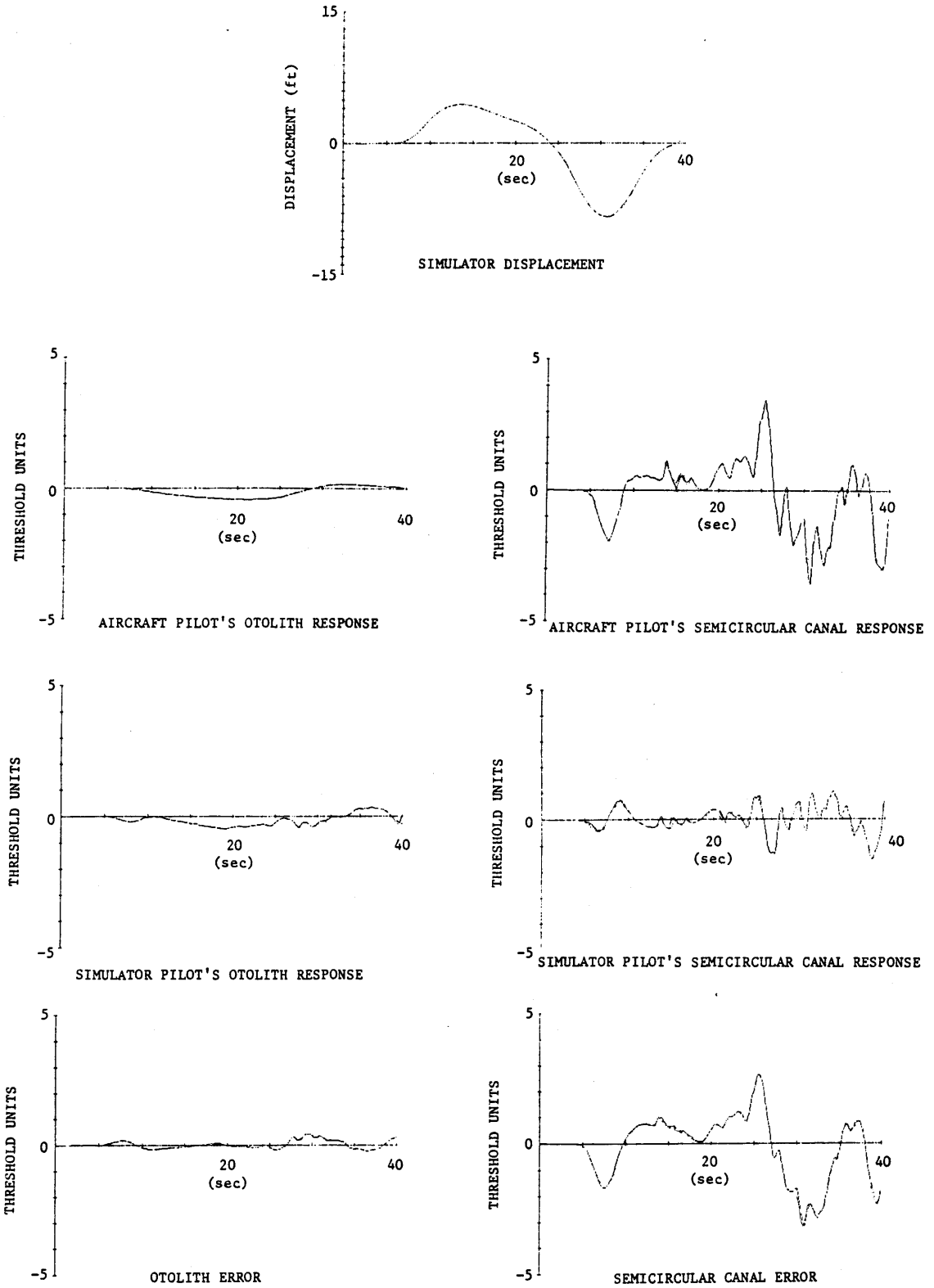

Figure 3-12. Time Response of the Ames Increased Omega Washout

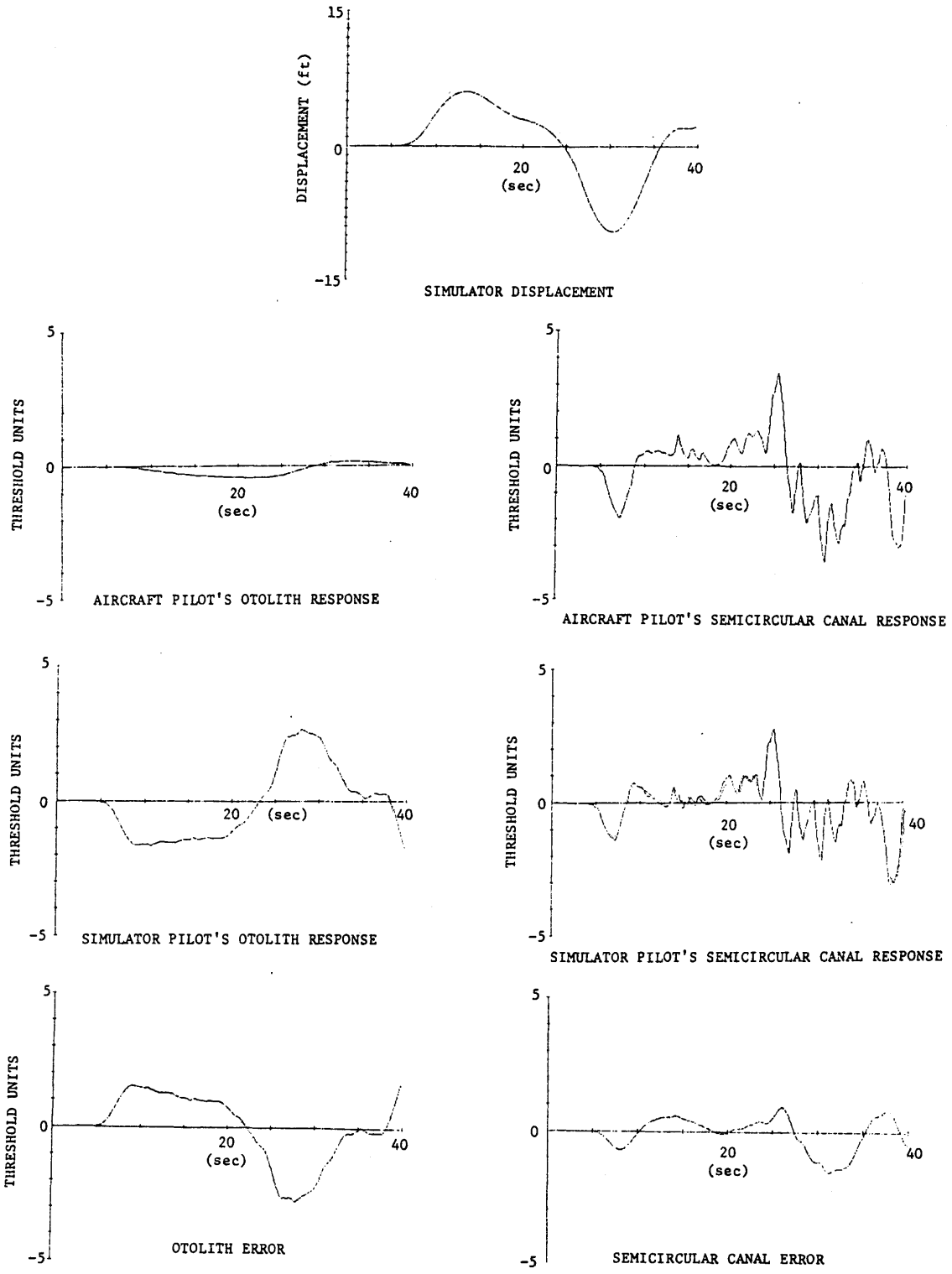

Figure 3-13. Time Response of the OWS Nominal Washout

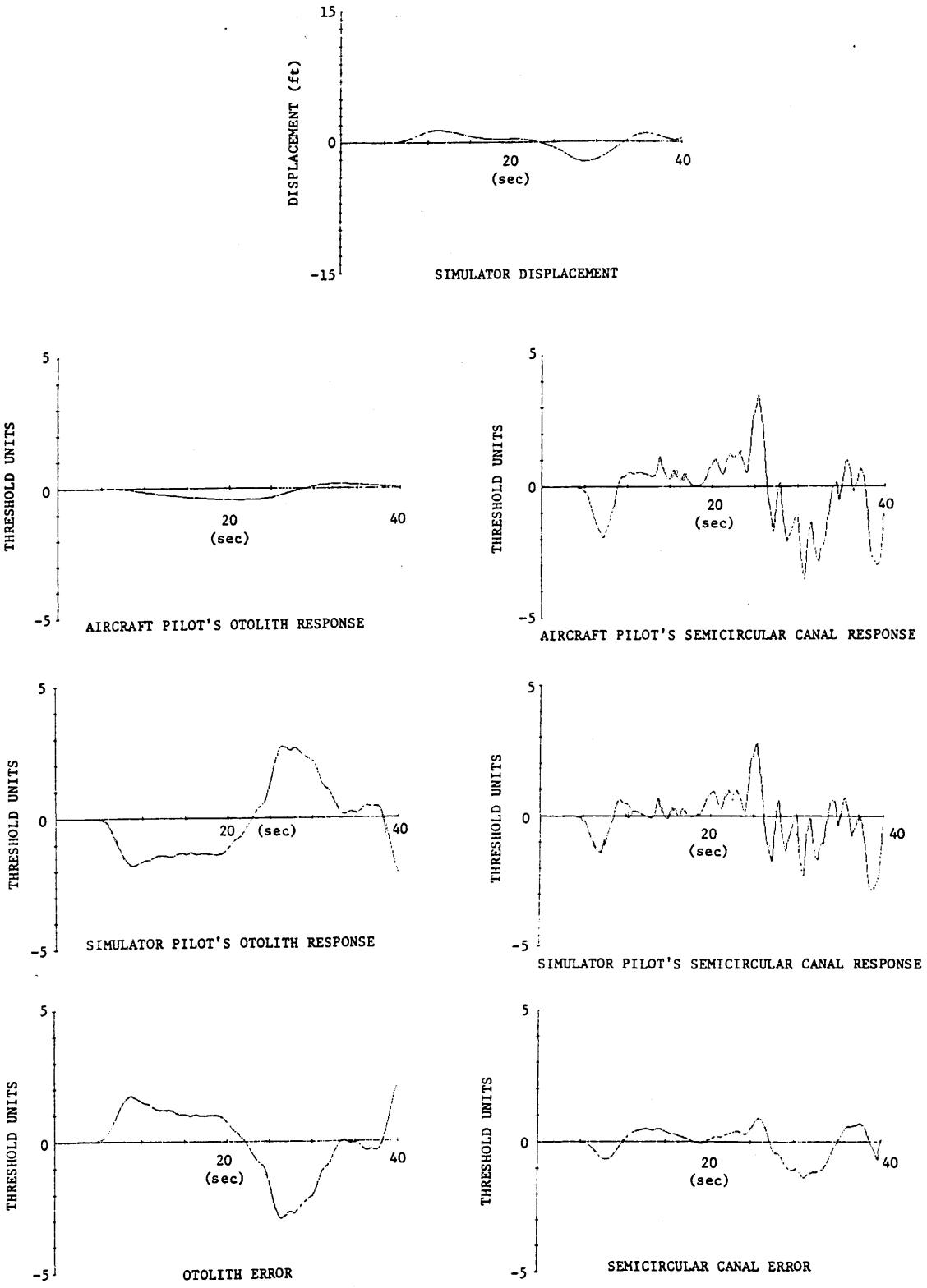

Figure 3-14. Time Response of the OWS Decreased Gain Washout

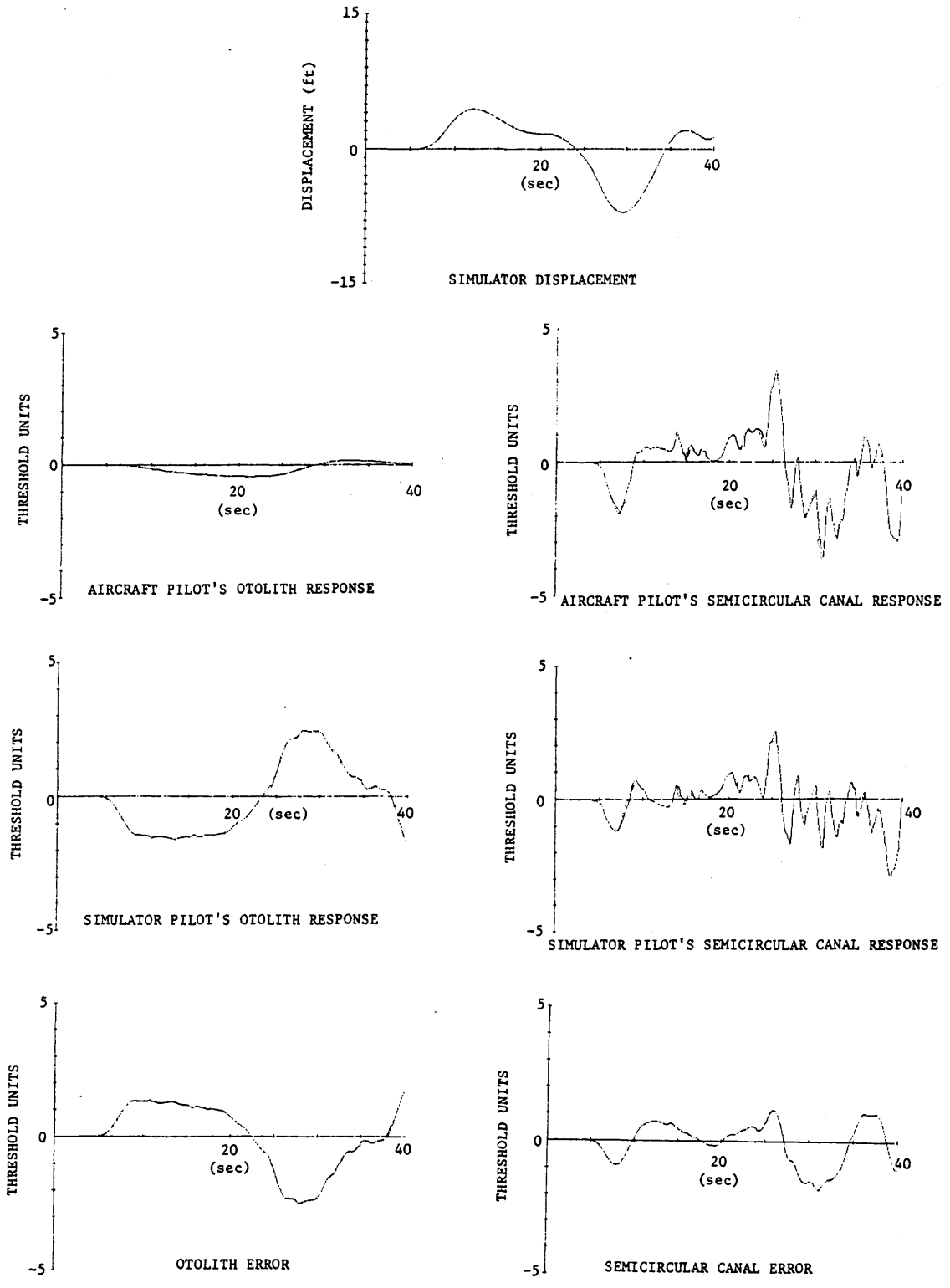

Figure 3-15. Time Response of the OWS High Otolith Weighting Washout

Table 3-4

SUMMED SQUARED VESTIBULAR ERRORS USING ACTUAL STICK COMMANDS

WASHOUT	OTOLITH ERROR	SEMICIRCULAR CANAL ERROR
AMES NOMINAL	56.6	1423
AMES DECREASED GAIN	7.9	1728
AMES INCREASED OMEGA	25.5	1702
OWS NOMINAL	1728	411.6
OWS DECREASED GAIN	1777	331.9
OWS HIGH OTOLITH WEIGHTING	1607	625.0

Table 3-5

SUMMED SQUARED VESTIBULAR ERRORS USING SQUARE WAVE STICK COMMANDS

WASHOUT	OTOLITH ERROR	SEMICIRCULAR CANAL ERROR
AMES NOMINAL	179	3241
AMES DECREASED GAIN	14.4	3678
AMES INCREASED OMEGA	58.2	3969
OWS NOMINAL	1570	1288
OWS DECREASED GAIN	1749	966
OWS HIGH OTOLITH WEIGHTING	1256	1876

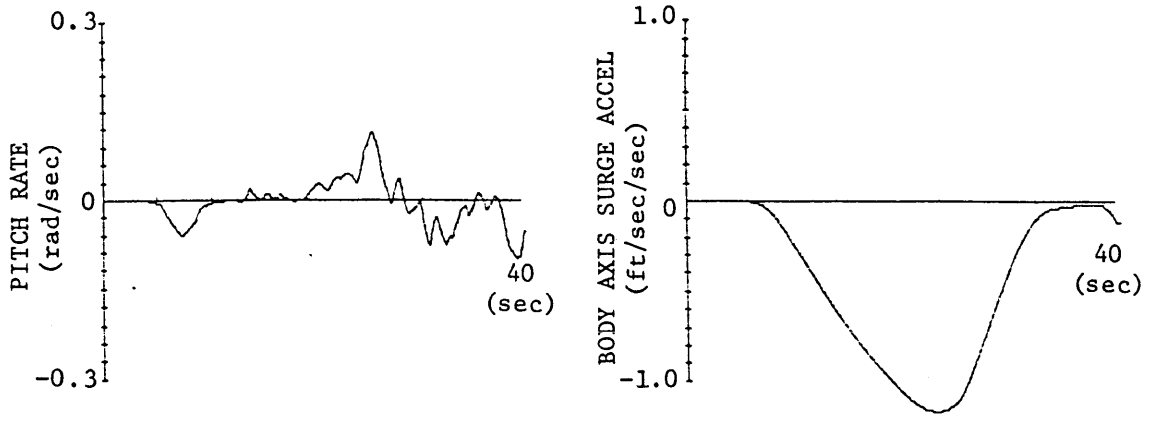

Figure 3-16. Actual Pilot Inputs

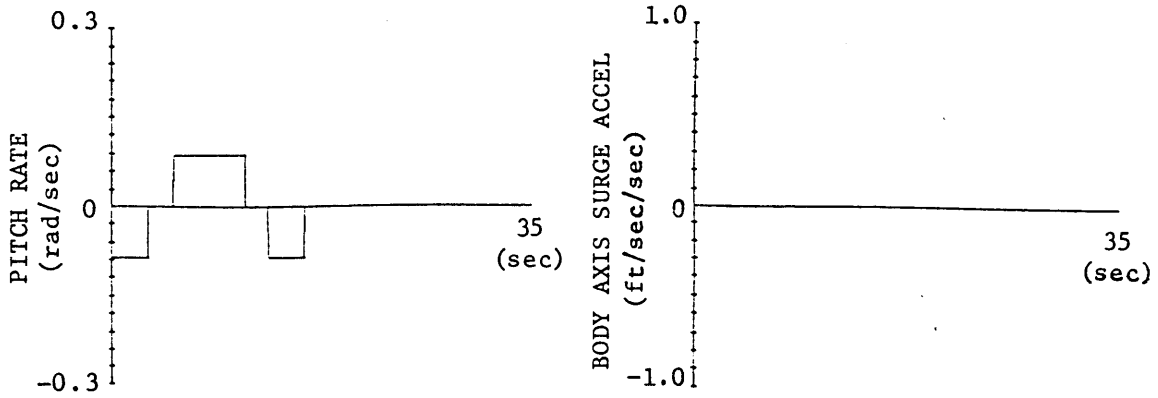

Figure 3-17. Simulated Pilot Inputs

with the OWS Nominal and Decreased Gain washouts, the otolith errors are greater than the semicircular canal errors even though theoretically the washouts should allow equal levels of error from each vestibular organ. Furthermore, the OWS High Otolith Weighting washout should allow greater semicircular canal error in order to reduce otolith error. Now if square waves are used for pilot inputs (Figure 3-17), the controller does the correct error balancing, as illustrated in Figure 3-18 and Table 3-5. For the purposes of comparison, the result of applying the same inputs to the Ames Nominal washout is shown in Figure 3-19. Actually in Table 3-5, the otolith errors are still slightly higher than semicircular canal errors, but this is because the otolith error is coupled to the simulator displacement cost term. To reduce otolith error the system would command large simulator excursions, but the displacement term reduces these commands thereby inducing some additional otolith error.

The reason excessive otolith error results when the actual pilot commands are used instead of square wave inputs can be explained by an analysis of the characteristics of the inputs. During the actual dash-quick stop maneuver, the pilot commands pitch down during seconds five through ten of the run; however, the pitch up command is not given until the twenty second point. As a result of this delay, the pilot inputs initially appear to have a DC component in pitch rate. This DC component is attenuated by the high-pass filters in block A_{12} of the OWS washouts; therefore, no DC linear acceleration is commanded to the motion base. However, the DC pitch rate component passes through the A_{22} block with no attenuation, thus commanding the simulator to pitch

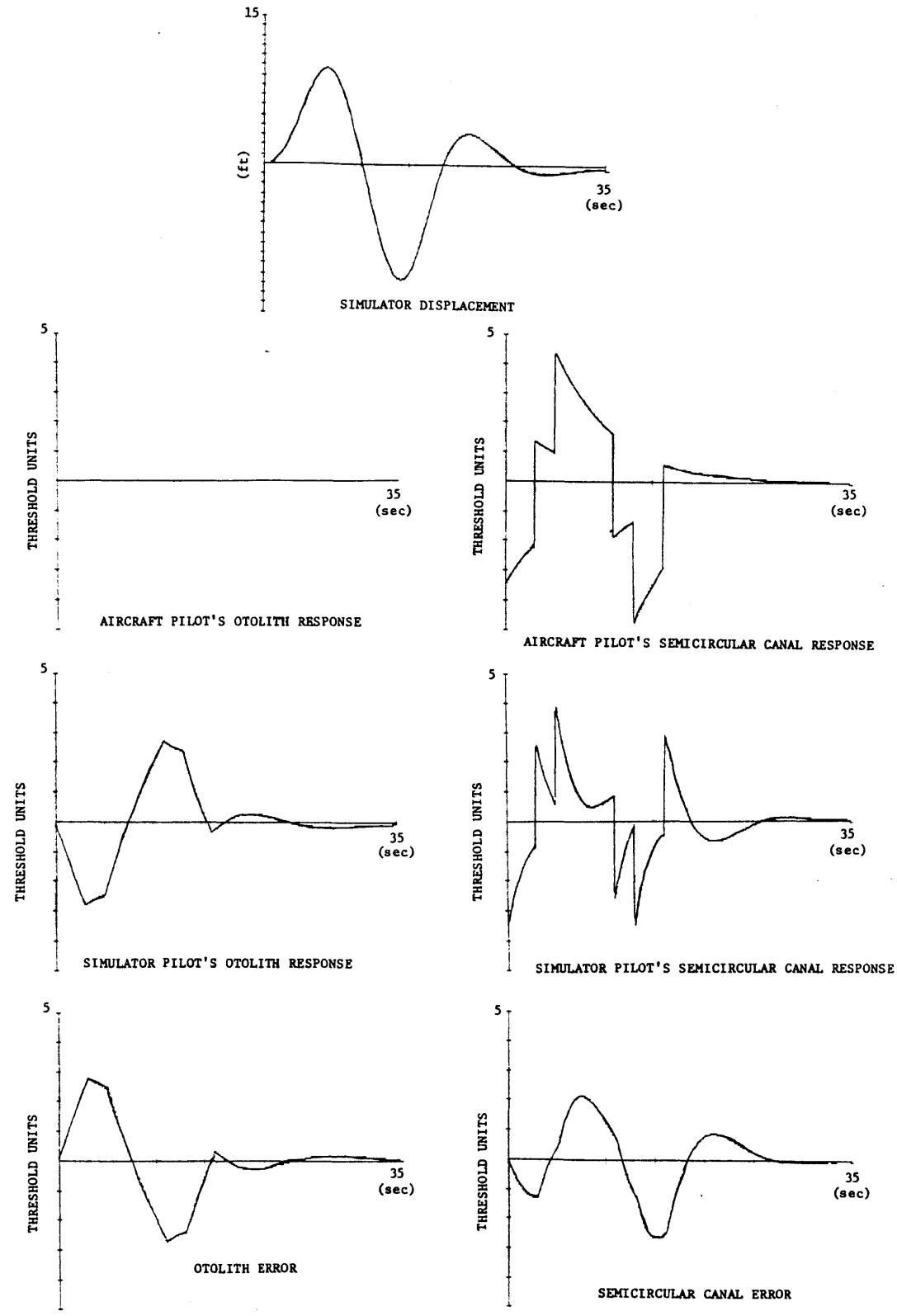

Figure 3-18. Time Response of OWS Nominal Washout

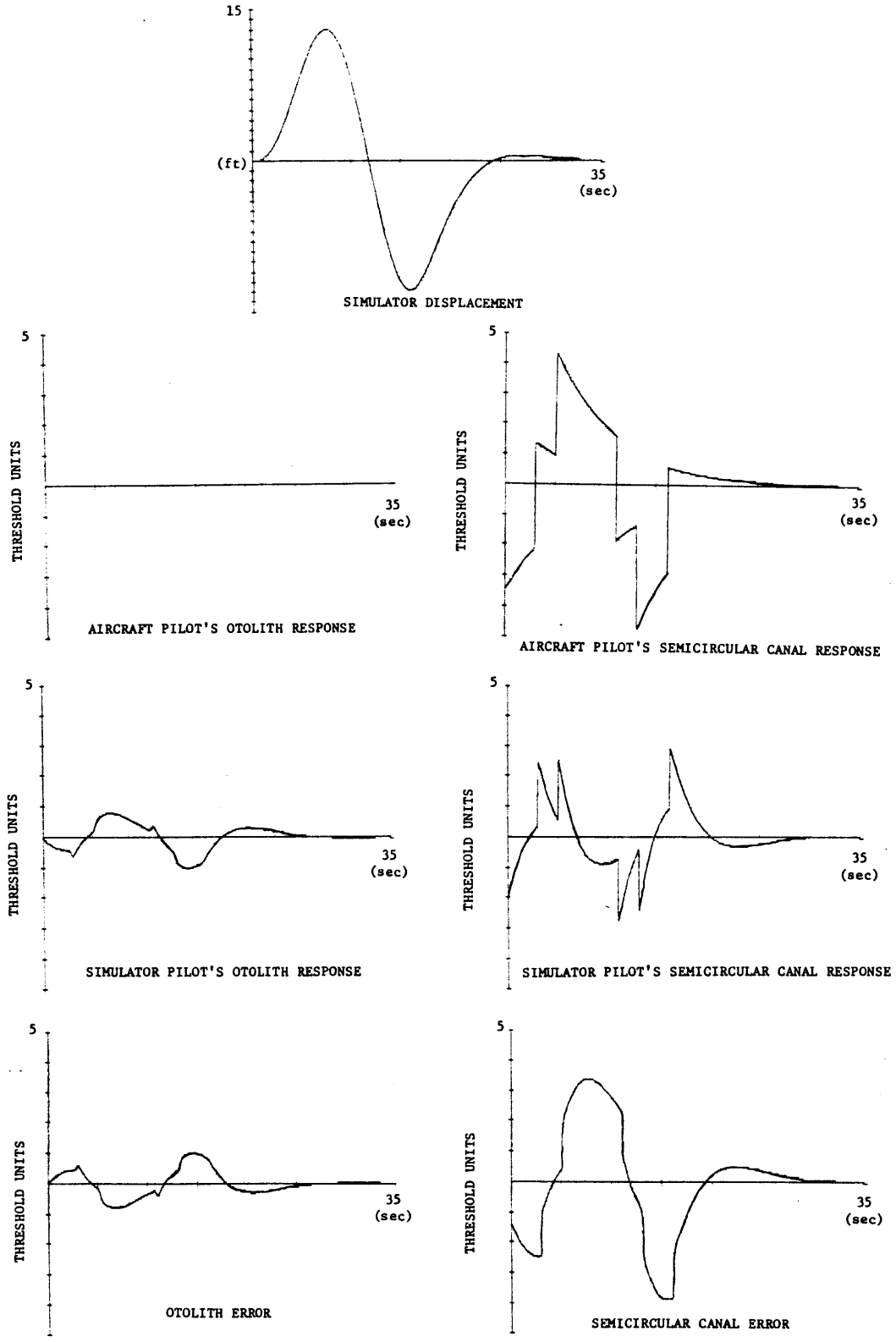

Figure 3-19. Time Response of the Ames Nominal Washout

down. This pitch angle is not properly coordinated by the washout since no linear acceleration is commanded; therefore, large otolith errors result. This effect is not evident with the square wave pilot inputs since the length of time between between pitch up and pitch down is very short; consequently, no large DC components are observed by the filters for any significant length of time.

3.2 Vehicle Dynamics

The vehicle dynamics used in this experiment are representative of a vectored thrust hovering aircraft, whose pitch stick input (del_e) to surge displacement transfer function is:

$$del_e \longrightarrow \boxed{\frac{-48.24}{(s)(s)(s+0.02)(s+2.0)(0.01s+1)}} \longrightarrow \text{surge accel}$$

A bode plot of this transfer function is shown in Figure 3-20.

3.3 Test Procedure

The evaluation of washouts was performed over a period of four days, during which four NASA helicopter test pilots served as subjects, three of whom had prior experience on the VMS. For each pilot, two test sessions were performed, each lasting approximately sixty minutes. Four motion cases (one fixed base and three motion washouts) were tested during each session; the order of presentation is listed in Table 3-6. Note that for each pilot, the three 'high fidelity' motion cases were compared in one session while the three 'low fidelity' cases were compared in the other session. A copy of the experimental procedure used to brief the pilots is listed in the Appendix.

To evaluate each particular washout, four trials of a tracking task

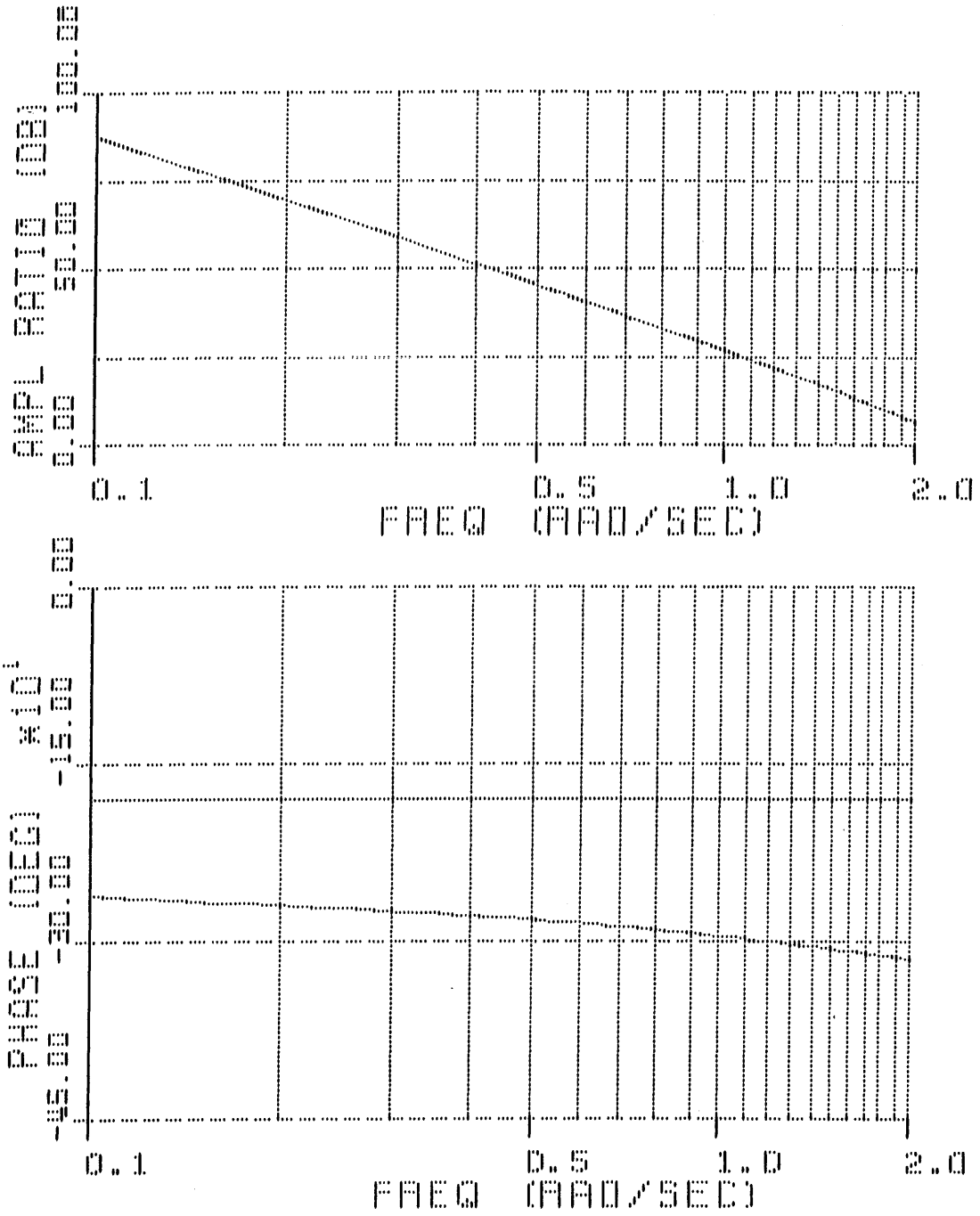

Figure 3-20. Bode Plot of Aircraft Dynamics

Table 3-6

PRESENTATION ORDER OF WASHOUTS

PILOT #1

SESSION #1

1. AMES DECREASED GAIN
2. OWS DECREASED GAIN
3. AMES INCREASED OMEGA

SESSION #2

1. AMES NOMINAL
2. OWS NOMINAL
3. OWS HIGH OTOLITH WEIGHTING

PILOT #2

SESSION #1

1. AMES INCREASED OMEGA
2. OWS DECREASED GAIN
3. AMES DECREASED GAIN

SESSION #2

1. OWS HIGH OTOLITH WEIGHTING
2. OWS NOMINAL
3. AMES NOMINAL

PILOT #3

SESSION #1

1. OWS HIGH OTOLITH WEIGHTING
2. OWS NOMINAL
3. AMES NOMINAL

SESSION #2

1. AMES INCREASED OMEGA
2. OWS DECREASED GAIN
3. AMES DECREASED GAIN

PILOT #4

SESSION #1

1. AMES NOMINAL
2. OWS NOMINAL
3. OWS HIGH OTOLITH WEIGHTING

SESSION #2

1. AMES DECREASED GAIN
2. OWS DECREASED GAIN
3. AMES INCREASED OMEGA

were performed, each trial lasting 75 seconds. The hovering vehicle was initially placed 108 ft behind, 28 ft to the right of, and 2 ft below the target vehicle, a "hovering" F-111. This aircraft was used since it was readily available in the data base of the computer generated imagery. Both the F-111 and the piloted hovercraft were placed at an initial altitude of 80 ft, thereby providing the pilot with good visual cues from the surrounding canyon scenery (see Figure 3-21). The pilot was told to remain this set distance behind the F-111 as the F-111's pitch angle was modulated by a five component sum of sines disturbance (Table 3-7). To reduce the possibility that the pilot could learn to predict the disturbance, a different combination of sines was used for each of the four tracking trials. The magnitude of each of the

Table 3-7. Magnitudes of Disturbance Components

	MAGNITUDE			
FREQUENCY	CASE #1	CASE #2	CASE #3	CASE #4
0.257 rad/sec	-1.0	1.0	-1.0	1.0
0.513	1.0	-1.0	1.0	-1.0
0.770	-1.0	1.0	-1.0	1.0
1.15	1.0	-1.0	-1.0	1.0
1.54	-1.0	1.0	1.0	-1.0

GAIN ON SUM OF COMPONENT FREQUENCIES = 0.06

component sine waves remained the same, but the phase was sometimes shifted 180 degrees, as shown in Table 3-7. As the F-111 pitched, the magnitude of its lift vector was adjusted such that the vertical component of lift always exactly countered the force due to gravity; therefore, the F-111 remained at a constant altitude. The horizontal

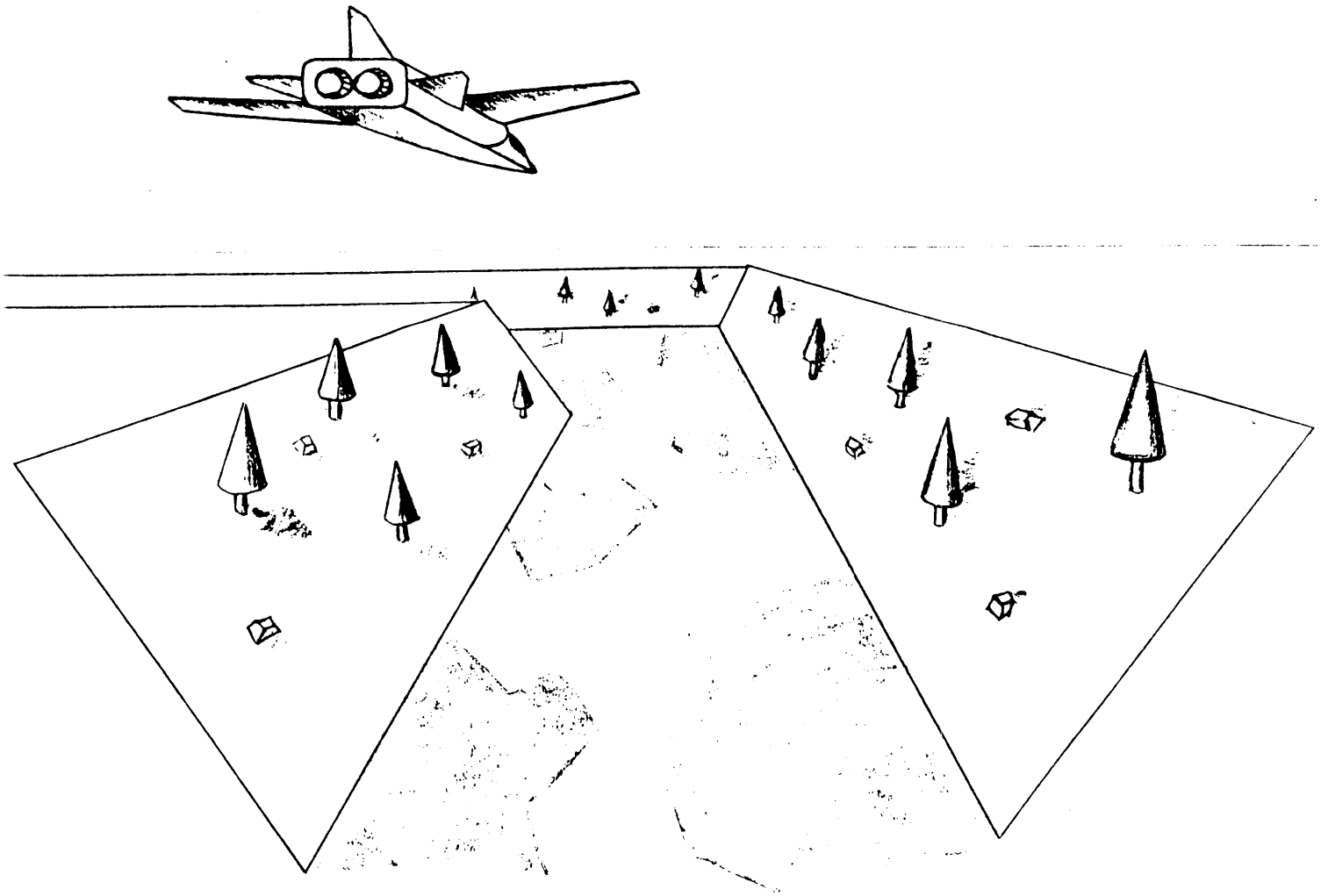

Figure 3-21. Visual Scene During the Tracking Task

component of the lift vector caused the F-111 to be randomly accelerated along the inertial surge axis. To facilitate off-line data analysis, the relative positions of the F-111 and the hovering vehicle were recorded along with the pilot stick inputs.

To further evaluate the washout characteristics, the hovering vehicle was placed in the center of the canyon at an altitude of 30 ft. The pilots would execute a dash-quick stop maneuver by pitching nose down approximately 10 deg, accelerating down the canyon, and pitching nose up to come to a stop over a road positioned approximately 1000 ft downrange. This maneuver was typically performed three times.

Finally, the pilots would perform a sinusoidal fore-aft pitching maneuver with a maximum pitch angle amplitude of 5 to 10 degrees at frequencies of 1,2 and 4 cycles/sec.

To quantify the pilots' opinions of the washouts, they first rated the handling qualities of the aircraft's pitch-surge axis using the Cooper-Harper rating scale (Figure 3-22). This is a standard scale with which all the test pilots have had extensive experience. Although the scale does not directly apply to the evaluation of simulator motion systems, it is useful for this purpose since any motion cues provided to the pilot yield lead information as to the future state of his aircraft. Consequently, any motion cues provided by the motion base of the simulator improve the pilot's ability to control the aircraft, thereby improving the handling quality rating.

The pilots were than asked to directly evaluate the simulator

HANDLING QUALITIES RATING SCALE

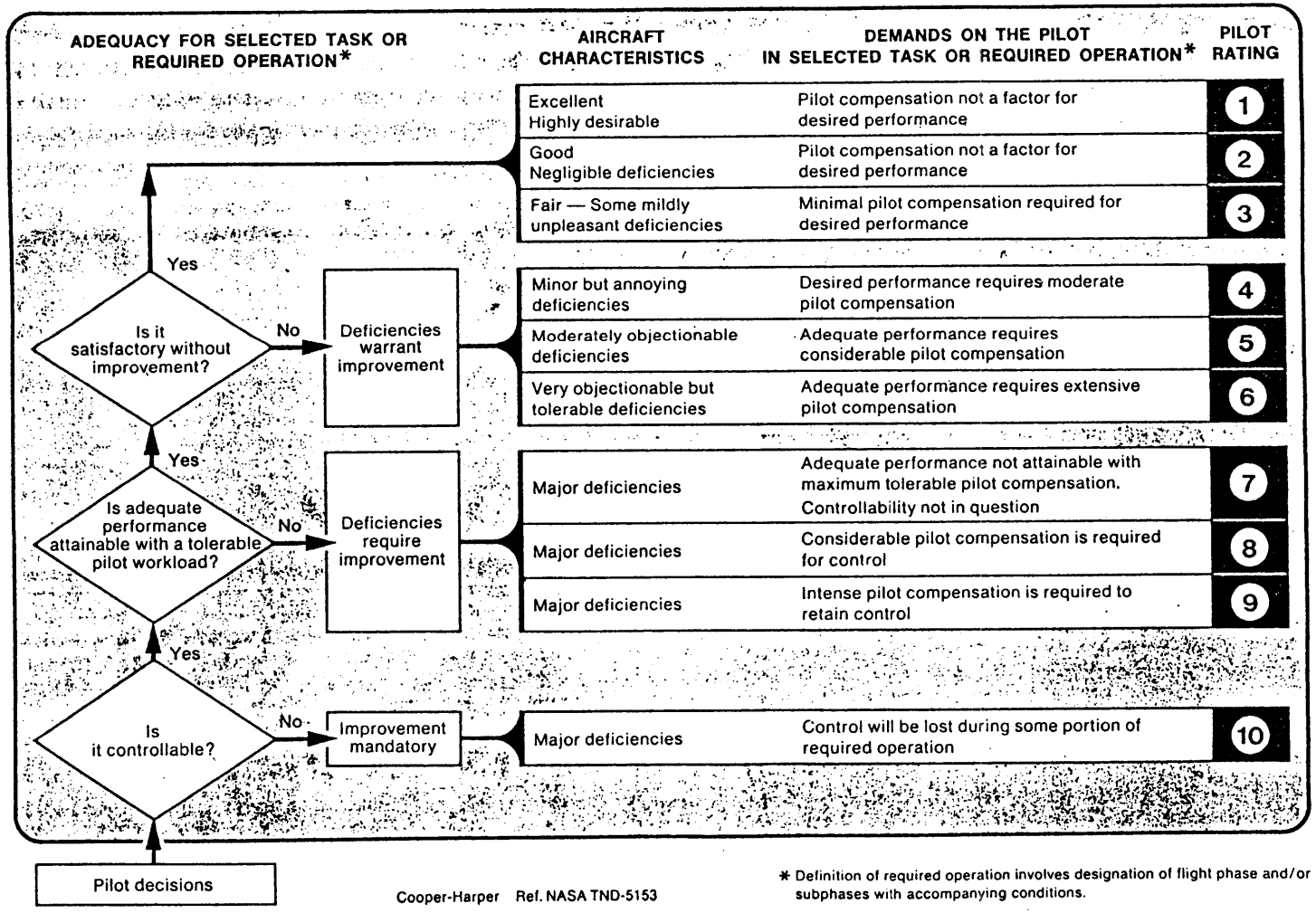

Figure 3-22. Cooper-Harper Handling Qualities Rating Scale

motion cues using a scale (Figure 3-23) developed by Steven Bussolari and John Stewart. Note that the motion categories include smoothness, sense, amplitude, phase lag, discomfort, disorientation, and overall feel. Also note that each scale contains specific anchor points in an attempt to standardize the ratings between pilots.

The results of the pilots' tracking task performance are presented in the following chapter along with a summary of their handling quality and motion evaluation ratings.

MOTION RATING SCALES

The motion of the simulator will be rated on the following seven scales:

Attribute	Rating 1	5
SMOOTHNESS:	extremely smooth-comparable with fixed base	extremely jerky limit of tolerance
SENSE:	definitely correct as in aircraft	totally reversed
AMPLITUDE:	no motion experienced	at least twice that expected
PHASE LAG:	none experienced	at least 180°
DISCOMFORT:	none experienced	cannot continue maneuver
DISORIENTATION:	none experienced	cannot perform maneuver
OVERALL:	excellent	extremely poor

Pilots will be asked to rate the motion during the Forward Step and Pitching Maneuvers. If they desire, they may fly the vehicle in the canyon to elucidate any particular attribute of the motion. Their comments will be recorded.

Note: To avoid encounters with the software limits during motion evaluation, pilots will be requested to keep pitch angle excursions within positive or negative 10 degrees.

Figure 3-23. Motion Rating Scale

4. Results and Discussion

4.0 Introduction

By analyzing the data from the experiments on the VMS, an attempt has been made to determine a valid measure of flight simulator motion fidelity and to assess the performance of the Optimal Washout System in comparison to a standard crossfeed washout system. Fidelity measures investigated include displacement tracking performance, velocity tracking performance, describing functions of the pilot model, handling quality ratings (HQR), and motion scale ratings.

4.1 Discussion of Tracking Task

In the tracking task, the pilots were instructed to remain a fixed distance from the lead aircraft as the lead aircraft was perturbed by a sum-of-sines disturbance. This distance was selected to be 108 ft, at which the pilots were positioned at the beginning of each run. Due to difficulties in controlling the high order dynamics of the hovercraft and in judging the distance to and detecting the motion of the F-111, the pilots could not perfectly track the lead aircraft. In general, the pilots tended to track with a position bias from the desired 108 ft set point with a variance about the biased point. The variance of the hovercraft's position from the bias point is defined as the Displacement Error Score (DES). The position bias and DES are calculated as follows:

$$\text{BIAS} = \sum_{i=1}^{N} \frac{\text{DISPLACEMENT ERROR}_i - 108'}{N}$$

$$DES = \sum_{i=1}^{N} \frac{(\text{DISPLACEMENT ERROR}_i - \text{MEAN DISPLACEMENT ERROR})^2}{N-1}$$

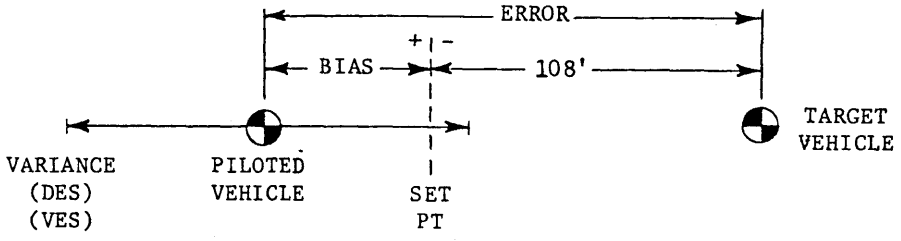

Because it may be easier for the pilots to detect a velocity error between the F-111 and their aircraft than it is to detect an absolute difference in distance, the Velocity Error Scores (VES) have also been analyzed. The VES's are the variance of the error between the velocities of the F-111 and the hovercraft. They are calculated using the following equation:

$$VES = \sum_{i=1}^{N} \frac{(\text{VELOCITY ERROR}_i - \text{MEAN VELOCITY ERROR})^2}{N-1}$$

It is presumed that, the pilot uses some combination of velocity error and displacement error feedback to perform the tracking task. However, due to the difficulty in simulataneously analyzing both displacement error and velocity error in terms of a multi-variable system [McRuer and Krendel 74], the analysis presented has been performed on the displacement and velocity data separately.

A list of the biases and variances for each trial is given in

Appendix C. Some data editing has been performed to remove any anomalous effects; for example, during some runs, the disturbance quickly switches from a large negative peak to a large positive peak. If the pilot is not fully alert, he has difficulty in properly tracking the lead aircraft and a large displacement error will result. Because this effect is evident in only two of 128 runs, it is not indicative of the overall performance; therefore, these segments have been edited out from the raw data. There are also sections near the end of some runs where the error increases greatly. These sections have also been editted since the pilot, due to fatigue, has probably lost total concentration and is not fully aware of the distance to the lead aircraft. This effect was evident in only four of the 128 runs.

4.2 Presentation of Tracking Performance Data

To illustrate the functional relationships between the various motion evaluation parameters, the following Figures are presented. The DES's for each pilot are shown in Figures 4-1 through 4-4 in which the second session fixed base run is plotted first to serve as a reference point, followed by the three Ames washouts, and finally the three OWS washouts. To demonstrate any learning effects present in the experiments, the performances during each washout have then been plotted in order of presentation (Figure 4-5 through 4-8). The horizontal lines at the top of each graph indicate that the performance during one washout (at the left end of the line) is significantly different from the performance during another washout (on the right end of the line). To better illustrate learning, each trial is plotted in order of presentation in Figures 4-9 through 4-12. Trials 1 through 4 and 17

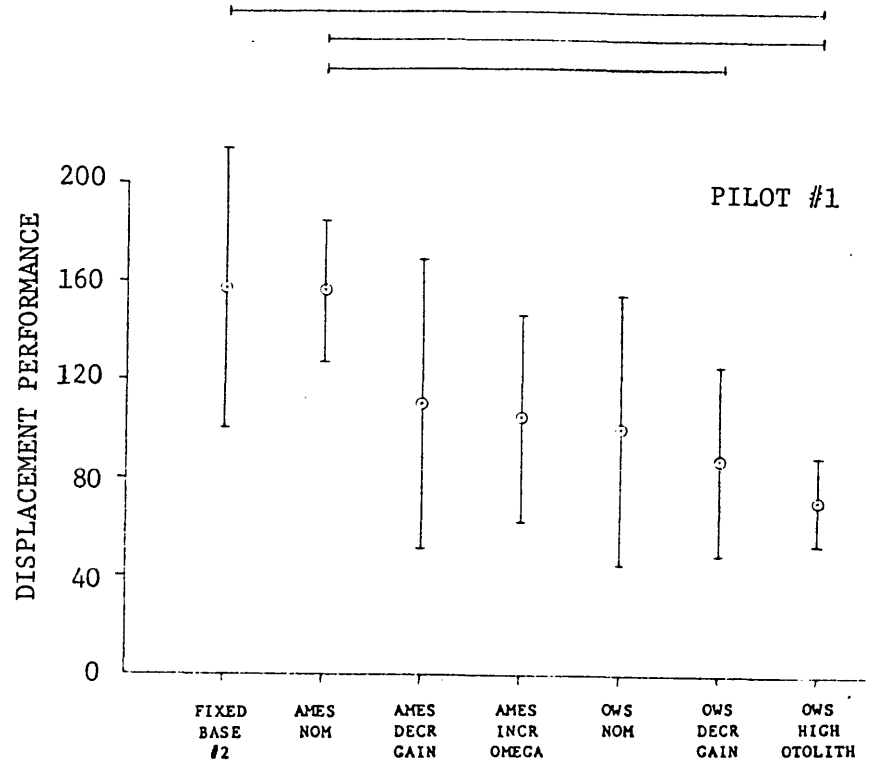

Figure 4-1. Displacement Performance vs Washout

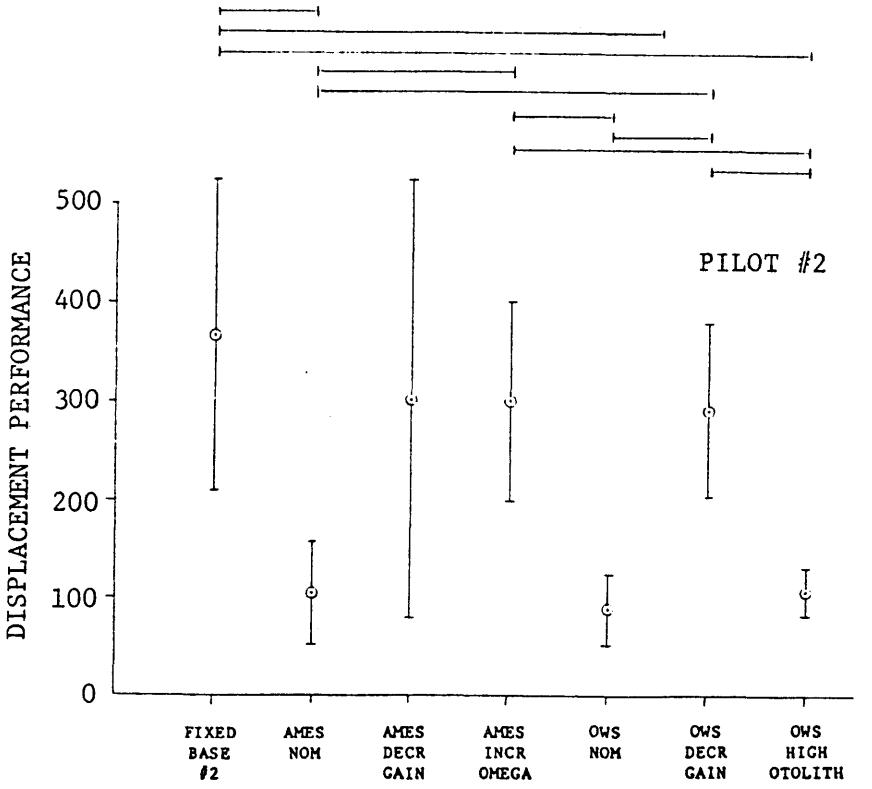

Figure 4-2. Displacement Performance vs Washout

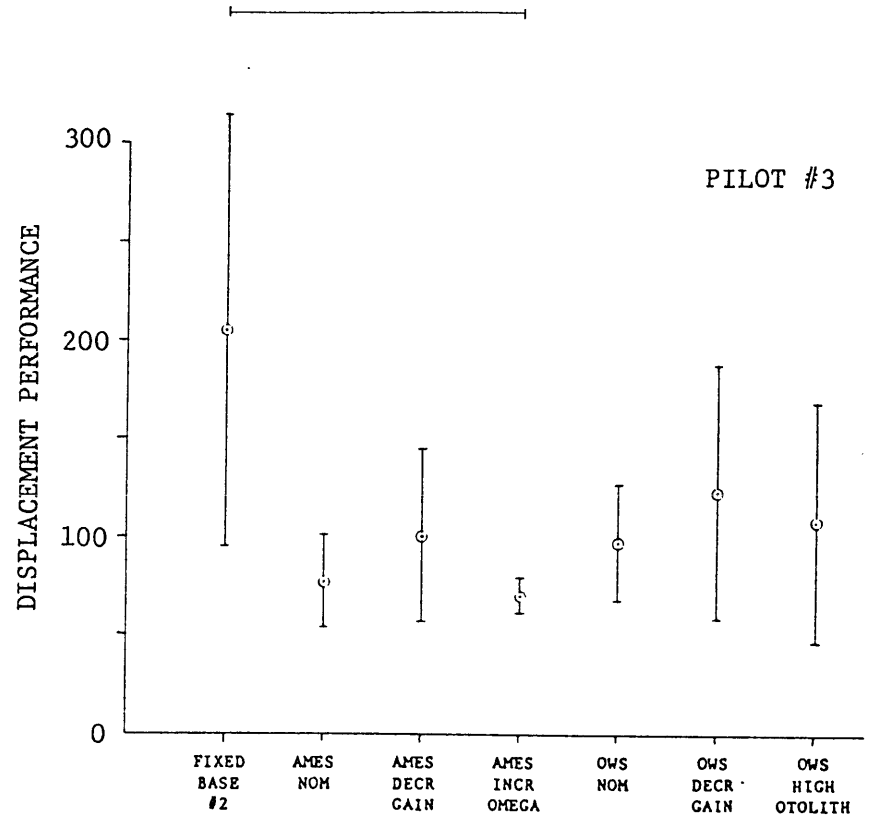

Figure 4-3. Displacement Performance vs Washout

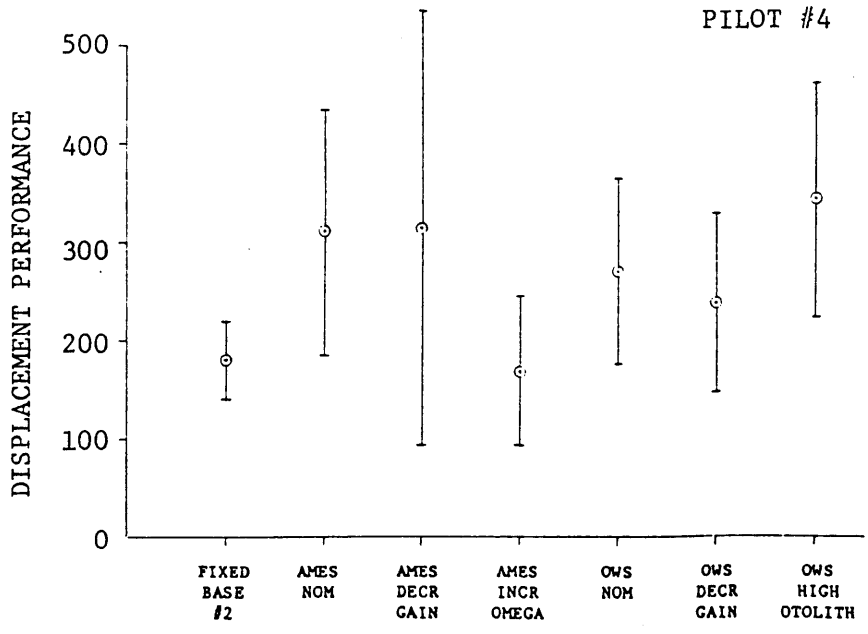

Figure 4-4. Displacement Performance vs Washout

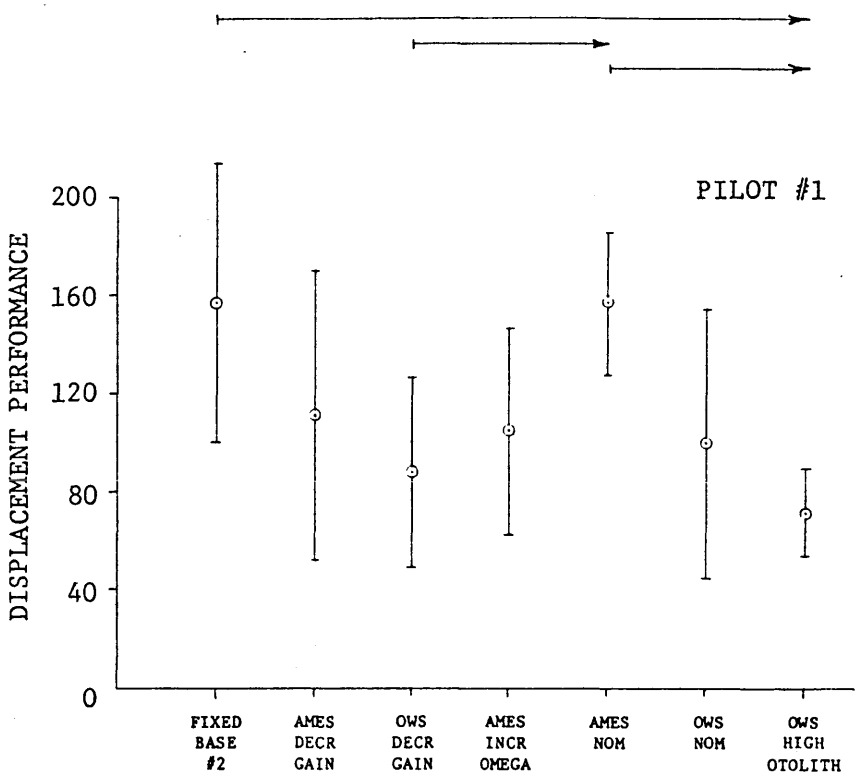

Figure 4-5. Displacement Performance vs Order

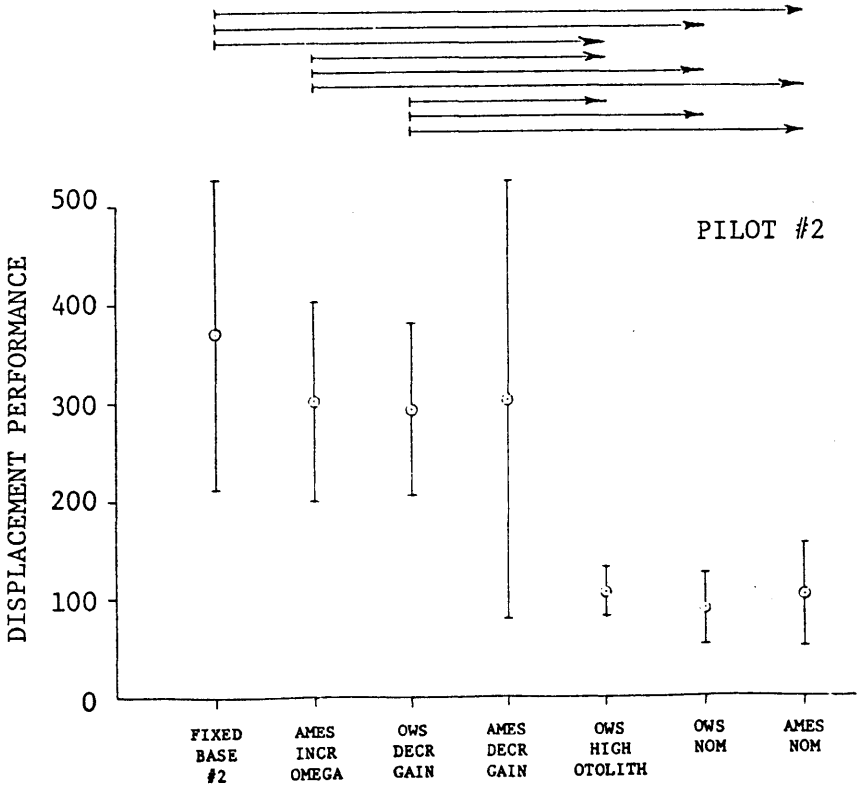

Figure 4-6. Displacement Performance vs Washout

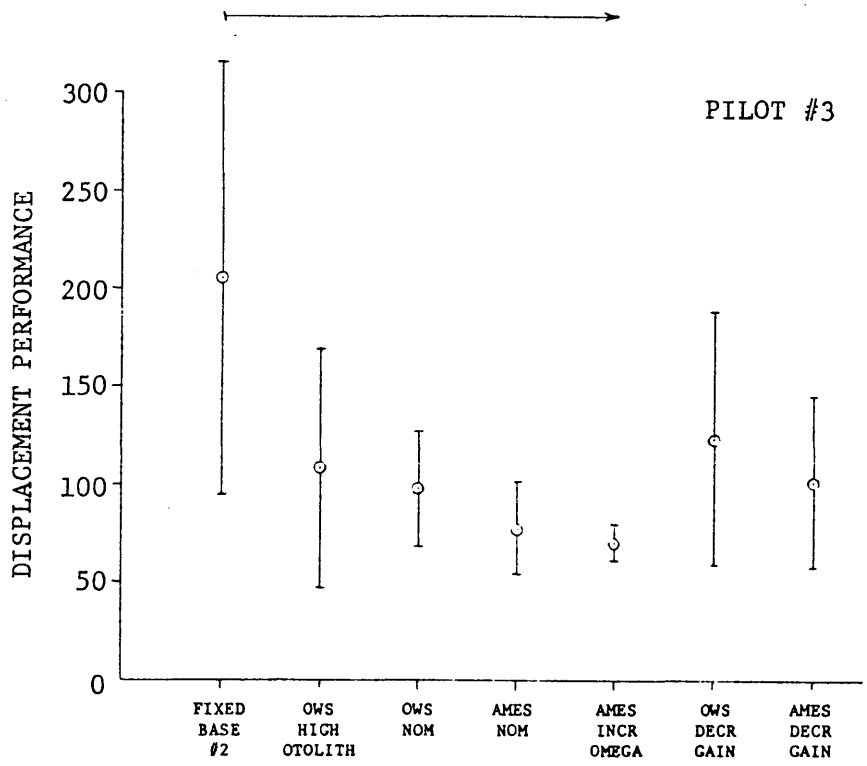

Figure 4-7. Displacement Performance vs Order

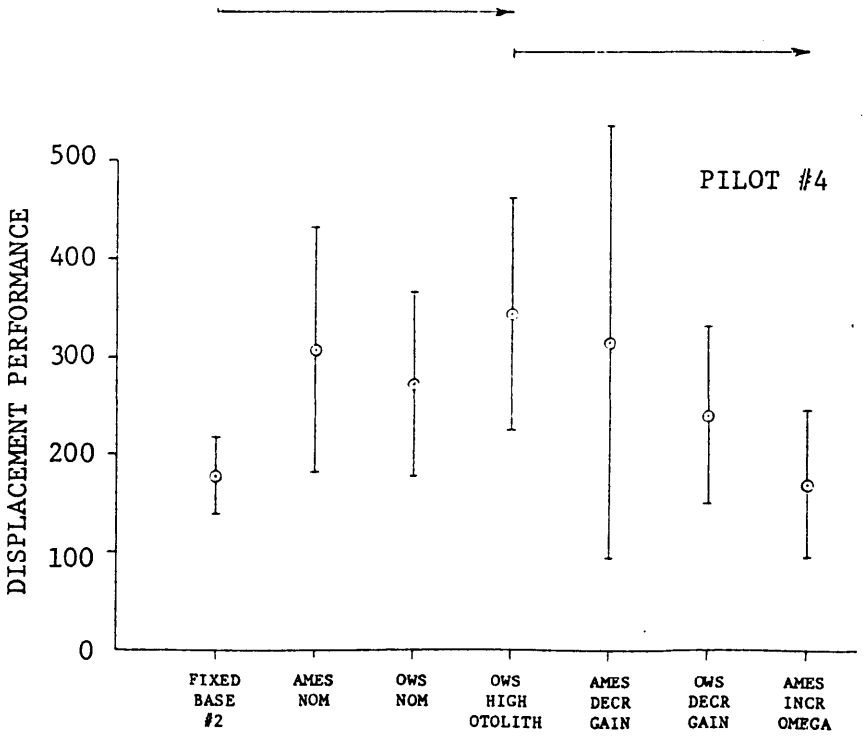

Figure 4-8. Displacement Performance vs Order

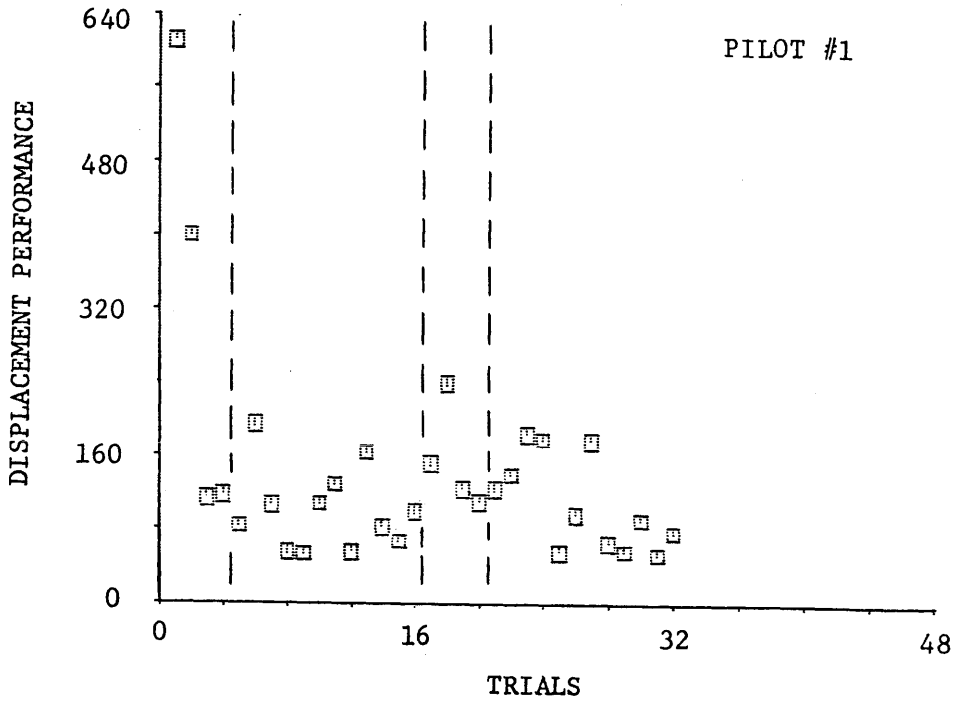

Figure 4-9. Displacement Performance vs Trial

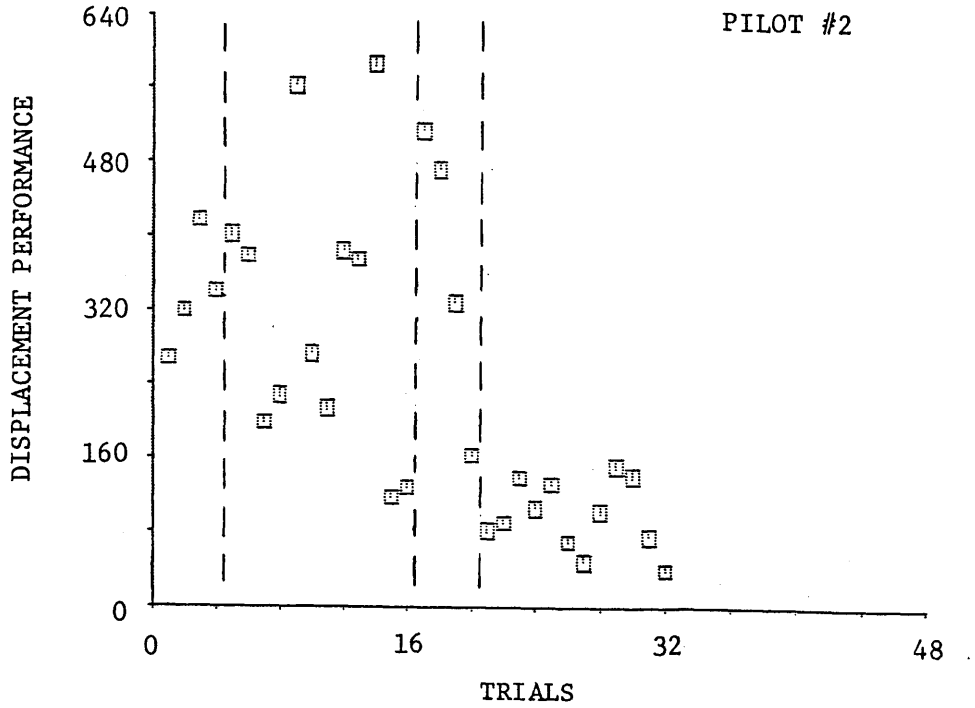

Figure 4-10. Displacement Performance vs Trial

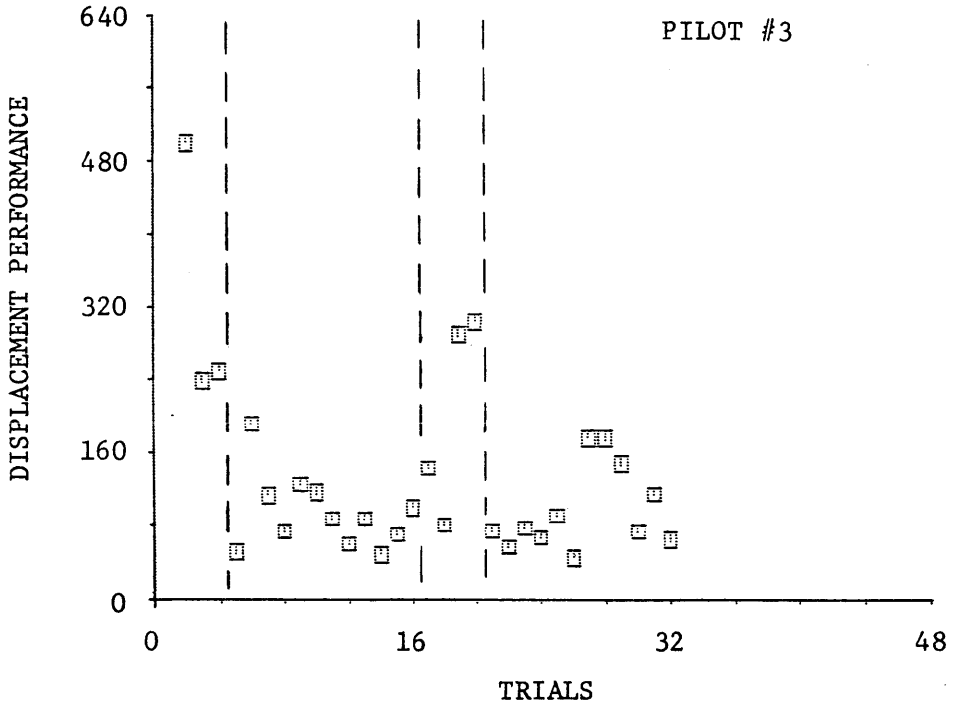

Figure 4-11. Displacement Performance vs Trial

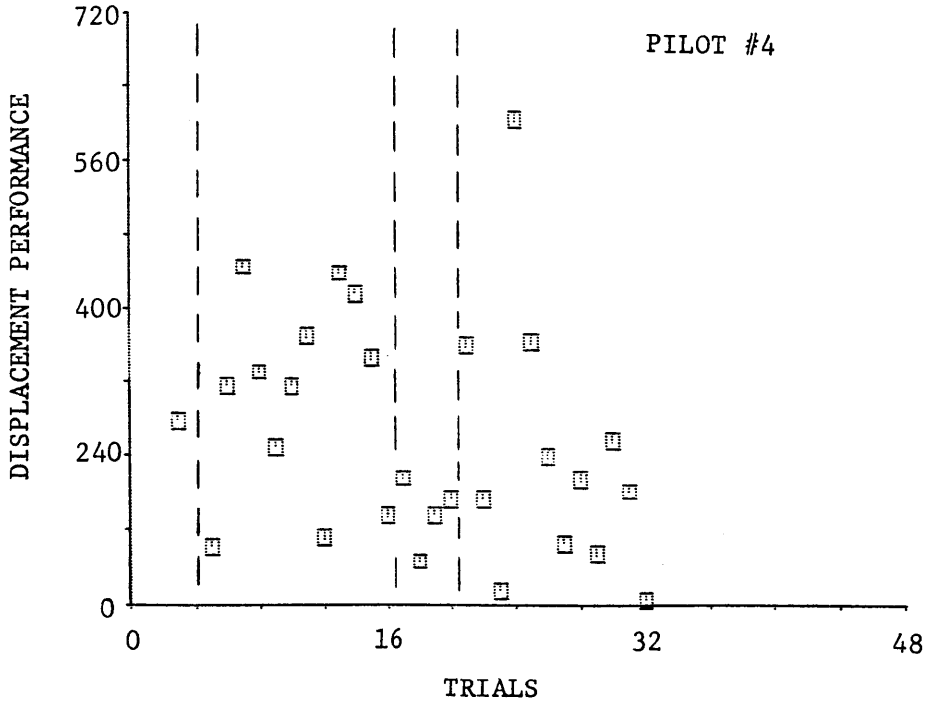

Figure 4-12. Displacement Performance vs Trial

through 20, bounded in the figures by dashed lines, are fixed base runs. Figures 4-13 through 4-16 illustrate the relationship between position bias and displacement performance. This relationship is expected since the rate of change of the angle subtended by the F-111 is greater if the pilot is closer to the lead aircraft; therefore, it is easier to detect and thereby track the motion of the F-111 if the pilot is closer to the F-111. Finally, to determine any relationship between handling quality ratings and performance, Figures 4-21 through 4-24 have been presented.

The same family of figures made for displacement have also been made for velocity tracking performance. The VES's have been plotted versus washouts in Figures 4-25 through 4-28, order effects are examined in Figures 4-29 through 4-36, position bias effects are illustrated in Figures 4-37 through 4-40, and the handling quality ratings are plotted versus performance in Figures 4-41 through 4-44.

The pilot comments for each of the washouts are presented in Appendix D.

4.3 Discussion of Tracking Performance Data

Due to the individual pilot characteristics, the data will be discussed for each pilot separately, from which generalizations shall be made for the entire population.

For Pilot #1, it is evident from Figure 4-1 that the variations of DES's between trials is typically greater than the difference in DES's between washouts; therefore, statistically there are no differences in performance between the three Ames washouts and two of the OWS washouts;

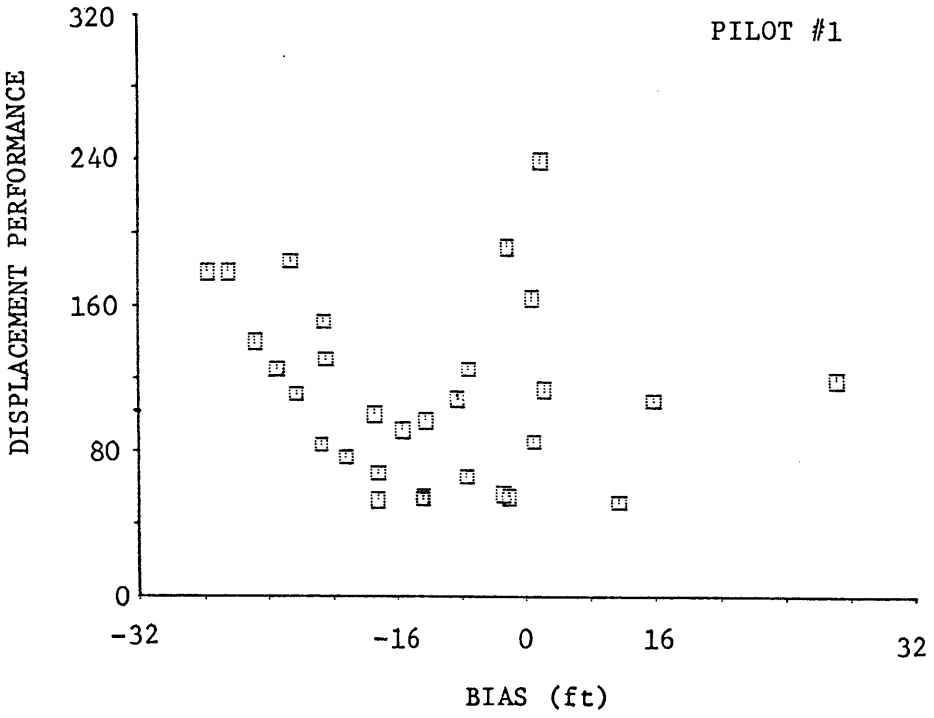

Figure 4-13. Displacement Performance vs Bias Position

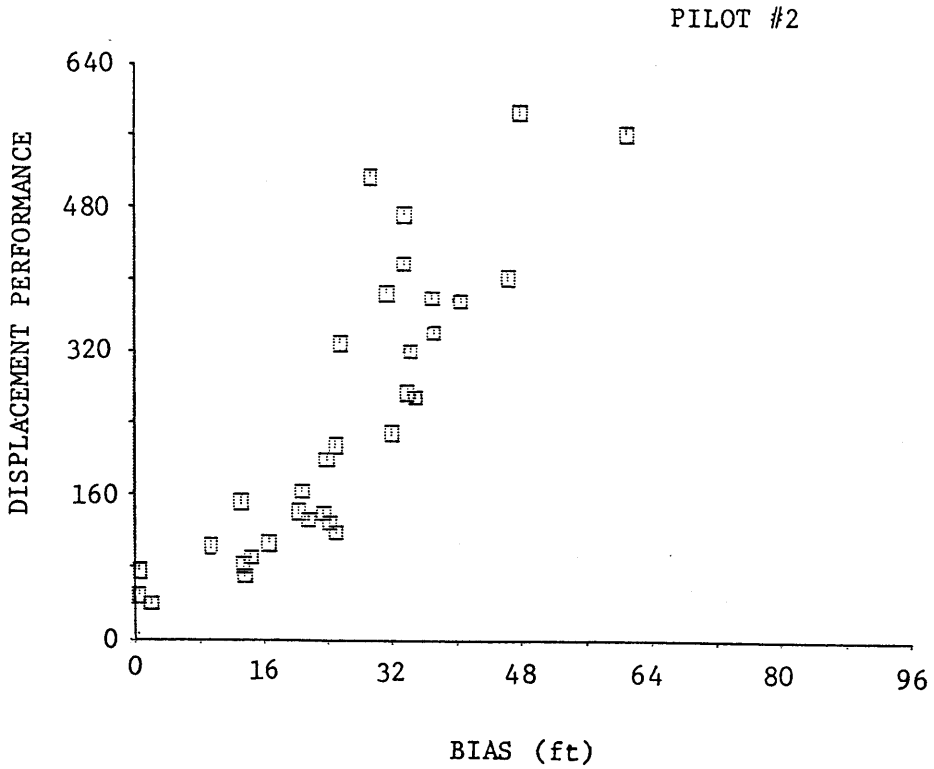

Figure 4-14. Displacement Performance vs Bias Position

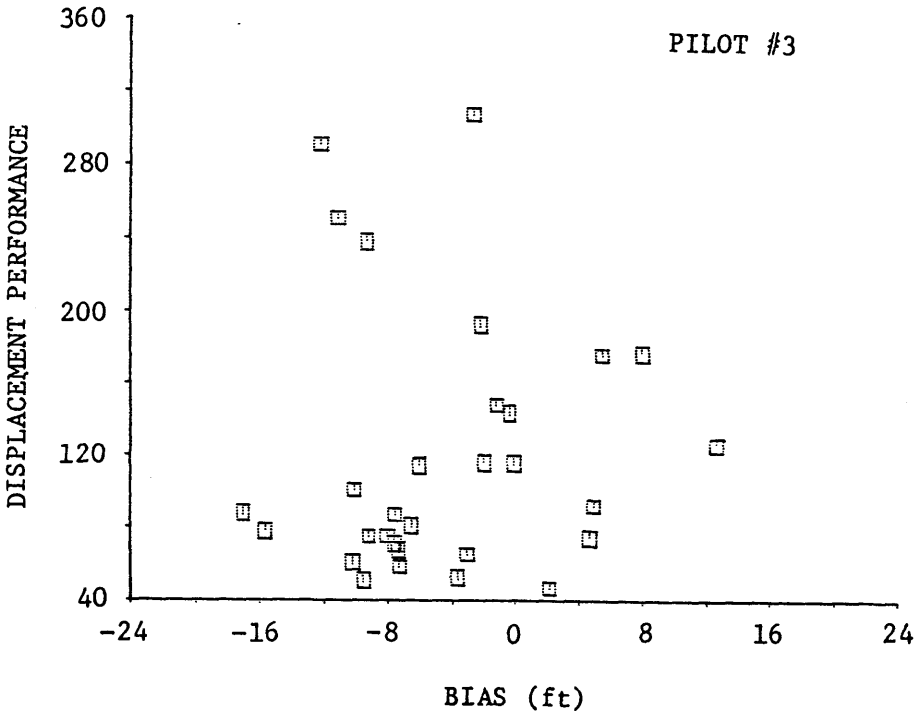

Figure 4-15. Displacement Performance vs Bias Position

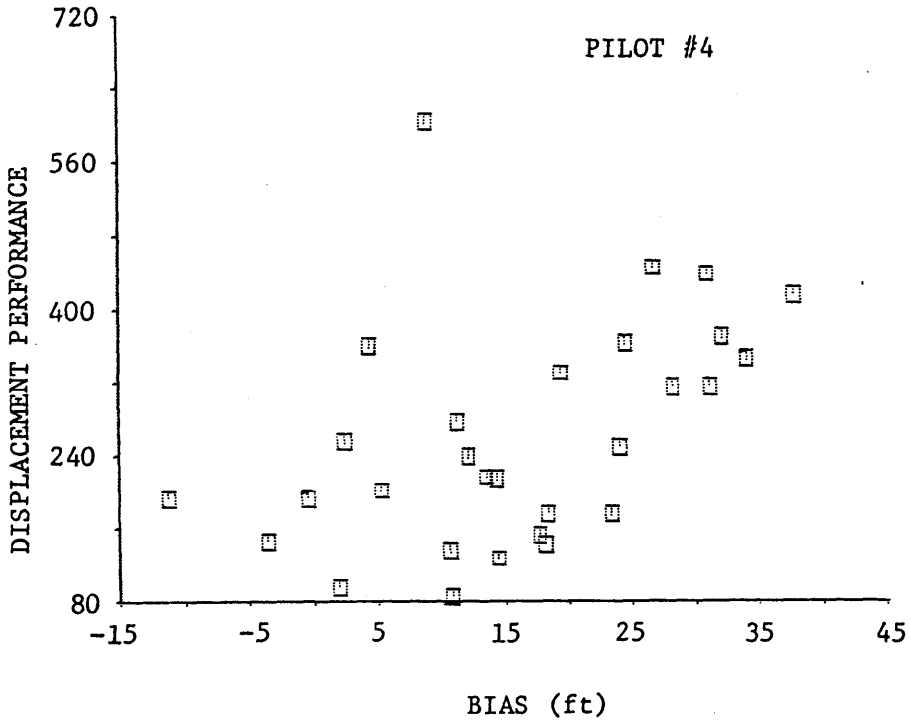

Figure 4-16. Displacement Performance vs Bias Position

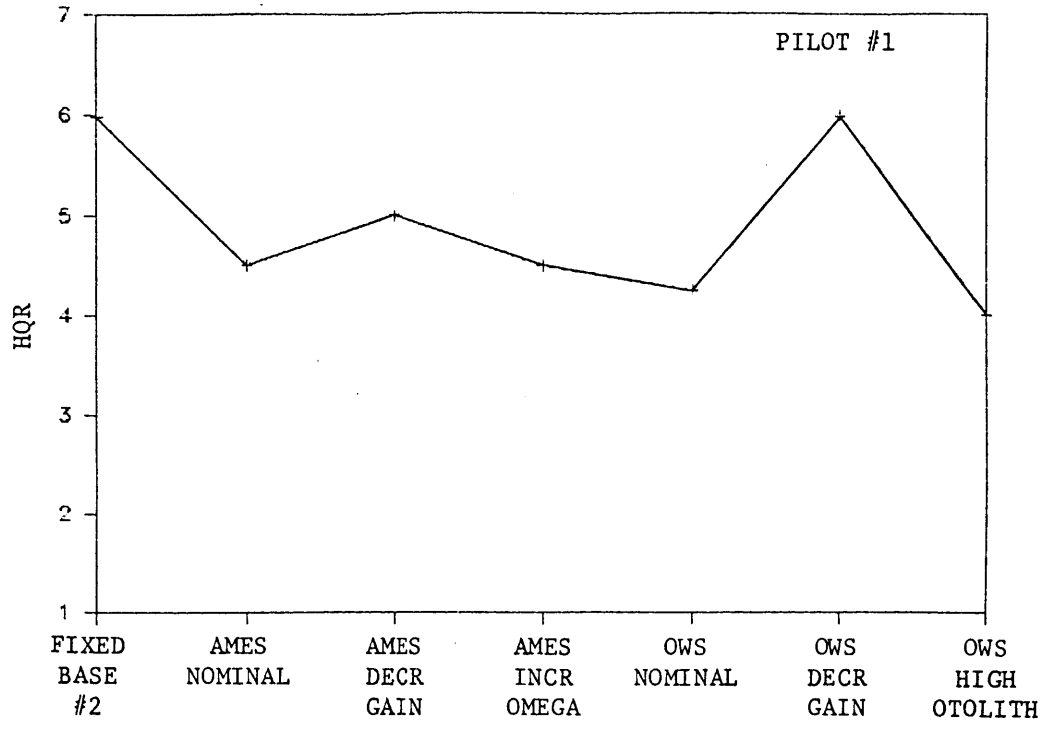

Figure 4-17. Cooper-Harper Ratings

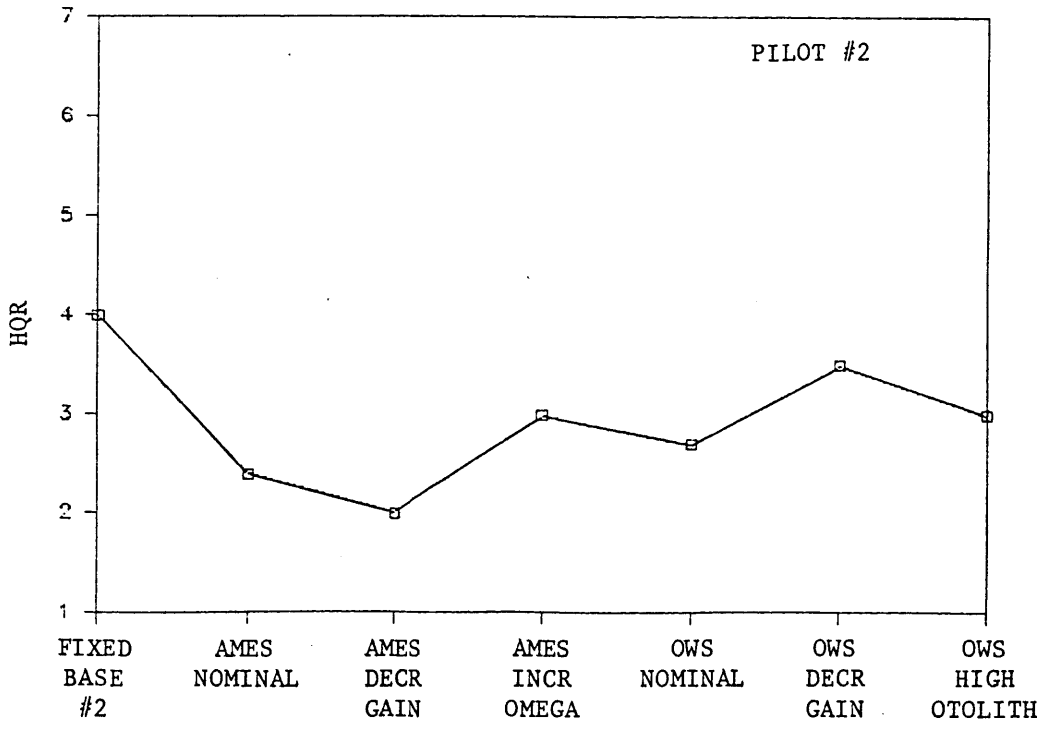

Figure 4-18. Cooper-Harper Ratings

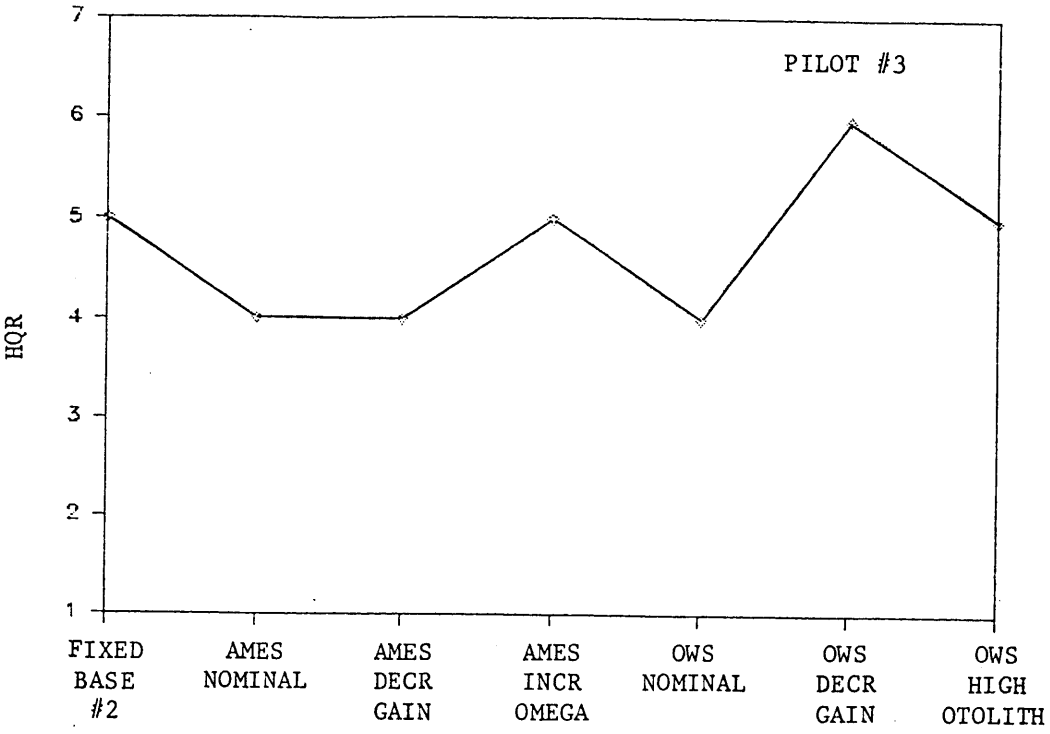

Figure 4-19. Cooper-Harper Ratings

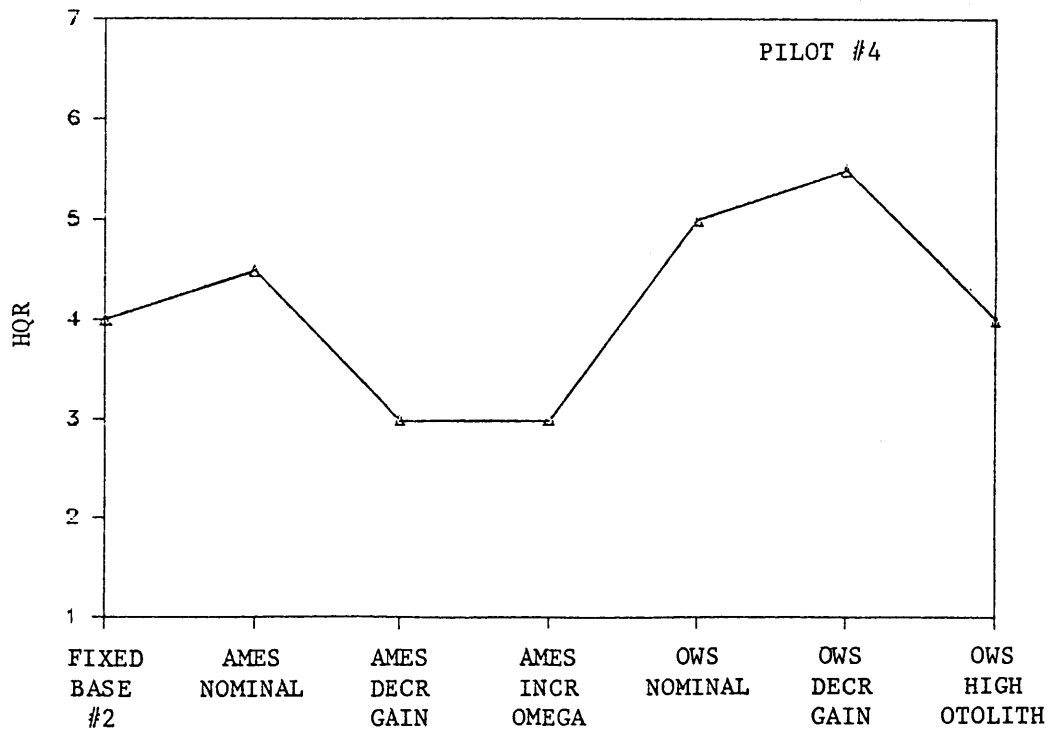

Figure 4-20. Cooper-Harper Ratings

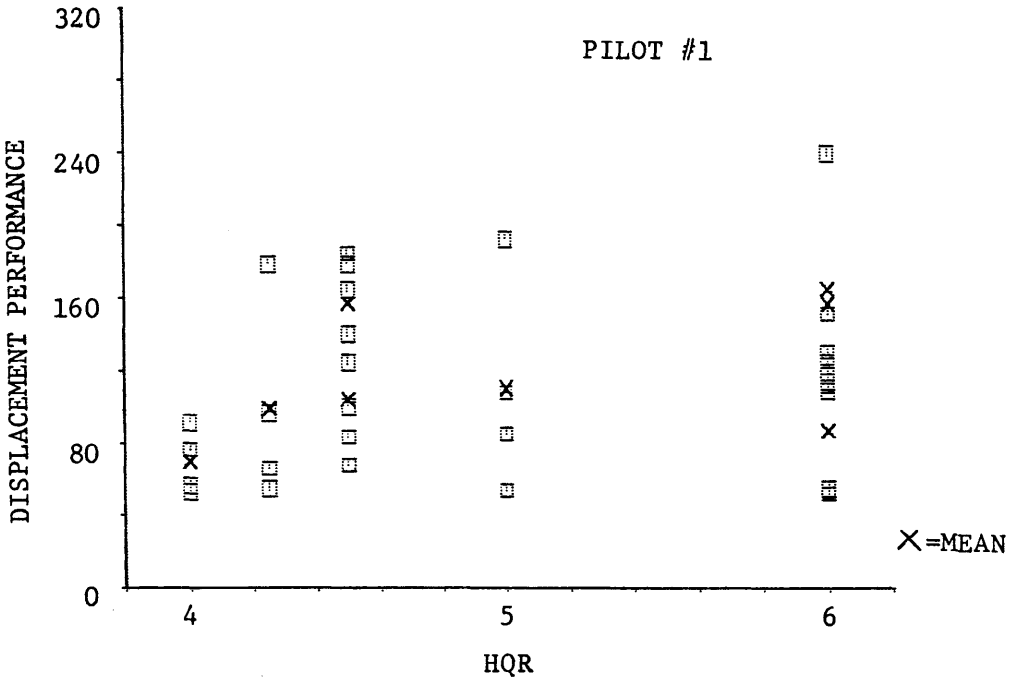

Figure 4-21. Displacement Performance vs HQR

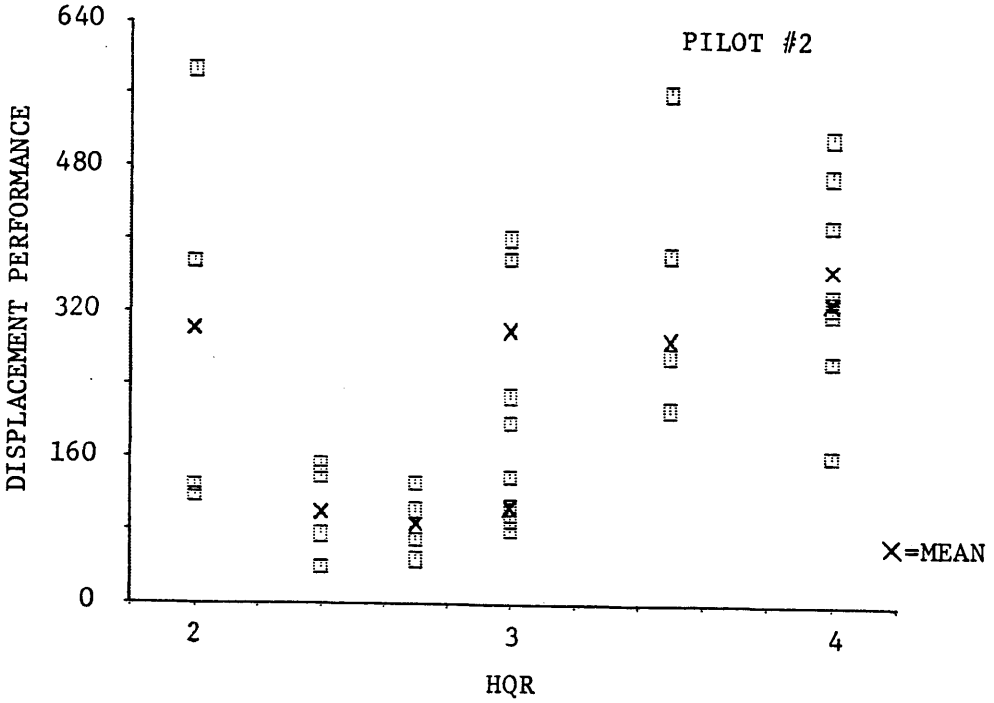

Figure 4-22. Displacement Performance vs HQR

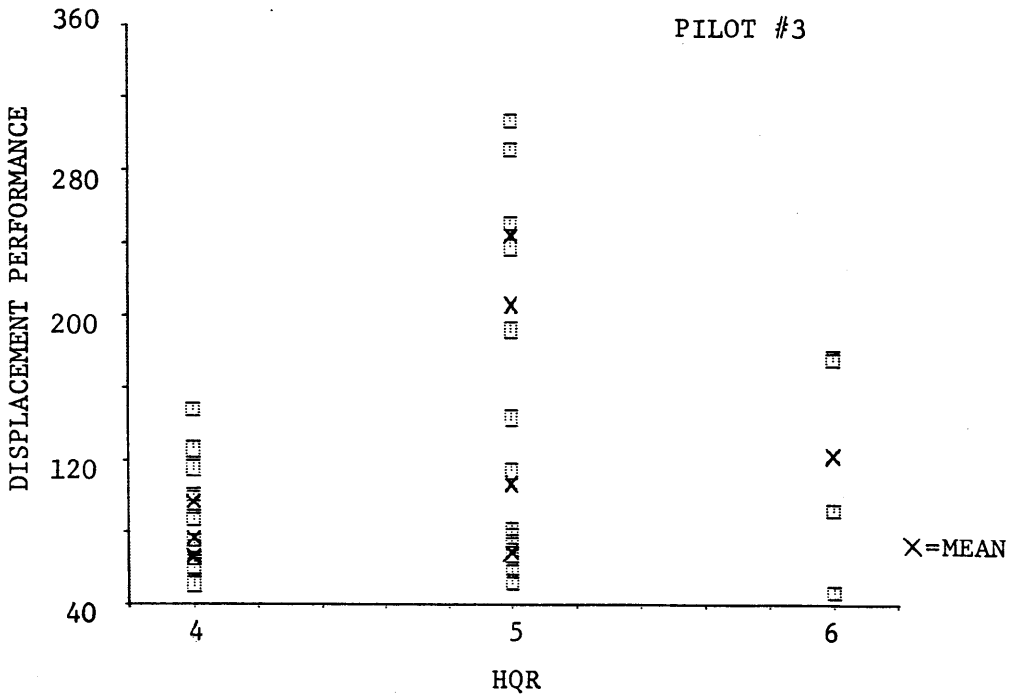

Figure 4-23. Displacement Performance vs HQR

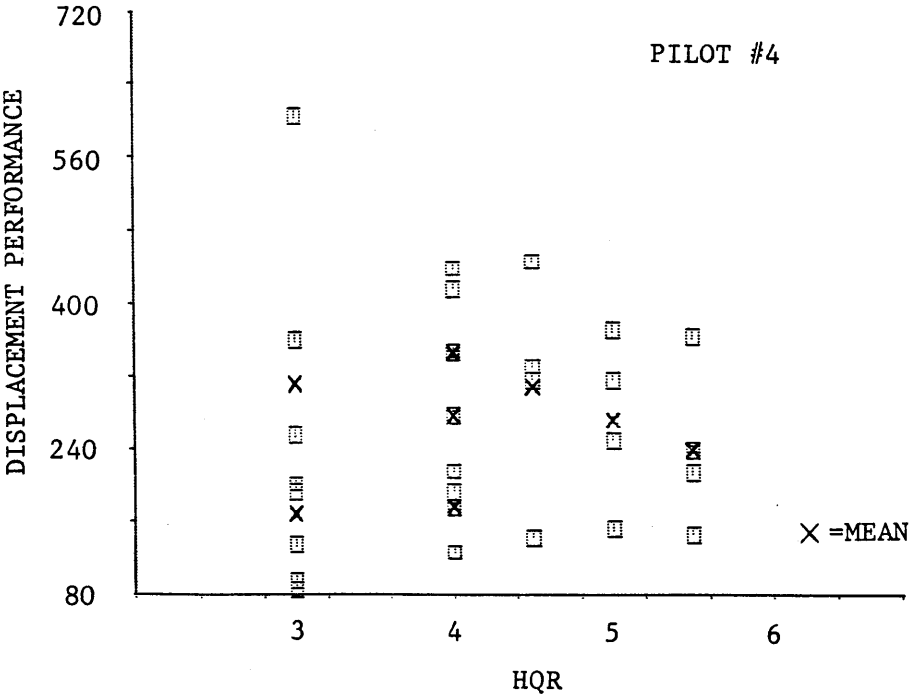

Figure 4-24. Displacement Performance vs HQR

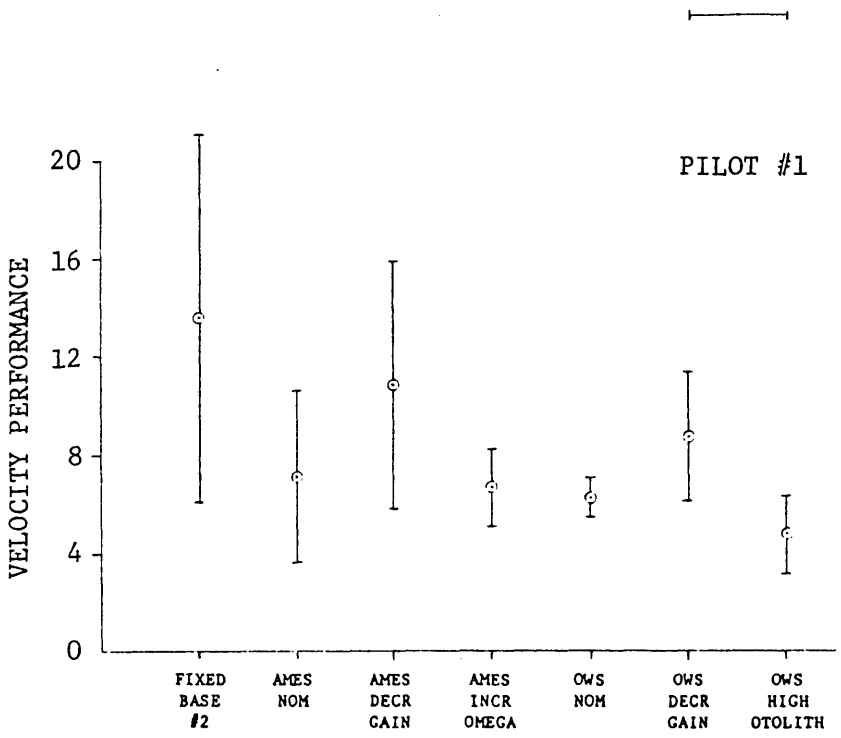

Figure 4-25. Velocity Performance vs Washout

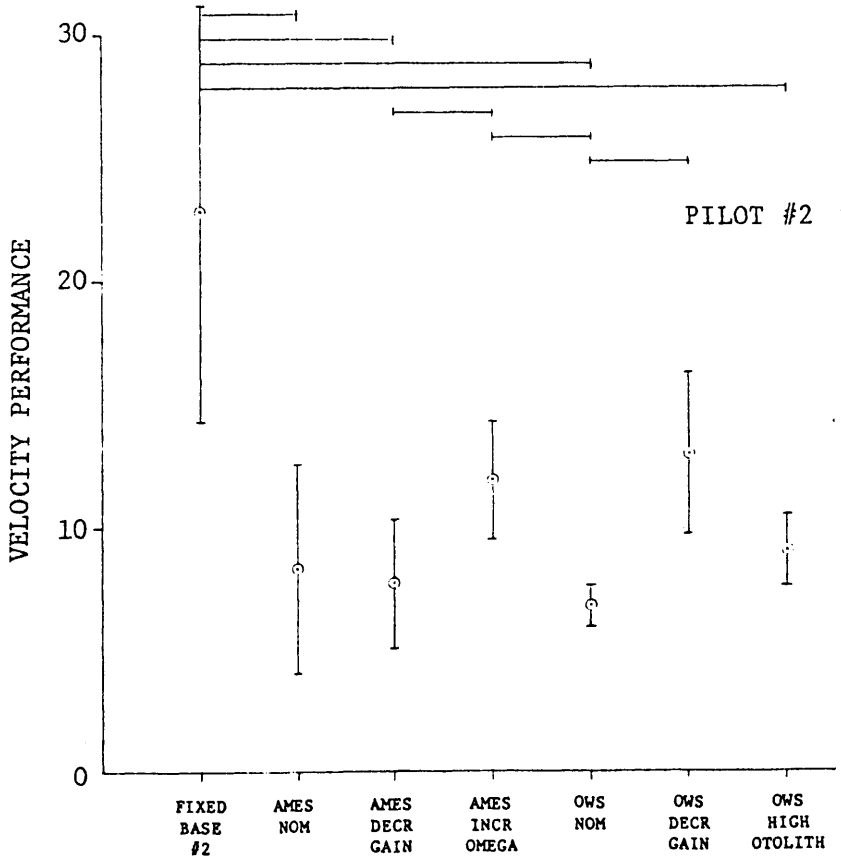

Figure 4-26. Velocity Performance vs Washout

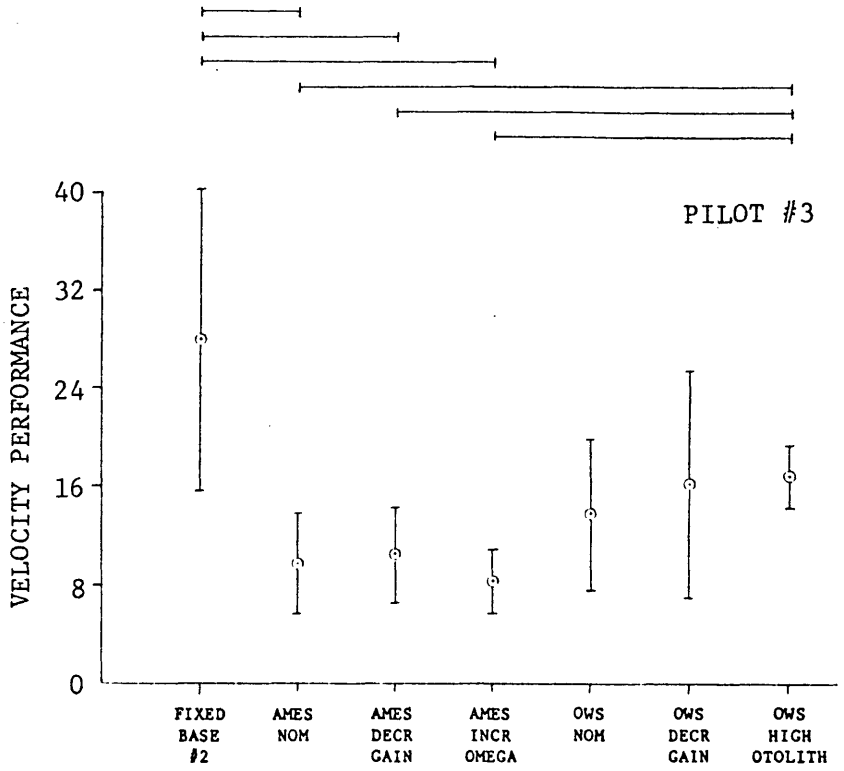

Figure 4-27. Velocity Performance vs Washout

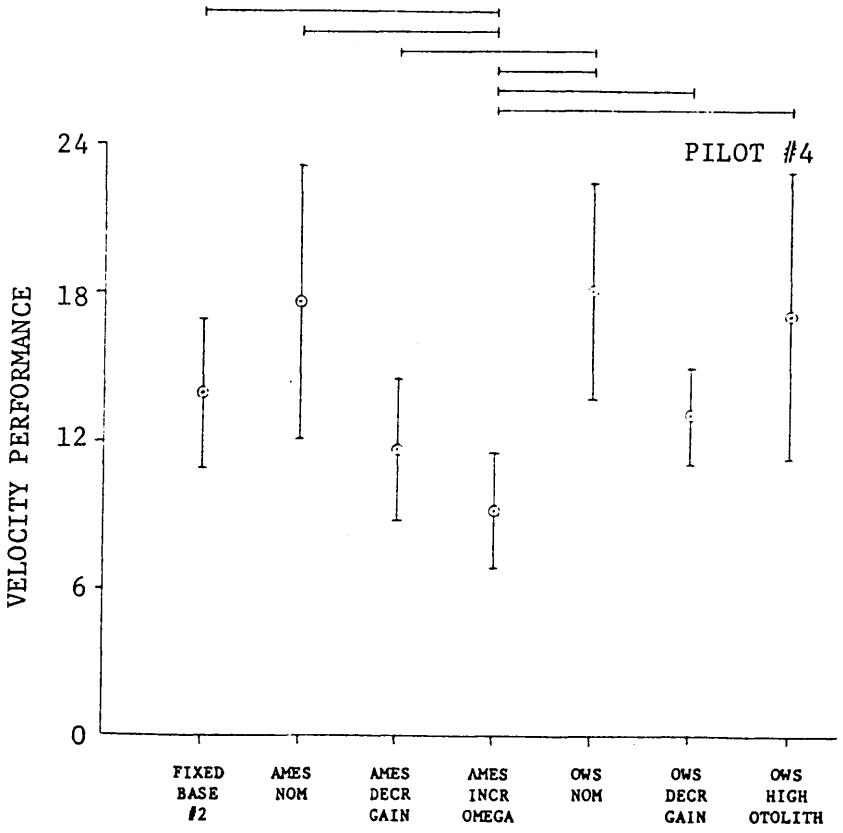

Figure 4-28. Velocity Performance vs Washout

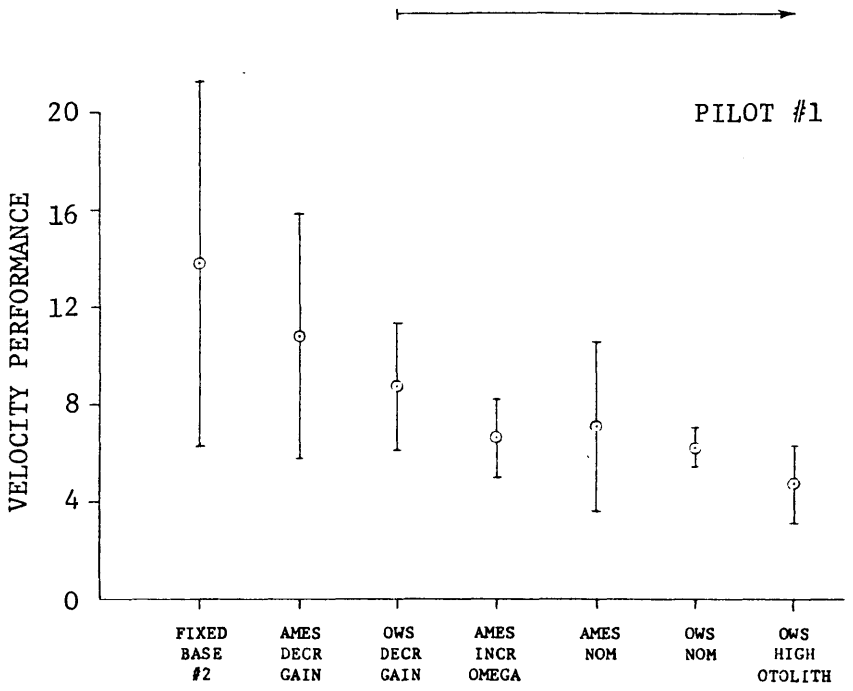

Figure 4-29. Velocity Performance vs Order

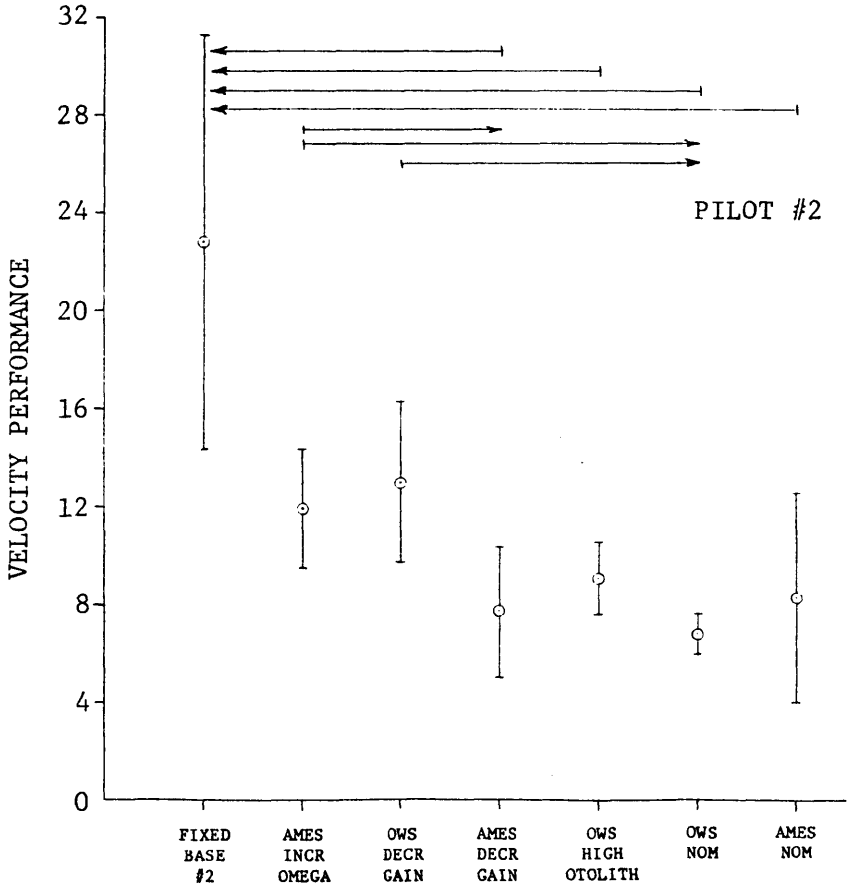

Figure 4-30. Velocity Performance vs Order

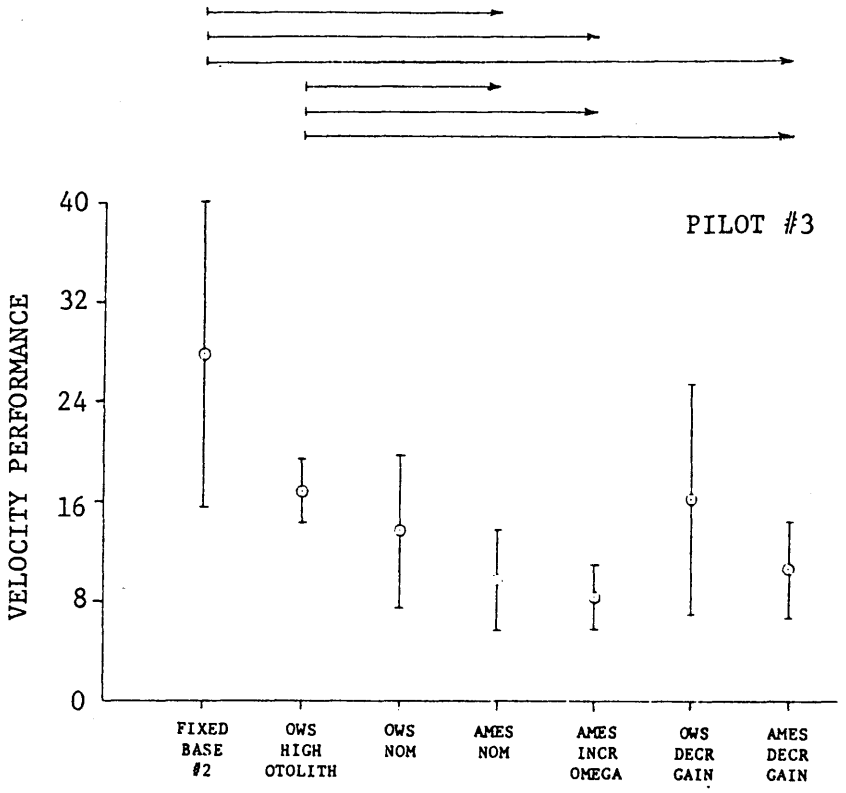

Figure 4-31. Velocity Performance vs Order

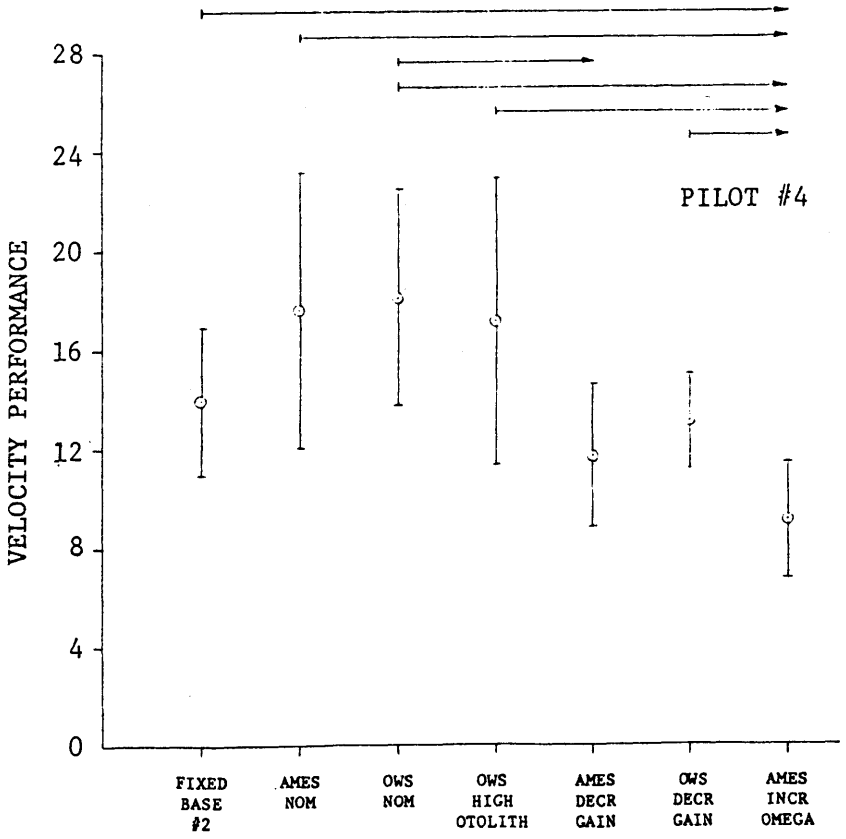

Figure 4-32. Velocity Performance vs Order

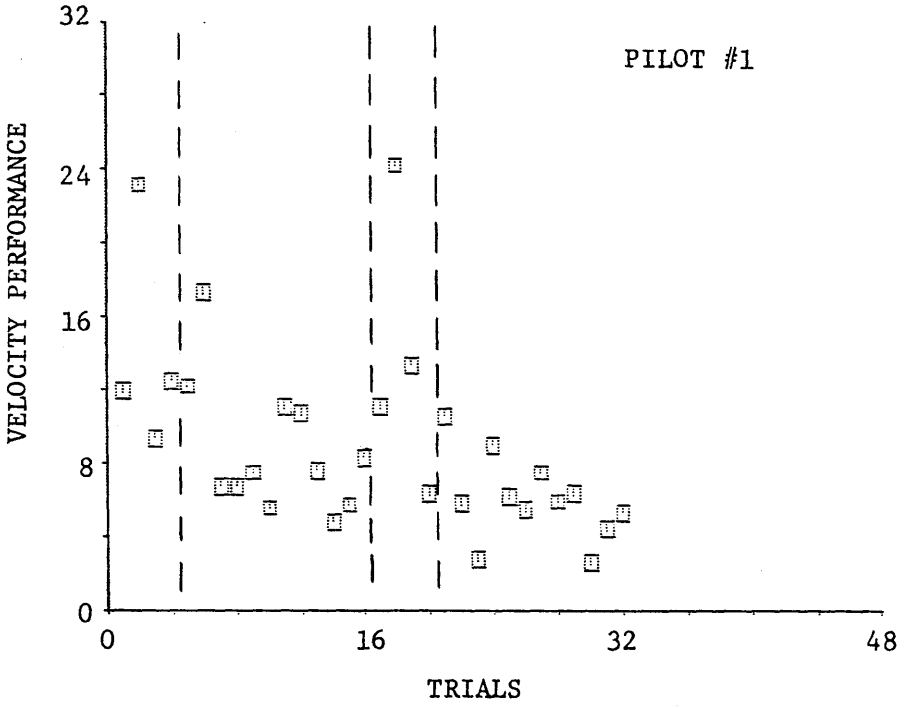

Figure 4-33. Velocity Performance vs Trial

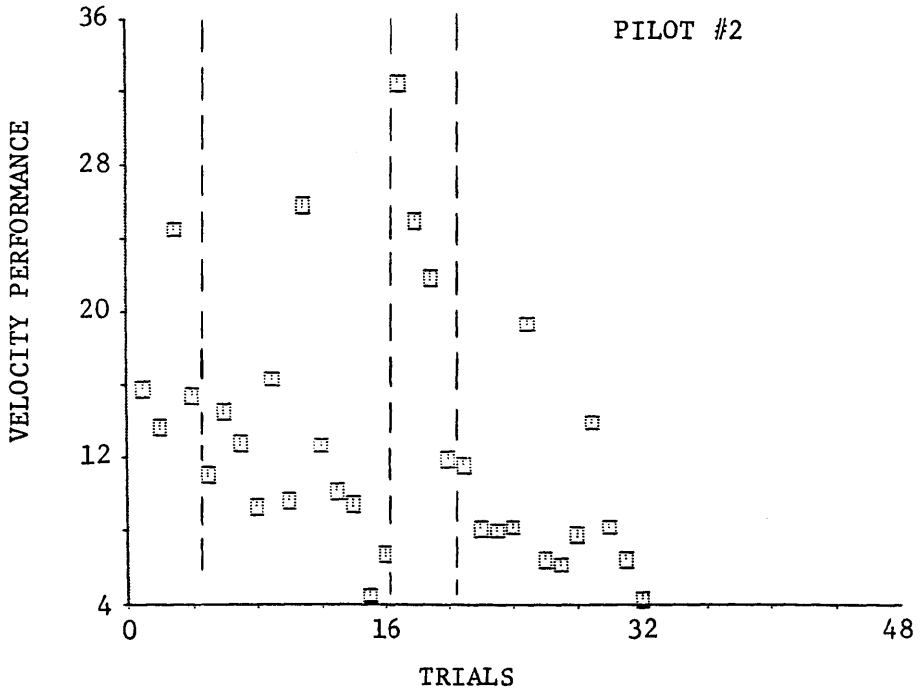

Figure 4-34. Velocity Performance vs Trial

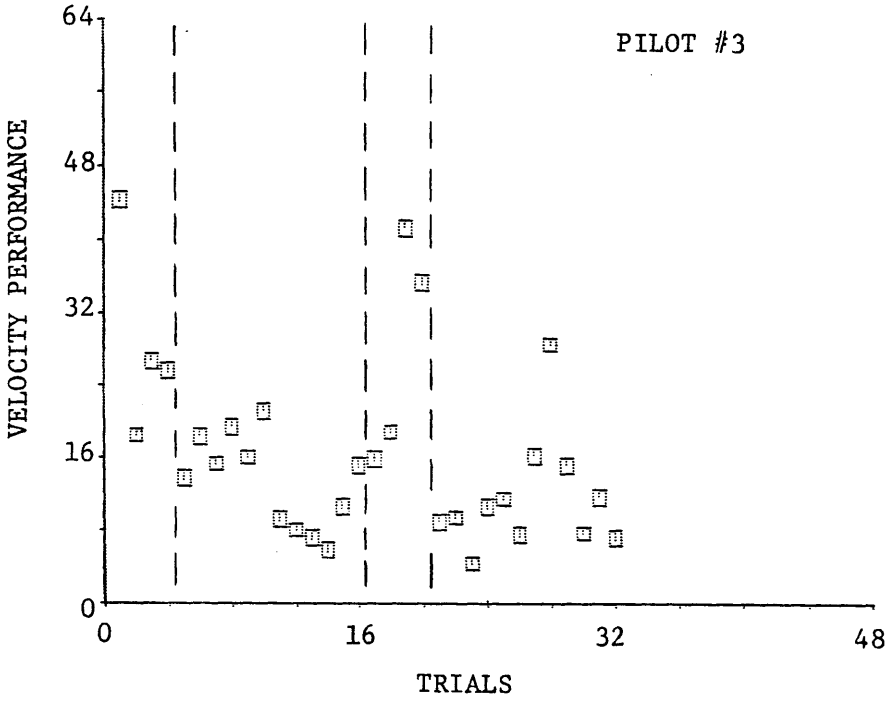

Figure 4-35. Velocity Performance vs Trial

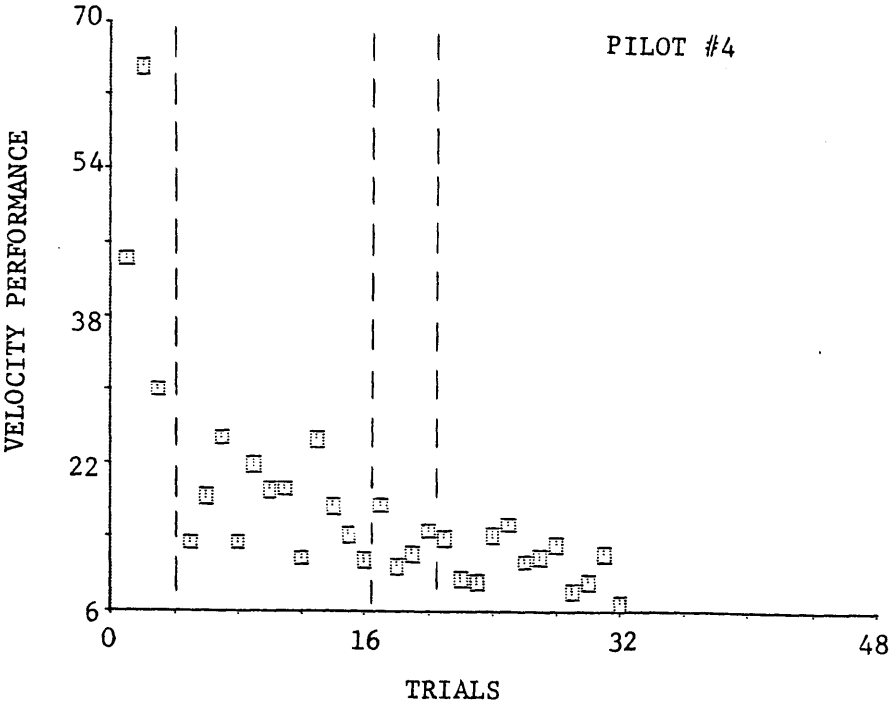

Figure 4-36. Velocity Performance vs Trial

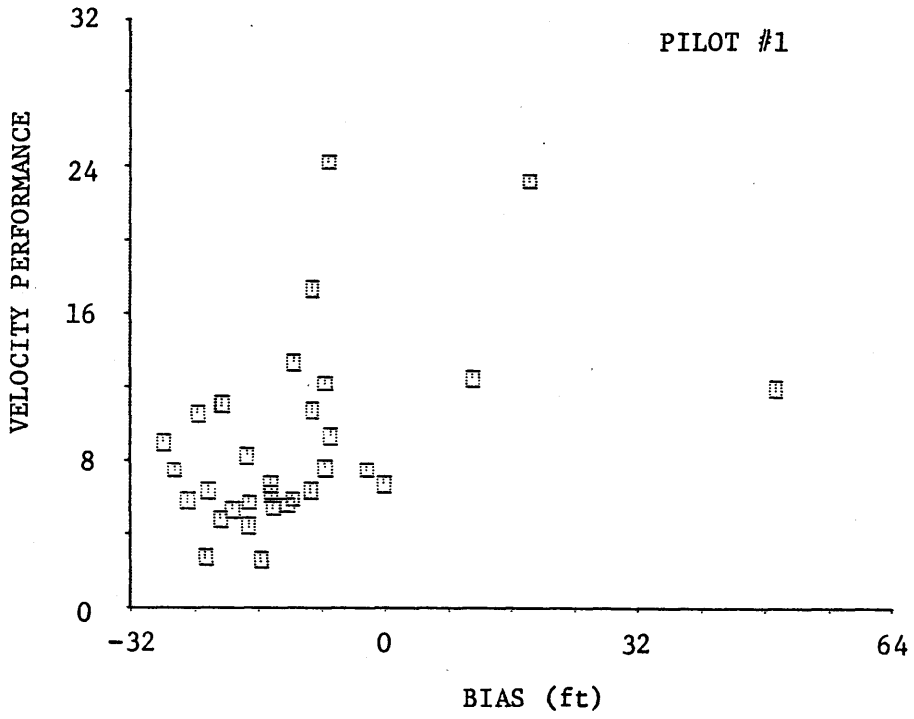

Figure 4-37. Velocity Performance vs Position Bias

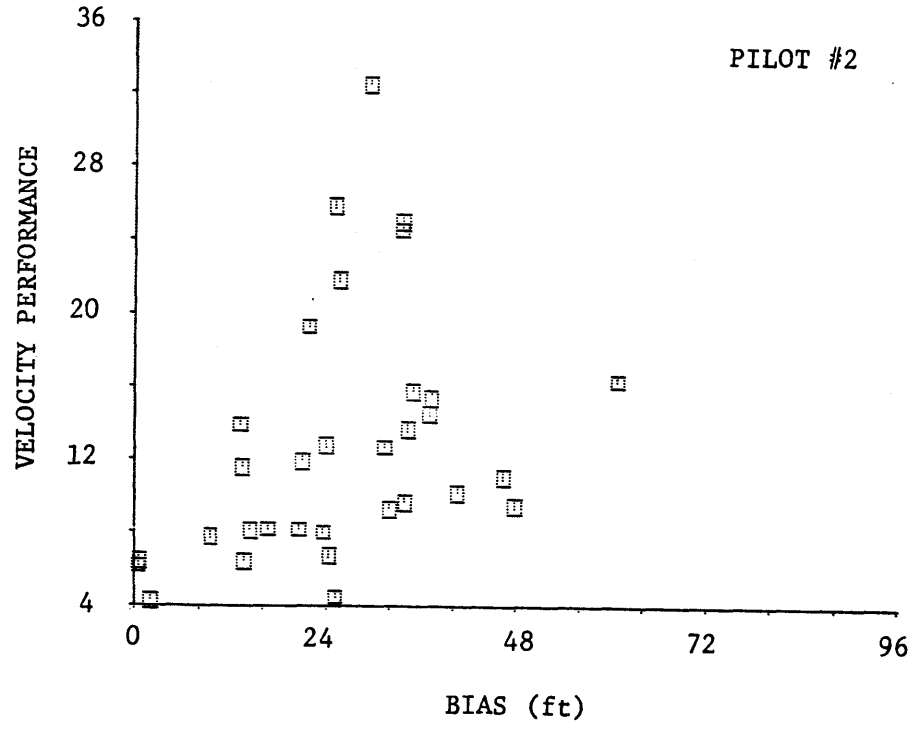

Figure 4-38. Velocity Performance vs Position Bias

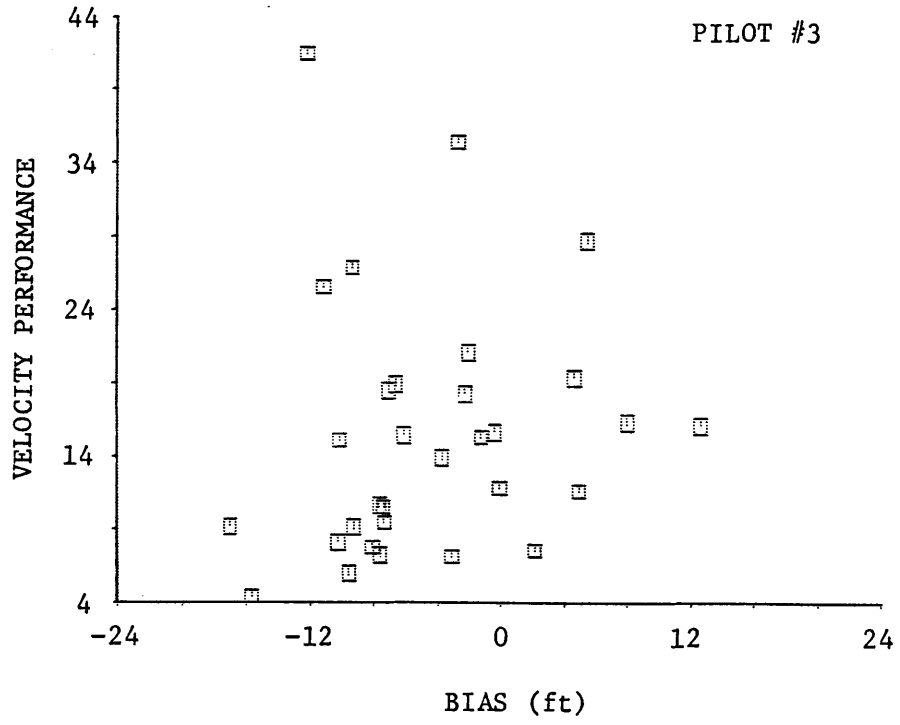

Figure 4-39. Velocity Performance vs Bias Position

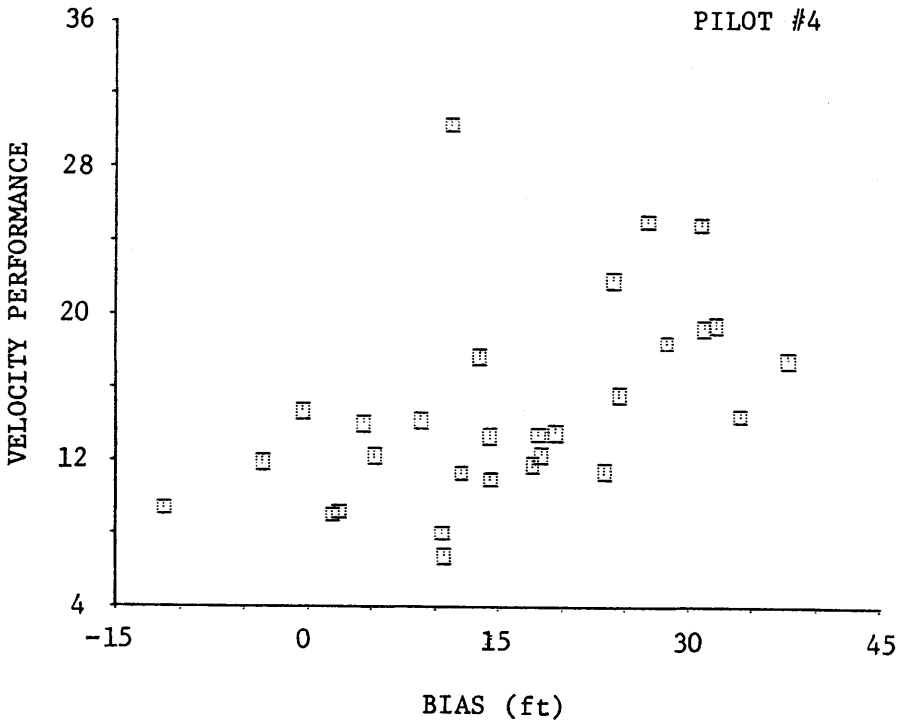

Figure 4-40. Velocity Performance vs Bias Position

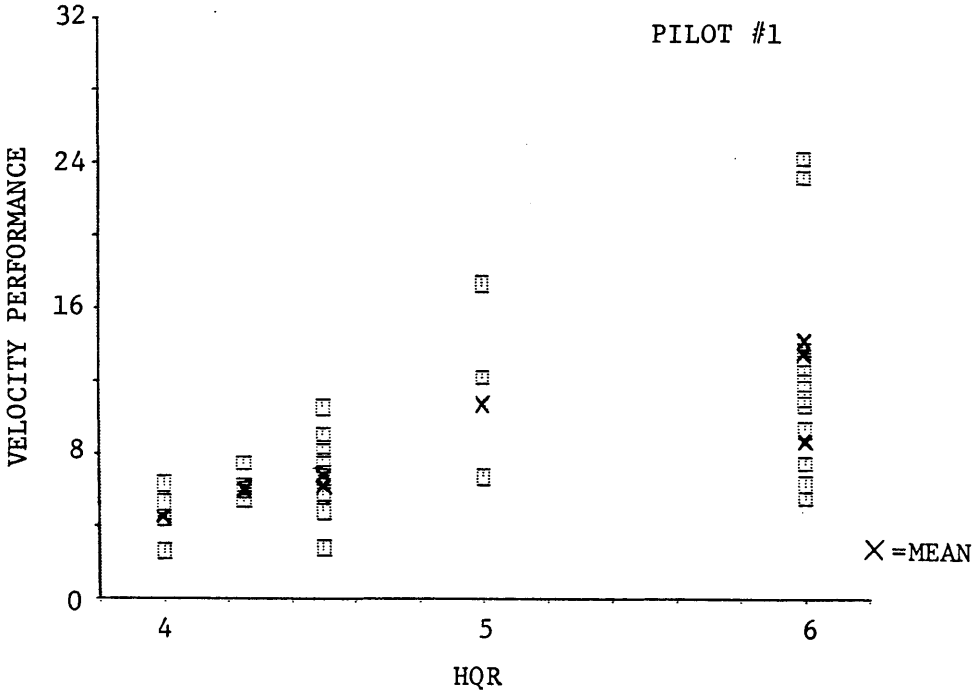

Figure 4-41. Velocity Performance vs HQR

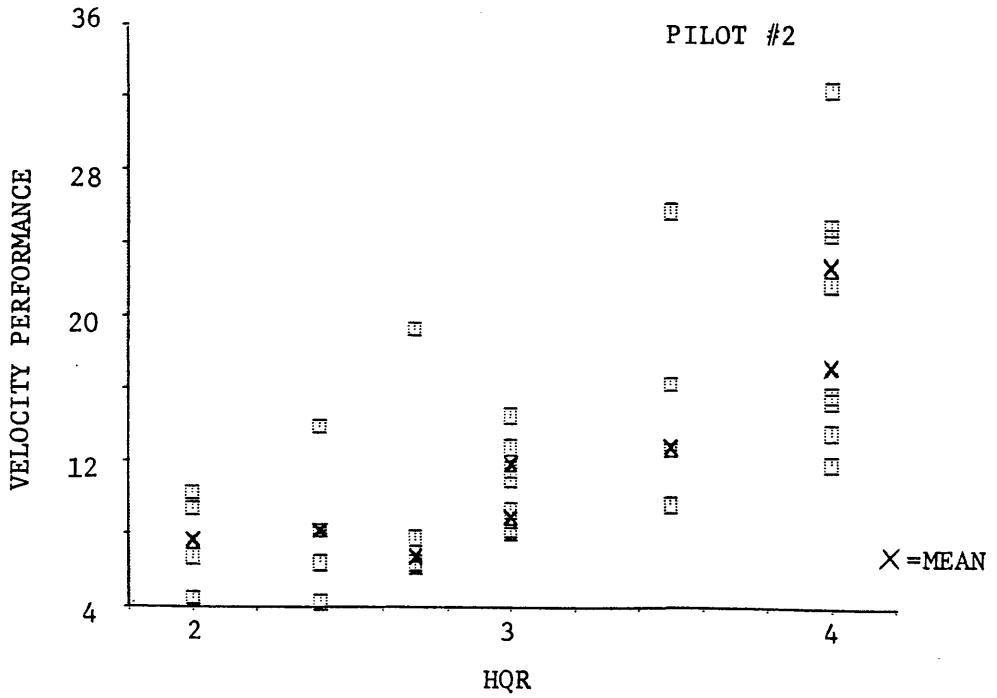

Figure 4-42. Velocity Performance vs HQR

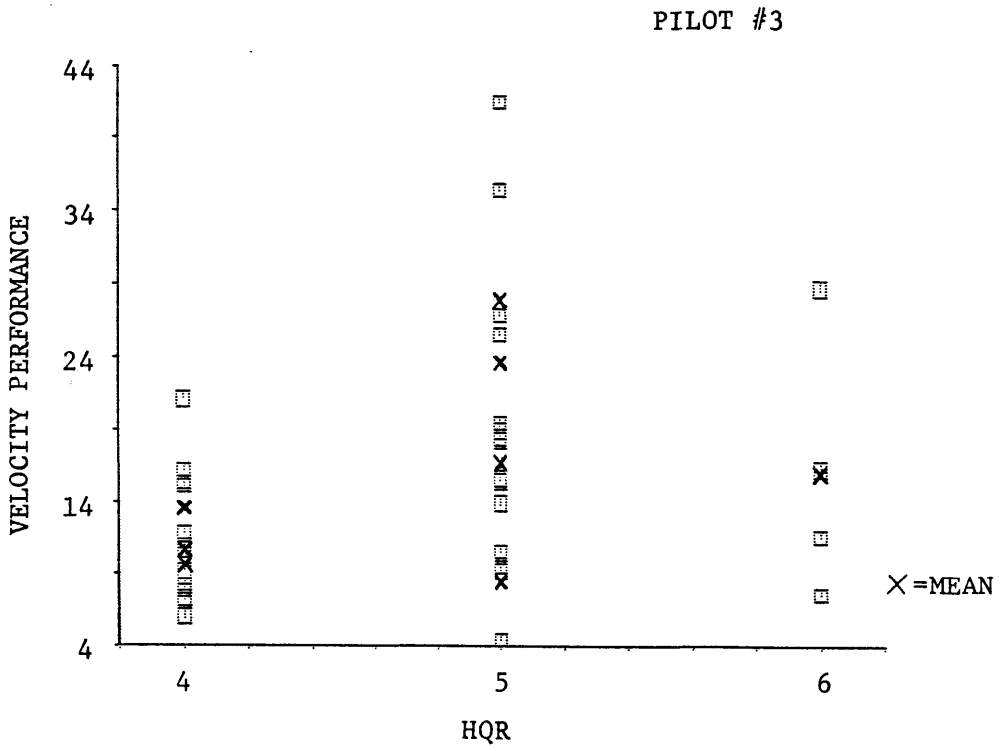

Figure 4-43. Velocity Performance vs HQR

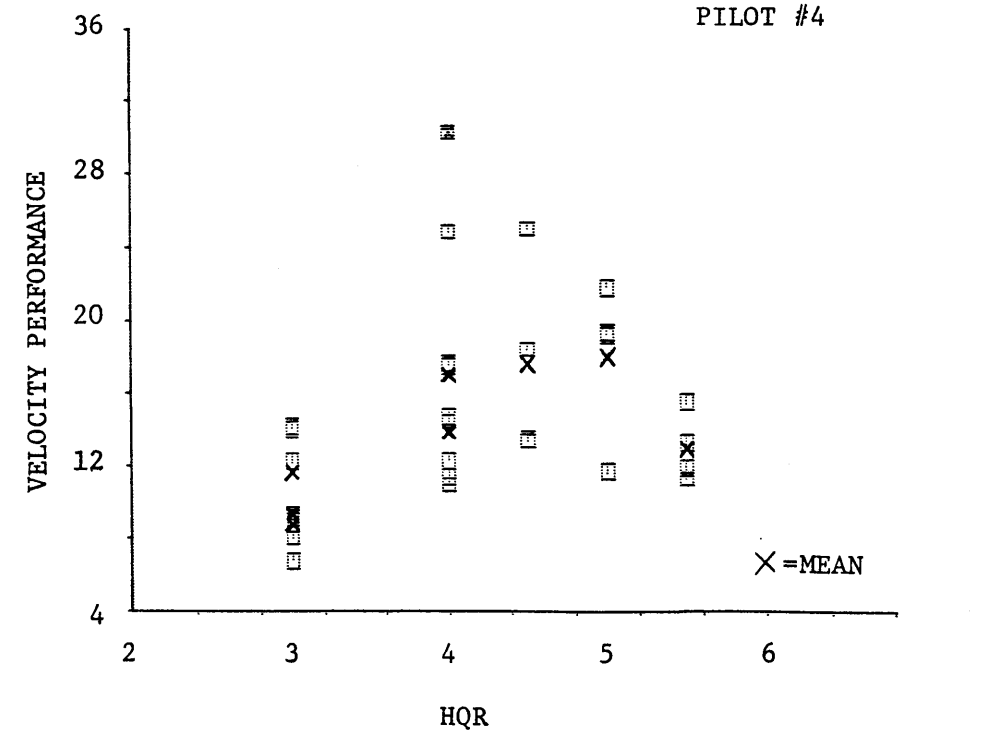

Figure 4-44. Velocity Performance vs HQR

however, performance with the OWS High Otolith Weighting washout is significantly better than with the Ames Nominal washout. Figure 4-9 illustrates that there is minimal correlation between the order of washout presentation and displacement performance (R=-0.07 considering all motion trials, R=-0.21 considering all trials in the first session); therefore, there are minimal learning effects after the first two fixed base trials of the first session. On the hypothesis that tracking performance improves if the pilot is closer to the lead aircraft, position bias has been plotted versus performance (Figure 4-13); however, there is no significant correlation (R=-0.17). Comparing the handling quality ratings to the DES's, Figure 4-21 confirms that there is little correlation (R=0.24) between the HQR's and the DES's. In summary, for Pilot #1, there are minimal order effects on displacement performance, there is no relationship between bias and performance, and there is no correlation between displacement performance and handling quality ratings.

Now looking at the velocity performances for Pilot #1 (Figure 4-25), there are fewer significant performance differences between washouts than there were in the displacement plots. However, Figures 4-29 through 4-33 do indicate a slight learning trend towards the reduction of velocity error (R=-0.56 considering all motion cases and R=-0.61 for all trials in the first session). The bias plot (Figure 4-37) indicates a slight correlation (R=0.43) between bias and performance, but in general, because the range of biases is so small, the effect of bias on performance is insignificant. Observing, Figure 4-41, there is a slight correlation (R=0.61) between the velocity

performance and the handling quality ratings. In the plot of the Cooper-Harper ratings (Figure 4-17), the pilot rates the Ames Nominal, the Ames Increased Omega, the OWS Nominal, and the OWS High Otolith washouts on the same level, but rates the Fixed Base, the Ames Decreased Gain, and the OWS Decreased Gain washouts worse. This corresponds to the data in Figure 4-25 in that the performance for Fixed Base, Ames Decreased Gain, and OWS Decreased Gain are all slightly worse than for the rest of the washouts. Although the two washouts that were presented first had the worst performances and the worst HQR's, it is unlikely that learning was the only factor in the handling quality ratings. The pilot indicates specific motion cues that were lacking in the first two washouts but were present in latter washouts (see pilot comments in Appendix D). In summary, for velocity performance, there was a slight learning effect and a slight correlation between performance and handling quality ratings.

For Pilot #2, the differences in displacement performance (Figure 4-2) is quite significant for a number of washouts. The performance with the Ames Nominal, OWS Nominal, and OWS High Otolith Weighting washouts are significantly better than the performance for the Fixed Base, Ames Increased Omega, and OWS Decreased Gain cases; unfortunately, the variability in the Ames Decreased Gain case makes impossible any conclusions about its rank relative to the other washouts. It appears that the pilot's performance was typically better during the second session of the experiment. This result can be attributed to three factors: to learning effects, to the possibility that the pilot had a bad day during the first session, or to the improved motion cues of the

washouts used during the second session. There appears to be minimal learning evident for this pilot. In Figure 4-10, although the performance on each trial is reasonably well correlated with the order of presentation when considering all the trials (R=-0.63) or when considering all trials with motion (R=-0.71); nevertheless, when considering only the trials in the first session, there is no correlation (R=-0.15), indicating that the level of performance during the second session is better than that of the first session, not that significant learning has taken place throughout the experiment. The possibility that the pilot had a bad first session is unlikely judging from the similar performance levels of the two fixed base cases. Therefore, the most likely explanation is that the pilot preferred the motion cues of the higher fidelity washouts. This is confirmed by pilot comments given during testing of the third washout; the pilot stated that the improved motion of that case over the two previous low fidelity washouts allowed him to move closer to the lead aircraft, but Figure 4-14 indicates a very strong relationship between the bias position and the performance level. The closer the pilot is to the lead aircraft, the better his performance; therefore, the improved motion of the washouts in the second session allowed him to move closer to the lead aircraft and thereby improve his performance. Comparing displacement performance with the handling quality ratings (Figure 4-22), there does appear to be a slight correlation between these two parameters. The pilot rates the Ames Nominal and Ames Decreased Gain washouts as the best, followed by the OWS Nominal and the OWS High Otolith Weighting cases. This trend is reflected in the DES's also, where the Ames

Nominal, OWS Nominal, and OWS High Otolith Weighting have equivalent performance ratings. In summary, there is no real learning effect in displacement performance, but there is improved performance with improved motion, probably a result of the pilot's confidence to move closer to the lead aircraft when sufficient motion cues were provided. Also, there is a slight correlation between the handling quality ratings and the displacement performance.

The velocity performance plot (Figure 4-26) for Pilot #2 displays the same relative shape as does the displacement plot, but the relative differences in means of the VES's is less than those of the DES's. Therefore between washouts, there are fewer significant performance differences for velocity than for displacement. Nevertheless, the variability of the Ames Decreased Gain case is much less in velocity than in displacement, thereby making it evident that a fairly high level of performance was achieved with this washout relative to the Ames Increased Omega and OWS Decreased Gain washouts. This corroborates with the pilot comment that he felt his performance improved with the Ames Decreased Gain washout; furthermore, this corroborates with the handling quality ratings: the Ames Decreased Gain washout was rated a 2, the Ames Increased Omega case was rated a 3, and the OWS Decreased Gain case was rated a 3.5 . For this pilot, there is a slight learning effect in velocity (R=-0.50), particularly in the first session, as illustrated in Figures 4-30 and 4-34. Figure 4-38 indicates that there is no correlation between position bias and performance; however, there is a fairly strong relationship between the handling quality ratings and the VES's (R=0.71).

With respect to the other pilots, Pilot #3 had the best average DES's for the motion cases, although between washouts, there is little difference in mean DES's; consequently, there are no significant differences between the washouts (see Figure 4-3). Observing Figure 4-7 and 4-11, there does appear to be a learning trend in the first session (R=-0.66), but most of this trend is due to the poor performance in the fixed base trials. If considering learning only over the first session motion runs, there is much less correlation (R=-0.37). Although the pilot does comment that he has observed some learning by the end of the second motion washout, it is not apparent in his performance. Figure 4-15 indicates that displacement performance is independent of position bias (R=0.05). Similarly, Figure 4-23 indicates that there is no correlation (R=0.26) between DES's and HQR's.

It is evident in Figure 4-27, that for Pilot #3, the velocity performances on the Ames washouts are significantly better than the performance with the OWS High Otolith Weighting case. Moreover, when the population of trials performed with the Ames washouts are compared with those performed with the OWS washouts, a t-test confirms that the overall performance on the Ames washouts is significantly better (p=99.3%) than the overall performance on the OWS washouts. It is not clear whether this is a result of better motion cues with the Ames washouts, or whether the analysis is biased by learning, since the first two washouts, during which the most significant learning would occur, were OWS washouts. Figures 4-31 and 4-35 do indicate a learning trend, mainly in the first session (R=-0.72), but again, it is not clear how much of this effect is a result of the washout characteristics and how

much is a result of learning. Pilot comments do indicate the pilot did notice some learning by the second washout of the first session. Figure 4-39 indicates that there is no correlation (R=0.12) between bias position and velocity performance. Figure 4-43 illustrates that the VES's are fairly independent of the handling quality ratings (R=0.31), mainly because there is little variation in mean performance with each washout. The changes in HQR's are therefore more likely a function of pilot workload which would increase when insufficient motion cues are present. In summary, there are few performance differences between washouts, although there is a learning trend which is more evident in the VES's than in the DES's. Judging from the pilot comments, this learning effect could have slightly biased the HQR for the OWS High Otolith Weighting case, which was the first washout presented. Finally, there appears to be no correlation between performance and the handling quality ratings.

The DES's for Pilot #4 are plotted in Figure 4-4. The only significant difference between washouts is that performance with the Ames Increased Omega case is better than that with the OWS High Otolith Weighting case. There appears to be no learning occurring after the first two fixed base runs of the first session (R=0.12). There is a slight correlation (R=0.46) between bias position and displacement performance (Figure 4-16), but no correlation (R=0.06) between the DES's and the handling quality ratings (Figure 4-24).

Now looking at the VES's in Figure 4-28, the performance differences between washouts are more apparent than for the DES's.

Observing Figures 4-32 and 4-36, there appears to be no learning effect in the first three washouts (R=-0.22), although significant learning did occur during the three fixed base runs. Generally, the performance with the three washouts of the second session appear to be better than that for the washouts of the first session. This difference can be explained by three possibilities: (1) sufficient learning occurred over the length of the experiment to affect the results between sessions, (2) the pilot preferred the lower fidelity washouts, or (3) the pilot had a bad first session. The first explanation, that the pilot experienced significant learning, contradicts the previous evidence that minimal learning occurred. The suggestion that the pilot's performance was better the second session because he preferred the lower fidelity washouts is unlikely. During the second washout presented the second session, the OWS Decreased Gain washout, even though the pilot had relatively good performance, he rated it a 6 and commented that it was the worst washout configuration he had tested so far. The final suggestion that the pilot had a bad day during the first session, is a possibility, but this is difficult to conclusively prove or disprove; however, it should be noted that this session was performed on a Monday morning and that it was the first session performed by any of the pilots; consequently, there were a number of operational difficulties and computer failures which may have frustrated the pilot. A comparison between bias position and velocity performance is given in Figure 4-40, which illustrates the slight correlation (R=0.50) between the two factors. Figure 4-42 illustrates the independence (R=0.30) of velocity performance and HQR's.

The correlation results for all pilots are summarized in Table 4-1.

4.4 Discussion of Pilot Model Describing Functions

To obtain the combined pilot-aircraft (open loop) describing function, the data from the tracking tasks was analyzed using an off-line NASA Ames routine. The analysis was first run using position error and later velocity error as the input to the pilot describing function. Pilot stick commands were used as the output. The information obtained from the program included amplitude ratios, phase angles, and signal to noise ratios of the pilot response at the five disturbance frequencies.

Unfortunately, for many of the data points, the signal to noise ratio is very small, especially at high frequencies; consequently, it is probable that the pilots were not necessarily using a linear control scheme. This corroborates one pilot's comments that he was utilizing a bang-bang control strategy. This is also substantiated by an FFT of the pilot stick inputs (Figure 4-45) where the dotted lines represent the disturbance frequencies. In Figure 4-45, it is evident that the frequency of the pilot's local peak amplitude is sometimes offset from the disturbance frequency. In other cases, there is a bimodal amplitude distribution about the disturbance frequency, with a low amplitude at the actual disturbance frequency; furthermore, there is a large remnant across the spectrum of interest. All of these factors, plus the fact that the there were large performance variations between trials for each pilot, makes definitive conclusions about specific features (crossover frequencies, phase margins) of the open loop transfer functions extremely difficult. To illustrate this point, a typical Bode plot of

Table 4-1. Summary of Correlations

CORRELATION WITH DISPLACEMENT PERFORMANCE

	PILOT #1	PILOT #2	PILOT #3	PILOT #4
ORDER	-.21	-.15	-.37	.12
BIAS	-.17	.87	.05	.46
HQR	.24	.43	.26	.06

CORRELATION WITH VELOCITY PERFORMANCE

	PILOT #1	PILOT #2	PILOT #3	PILOT #4
ORDER	-.61	-.50	-.72	-.47
BIAS	.43	.37	.12	.50
HQR	.61	.71	.31	.30

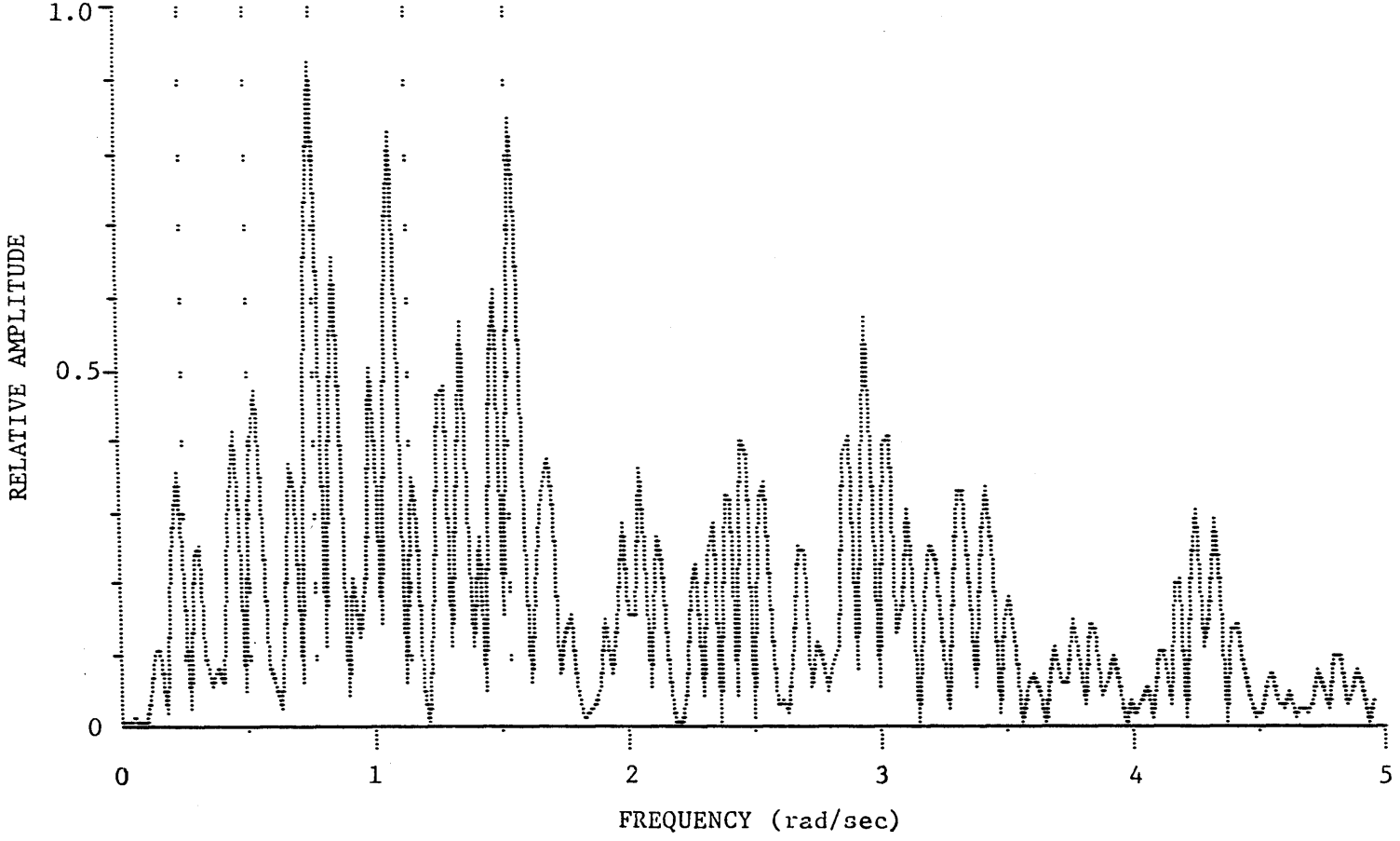

Figure 4-45. Spectrum of Pilot Inputs

the combined pilot-aircraft describing function is presented in Figure 4-46. The crossover frequency is difficult to determine because of the large variability among trials. Furthermore, the results shown are affected by the poor signal to noise ratio in the region of interest. It is however interesting to note that the phase lags are all near 180 degrees, indicating a marginally stable response. This is expected due to the high order dynamics of the hovercraft plant and to the difficulty of performing the tracking task. It is possible that if the pilots had been instructed to track the lead aircraft from a closer point the performance would have been more consistent, the signal to noise ratio would have improved, and there would have been significant differences among washouts for each of the describing functions.

Some general observations about the describing functions are that Pilot #3 had the most linear slopes and therefore, probably had the most linear control strategy. This pilot also had the best performance ratings, although his gains are slightly less than those for Pilot's #1 and #2. In general, Pilot #4 had the best phase margin.

4.5 Discussion of the Motion Rating Scale

The motion ratings for each pilot are summarized in Table 4-2. Unfortunately, due to pilot rating idiosyncrasies, it is difficult to draw conclusions from the ratings when evaluating over the entire population; however, dealing with each pilot separately, it is possible to obtain some fairly significant results by correlating each motion evaluation parameter with the overall motion rating (Table 4-3). For Pilot #1, sense, discomfort, and disorientation correlate well with the

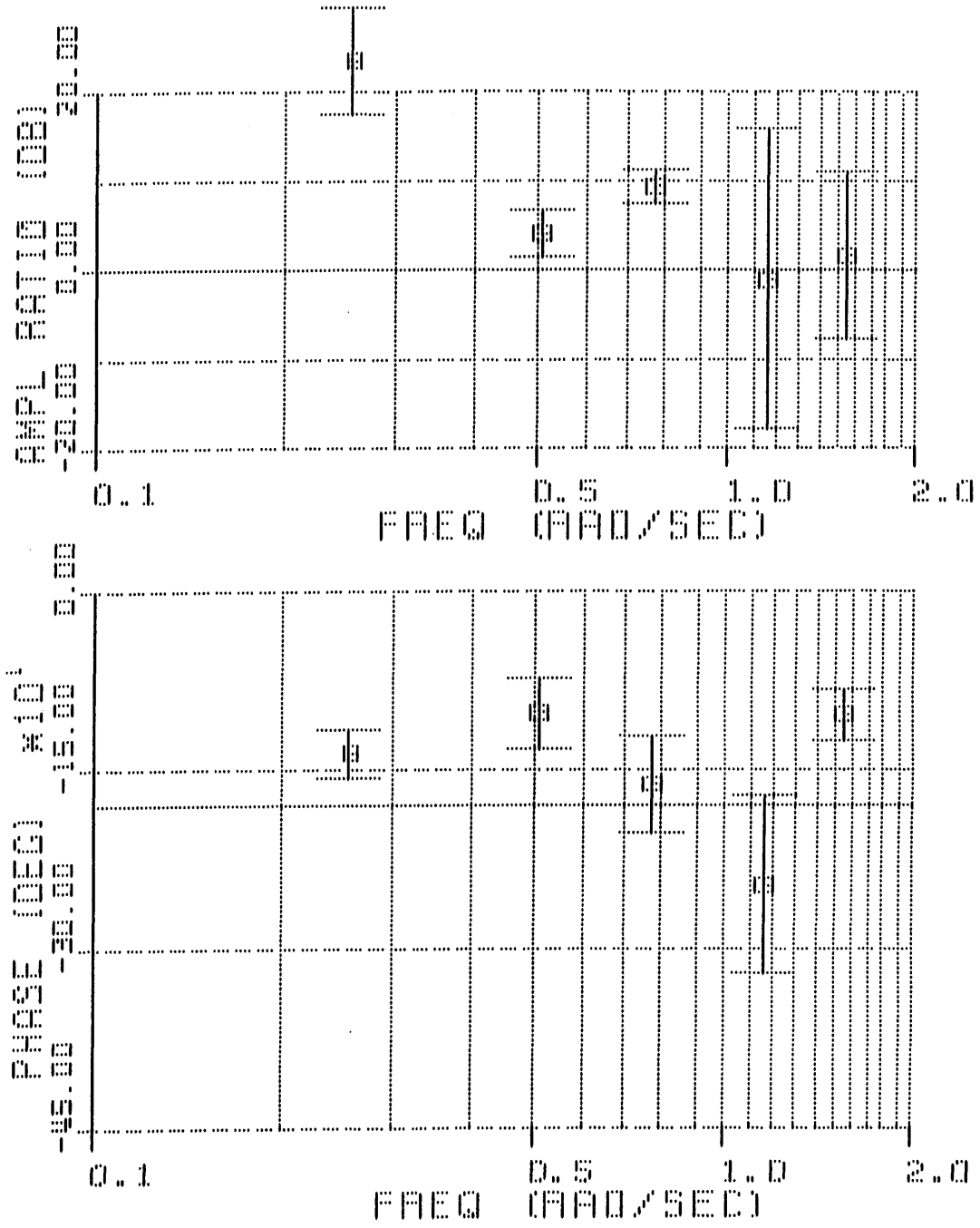

Figure 4-46. Bode Plot of Typical Pilot-Aircraft Describing Function

WASHOUT	MOTION RATING CATEGORIES						
	SMOOTHNESS	SENSE	AMPLITUDE	PHASE LAG	DISCOMFORT	DISORIENTATION	OVERALL
PILOT #1							
Ames Nominal	1.5	1.0	3.0	1.0	1.0	1.0	1.75
Ames Decreased Gain	1.5	1.75	2.0	1.0	1.0	1.0	2.0
Ames Increased Omega	1.5	1.0	3.0	1.0	1.0	1.0	1.5
OWS Nominal	1.5	1.0	3.0	2.25	1.0	1.0	2.0
OWS Decreased Gain	1.5	3.0	3.0	4.0	2.5	2.5	3.0
OWS High Otolith Weighting	1.5	1.0	3.0	1.5	1.0	1.0	1.5
PILOT #2							
Ames Nominal	3.5	1.3	2.7	1.2	1.0	1.0	1.3
Ames Decreased Gain	1.25	1.0	3.0	1.0	1.0	1.0	1.2
Ames Increased Omega	2.5	1.5	2.5	1.5	1.2	1.0	1.5
OWS Nominal	2.5	1.2	2.7	1.2	1.0	1.0	1.3
OWS Decreased Gain	2.0	1.5	2.5	1.5	1.5	1.5	1.5
OWS High Otolith Weighting	2.5	1.5	2.7	1.7	1.3	1.2	1.5
PILOT #3							
Ames Nominal	2.0	1.0	3.0	2.0	1.0	1.0	2.0
Ames Decreased Gain	2.0	1.0	3.0	4.0	1.0	1.0	2.0
Ames Increased Omega	2.0	1.0	3.0	3.0	1.0	1.0	2.0
OWS Nominal	2.0	1.0	4.0	3.0	2.0	1.0	2.0
OWS Decreased Gain	2.0	1.0	2.0	4.0	1.0	1.0	4.0
OWS High Otolith Weighting	2.0	2.0	4.0	2.0	1.0	2.0	2.0
PILOT #4							
Ames Nominal	2.0	1.0	3.0	*	1.0	1.0	2.0
Ames Decreased Gain	1.5	1.0	3.0	2.0	3.0	1.0	1.5
Ames Increased Omega	1.0	1.0	3.0	3.0	3.5	1.0	1.5
OWS Nominal	2.0	1.0	3.0	2.0	3.0	1.0	4.0
OWS Decreased Gain	3.0	3.0	4.0	4.0	5.0	3.0	5.0
OWS High Otolith Weighting	2.0	1.0	3.0	*	5.0	1.0	5.0

*no rating given

Table 4-2. Motion Rating Categories

Table 4-3

CORRELATION OF EACH MOTION RATING CATEGORY TO "OVERALL MOTION" RATINGS

	PILOT #1	PILOT #2	PILOT #3	PILOT #4
SMOOTHNESS	0.0	0.25	0.0	0.77
SENSE	0.93	0.97	-0.20	0.53
AMPLITUDE	0.0	-0.83	-0.76	0.53
LAG	0.78	0.96	0.55	0.70
DISCOMFORT	0.94	0.85	-0.31	0.70
DISORIENTATION	0.94	0.60	-0.20	0.53

overall motion rating; however discomfort and disorientation are probably the result of poor sense rather than being separate factors of the washout. For Pilot #2, there are significant correlations of sense and lag to the overall rating. For Pilot #3, the most significant correlation is with amplitude, while for Pilot #4, the most significant correlation is with smoothness.

To illustrate any correlation between the handling quality ratings and the overall motion rating, Table 4-4 has been constructed. For Pilots #1 and #2, there is fairly significant correlation between the the HQR's and the overall motion rating (R=0.91 for both pilots). The two other pilots exhibited less correlation (R=0.80 for Pilot #3 and R=0.72 for Pilot #4).

Table 4-4

COMPARISON OF "OVERALL MOTION" RATING TO HANDLING QUALITY RATINGS

WASHOUT	MOTION RATING	HANDLING QUALITY RATING
Pilot #1		
Ames Nominal	1.75	4.5
Ames Decreased Gain	2.0	5.0
Ames Increased Omega	1.5	4.5
OWS Nominal	2.0	4.25
OWS Decreased Gain	3.0	6.0
OWS High Otolith Weighting	1.5	4.0
Pilot #2		
Ames Nominal	1.3	2.4
Ames Decreased Gain	1.2	2.0
Ames Increased Omega	1.5	3.0
OWS Nominal	1.3	2.7
OWS Decreased Gain	1.5	1.5
OWS High Otolith Weighting	1.5	3.0
Pilot #3		
Ames Nominal	2.0	4.0
Ames Decreased Gain	2.0	4.0
Ames Increased Omega	2.0	5.0
OWS Nominal	2.0	4.0
OWS Decreased Gain	4.0	6.0
OWS High Otolith Weighting	2.0	5.0
Pilot #4		
Ames Nominal	2.0	4.5
Ames Decreased Gain	1.5	3.0
Ames Increased Omega	1.5	3.0
OWS Nominal	4.0	5.0
OWS Decreased Gain	5.0	5.5
OWS High Otolith Weighting	5.0	4.0

5. Conclusions and Recommendations

5.0 Motion Evaluation Techniques

1. From the experimental results, it is evident that even with highly trained test pilots, there is great variability in performance among trials and among pilots; consequently, performance, though widely used as an indicator of motion fidelity, is not necessarily a valid or consistent measure. In our experiments, performance was affected by learning (especially in velocity performance), by position bias, and by the difficulty of executing the assigned task. Furthermore, the tracking performance scores generally are not well correlated with the pilot comments or with the handling quality ratings.

2. The use of pilot describing function charateristics to indicate motion fidelity is also not necessarily valid. As with performance, the describing function characteristics are smeared by the performance variability among trials and by possible non-linear (bang-bang) pilot control schemes, both of which are probably a function of the difficulty of the task.

3. Even though the pilots were actually using HQR's to rate the handling qualities of the aircraft, for our experiments, the HQR's appear to be sensitive to the washout designs and are reasonably good indicators of motion fidelity. This is expected since the ratings indicate how much pilot compensation is required to control the aircraft. The amount of compensation is affected by the motion cues provided; therefore the

HQR's are relevant. In the experiments, the ratings are fairly consistent with pilot comments and they display no significant learning trends. Although the HQR's do not exhibit consistent magnitude levels between pilots, the shapes of the HQR versus washout plots are reasonably consistent between pilots.

4. The motion rating scale was reasonably successful in highlighting the strengths and deficiencies of the washouts, although a more precise definition of the various terms in the scale would be advantagous. When the overall motion rating is correlated with each of the motion parameter categories, sense is best correlated for Pilot #1, sense and lag are best correlated for Pilot #2, amplitude is best correlated for Pilot #3, and smoothness is best correlated for Pilot #4; therefore, the pilots either associate different motion qualities to the fidelity of motion or they have different interpretations of the motion scale categories.

5.1 Control System Improvements

1. One of the major goals of this experiment was to illustrate that the minimization of vestibular error is a reasonable technique for the design of washout systems. In general, the pilot comments and ratings justify the technique; however, relative to the experiments described here, better HQR's and pilot comments can probably be obtained for the OWS washouts by correcting the low gain inadvertantly used in the otolith model. The pilots appear to prefer the more coordinated washouts; therefore, more weight should be placed on the otolith error when designing future washouts, as was done with the OWS High Otolith

washout. Although HQR's with the OWS High Otolith Weighting washout (2:1 otolith to semicircular canal weighting) were not significantly better than those for the OWS Nominal washout (1:1 otolith to semicircular canal weighting), the HQR's for all OWS washouts may have been mainly affected by the lack of pitch angle coordination during the dash-quick stop maneuvers. This effect can be removed by filtering out the DC components of the aircraft pitch rate and thereby improving the coordination of the OWS washouts.

2. A possible improvement in the washout system could be obtained by implementing the sign-sensitive cost as proposed by Ish-Shalom [Ish-Shalom 82]. This sign-sensitive cost minimizes the motion cues to the simulator pilot that are in the direction opposite to the motion cues experienced by the aircraft pilot. For example, the motion sensations due to the accelerations commanded to keep the simulator within travel limits are minimized if the aircraft pilot is not sesnsing accelerations in the same direction.

3. In order to fully maximize the motion base capabilites, a combined visual-vestibular model should be developed and implemented into the current control system format. This would allow the washout system to better estimate the pilot's perception of motion since both visual and vestibular influences on perception are considered.

5.2 Possible Improvements in Experimental Procedures

1. To facilitate the development of more definitive conclusions, learning effects during the experiments should be minimized; therefore the pilots should be allowed greater time to learn the task before data

is taken.

2. To help the pilots learn the proper tracking distance to the lead aircraft, the pilots should be positioned at the set point and told that they are at the desired tracking distance. Their position should then be incrementally deviated on either side of the desired set point and the pilots told their distance from the set point. In this way, they can develop a feel for their distance from the lead aircraft before data is taken.

3. A common set of runs should be made in each session to allow the evaluation of session effects on performance. The extreme learning during the first session fixed base runs made comparison of performance to the second session fixed base runs impossible.

4. More realistic flight tasks should be used to evaluate the motion washout characteristics. Though the tasks used in this study were helpful in highlighting the differences between washouts, some of the bothersome washout characteristics observed during the tests may not arise during typical flight operations in the simulator. Therefore, some washouts that were rated poorly during the rather atypical flight maneuvers performed in the tests, may be entirely adequate for normal flight missions.

5.3 An Extended Motion Fidelity Test

1. To determine the relationship of motion fidelity to motion evaluation scales and pilot performance, the pilots could perform a set of tracking runs in the simulator with no motion, a set of runs in the simulator

with varying degrees of motion, and a set of runs in an actual helicopter using the same visuals as in the simulator. The graphic images could be transmitted from the ground and displayed on CRT's in the cab. Current helicopters designed to evaluate single pilot cockpits could be utilized for the experiment since they have one completely enclosed cockpit with visuals supplied only through video terminals. A backup pilot is also onboard to take over the controls should any emergency arise. This type of testing would permit performance in the simulator to be compared to performance in the aircraft; furthermore, transfer of training could be evaluated.

References

Correia, M.J., and Guedry, Jr., F.E., "The Vestibular System: Basic Biophysical and Physiological Mechanisms", Chapter 8 in Handbook of Behavioral Nuerobiology, 1, Sensory Integration, Masterson, R.B., Plenum, N.Y., 1978.

Fuller, R.,G., An Evaluation of the Fidelity of Motion Simulators Using a Model of Human Dynamic Orientation, Master's Thesis, Naval Postgraduate School, Monterey, CA, 1977.

Hosman, R.J.A.W., and van der Vaart, J.C., Vestibular models and thresholds of motion perception. Results of tests in a flight simulator. Delft University, Dept. of Aerospace Engineering Report LR-265, 1978.

Ish-Shalom, J. Design of Optimal Motion for Flight Simulators, Ph.D. Thesis, Massachusetts Institute of Technology, Cambridge, MA 1982.

Iurato, S., Submicroscopic structure of the inner ear. Oxford: Pergamon Press, Ltd., 1967.

Jewell, W.F., and Jex, H.R., A second order washout filter with a time-varying break frequency. Systems Technology Inc. WP-1094-9, 1978.

McRuer, D.T., Krendel, E.S., Mathematical Models of Human Pilot Behaviour, Agardograph No. 188, 1974.

Ormsby, C.C., Model of Human Dynamic Orientation, Ph.D. Thesis, Massachusetts Institute of Technology, Cambridge, MA, 1974.

Parrish, R.V., and Martin, D.J., Jr., Comparison of a Linear and a Non-linear Washout for Motion Simulation Utilizing Objective and Subjective Data from CTOL Transport Landing Approaches, NASA TN D-8157, 1976.

Parrish, R.V, Dieudonne, J.E., Bowles, R.L., and Martin, D.J., Coordinated adaptive washout for mtion simulators, AIAA Paper No. 73-930, 1973.

Reidel, S.A., and Hoffman, L.G., Preliminary investigation of a new nonlinear washout scheme, Systems Technology Inc., Wp-1110-1, 1977.

Reidel, S.A., and Hoffman, L.G., Investigation of nonlinear motion simulator washout schemes. 14th Annual Conference on Manual Control, USC, 1978.

Sinacori, J.B., A brief survey of motion simulators' drive logic with emphasis on the roll axis, Systems Technology Inc. WP-1094-2, 1977.

Sinacori, J.B., Stapleford, R.L., Jewell, W.F., and Lehman, J.M.,

Researchers Guide to the NASA Ames Flight Simulator for Advanced Aircraft, Systems Technology Inc. STI-TR-1074-1, 1977.

Sivan, R., Ish-Shalom, J. and Huang, J.K., An optimal control approach to the design of moving flight simulators. IEEE Trans. on Systems, Man, and Cybernetics, SMC-12:818-827, 1982.

Sull, Ivan R.B., Die Anwendung Vestibularer Modelle in Filteranlagen fur Flugsimulatorbewegungen: Versuchsauswertung. Ph.D. Thesis, Mach Institute, Bremen, 1960.

Wersall, J., Studies on the structure and innervation of the sensory epithelium of the cristae ampullares in the guinea pig. Acta Otolaryng. Suppl. 126, 1956.

Young, L.R., Role of the vestibular system in posture and movement. In: Medical Physiology Vol. I (V.B. Mountcastle, ed), St. Louis:Mosby Co., pp. 704-721, 1974.

Young, L.R., Oman, C.M., Curry, R.E., and Dichgans, J.M., A descriptive model of multi-sensor human spatial orientation with applications to visually induced sensations of motion, AIAA Paper No. 73-915, 1973.

APPENDIX A

WASHOUT SOFTWARE

```
C THIS ROUTINE CALCULATES THE WASHOUT COMMANDS
      SUBROUTINE WASH
C
      DIMENSION STATES(10)
      DIMENSION CONTRL(2),AAC(3,3),BAC(3,2),ACST(3)
      DIMENSION SIMCTL(2),ASIM(5,5),BSIM(5,2),SIMST(5)
      DIMENSION FDBK(2,10)
C
C-----------------------------------------------------------------------
C THESE ARE ALL PARAMETERS FROM THE AMES WASHOUT ROUTINES. THE ONLY
C  AMES PARAMETERS ACTUALLY REQUIRED IN THIS ROUTINE ARE: IMODE, AXIN,
C  AYIN,ZSDD,THES,PHIS,XDDO,YDDO,PDA,QDA,THETR,PHIR,RDA,DT
      COMMON/IFLAGS/IMODE,I90
      COMMON/STATE/AXIN,AYIN,AZIN,PDA,QDA,RDA,THETR,PHIR
      COMMON/OUTPUT/DUM1,DUM2,DUM3,YS,YSD,YSDD,ZS,ZSD,ZSDD,PSIS,PSISD,
      1       PSISDD,THES,THESD,THESDD,PHIS,PHISD,PHISDD
      COMMON/MISC/ODT,DT,GS,HCG,ZBIA,XDDO,YDDO,PIN,QIN
C-----------------------------------------------------------------------
C
C
C SIMACC TRANSFERS TO THIS ROUTINE, THE CAB SURGE ACCEL FROM THE PREVIOUS
C   ITERATION AS CALCULATED IN THE LIMITING LOGIC OF TRANFL. XSDD IS USED
C   TO UPDATE THE SIMULATOR STATES FOR THIS ITERATION.
      COMMON/SIMACC/SIMACC
C
C
C THESE STATEMENTS COMMUNICATE WITH OUR SUBROUTINE LOAD WHICH CONTAINS
C   THE DYNAMICS AND FEEDBACK MATRICES.
      COMMON/ACVEST/AAC,BAC
      COMMON/SIM/ASIM,BSIM
      COMMON/FDBK/FDBK
C
C
C ON THE FIRST PASS, LOAD THE DYNAMICS AND FEEDBACK MATRICES
      IF(IMODE.LE.0) CALL LOAD
C
C
C*************************************************************************
C TRANSFORM THE AIRCRAFT BODY AXIS LINEAR ACCELERATION AND ANGULAR
C   VELOCITY TO INERTIAL AXES.
C.....................I90=0.....................................
      IF (I90.EQ.1) GO TO 10
C
C NEXT LINE WAS CHANGED 7-11-84 TO NEGATE THE G-TILT EFFECTS IN THE ACCEL DATA
C
      CONTRL(1)= AYIN+GS*COS(THETR)*SIN(PHIR)-ZSDD*PHIS+YDDO
      CONTRL(2)= PDA+THETR*RDA
      GO TO 20
C
C.....................I90=1.....................................
C
C NEXT LINE WAS CHANGED 7-11-84 TO NEGATE THE G-TILT EFFECTS IN THE ACCEL DATA
10    CONTRL(1)= AXIN-GS*SIN(THETR)+ZSDD*THES+XDDO
      CONTRL(2)= QDA-PHIR*RDA
C
C
C*************************************************************************
C
C
```

```
C THIS SUBROUTINE CALCULATES THE NEW STATES OF
C   THE DYNAMICAL SYSTEM
C
      SUBROUTINE STVAR(CONTRL,DYNMAT,BMAT,N,M,STATES,DT)
C
      DIMENSION CONTRL(M), DYNMAT(N,N), BMAT(N,M), STATES(N)
      DIMENSION TEMP1(10), TEMP2(10)
C
C-----------------------------------------------------------------------
C                                                              DIMENSION |
C      CONTRL  = CONTROL INPUT VECTOR                          (M X 1)   |
C      DYNMAT  = SYSTEM DYNAMIC EQUATION MATRIX                (N X N)   |
C      BMAT    = CONTROL SENSITIVITY MATRIX                    (N X M)   |
C      OUTMAT  = OUTPUT SCALING MATRIX                         (NPX N)   |
C      DMAT    = FEED-FORWARD SCALING MATRIX                   (NPX M)   |
C      N       = DIMENSION OF THE STATE VECTOR                           |
C      M       = DIMENSION OF THE CONTROL VECTOR                         |
C      NP      = DIMENSION OF THE OUTPUT VECTOR                          |
C      STATES  = STATE VECTOR OF THE SYSTEM                    (N X 1)   |
C      DT      = TIME STEP SIZE                                          |
C      YOUT    = OUTPUT VECTOR                                 (NPX 1)   |
C      TEMP1   = TEMPORARY STORAGE VECTOR                      ( 10  )   |
C      TEMP2   = TEMPORARY STORAGE VECTOR                      ( 10  )   |
C                                                                        |
C   THIS ROUTINE CALCULATES:                                             |
C      STATES=STATES+(DYNMAT*STATES+BMAT*CONTRL)*DT                      |
C                                                                        |
C-----------------------------------------------------------------------
C
C CALCULATE THE PRODUCT OF DYNMAT AND STATES
      CALL PRDUCT(DYNMAT,N,N,STATES,TEMP1)
C CALCULATE THE PRODUCT OF BMAT AND CONTRL
      CALL PRDUCT(BMAT,N,M,CONTRL,TEMP2)
C CALCULATE THE DERIVATIVES OF THE STATES, INTEGRATE THEM, AND ADD TO
C    THE PRESENT STATES
      DO 10 INDEX=1,N
10    STATES(INDEX)=STATES(INDEX)+(TEMP1(INDEX)+TEMP2(INDEX))*DT
C
C
      RETURN
      END



C THIS SUBROUTINE CALCULATES THE PRODUCT OF AN ARRAY AND A VECTOR
      SUBROUTINE PRDUCT(ARRAY1,NROW1,NCOL1,VECTOR,RESULT)
C
      DIMENSION ARRAY1(NROW1,NCOL1), VECTOR(NCOL1), RESULT(NROW1)
C
C-----------------------------------------------------------------------
C    ARRAY1= THE ARRAY TO BE MULTIPLIED                                  |
C    VECTOR= THE VECTOR MULTIPLYING THE MATRIX                           |
C    RESULT= THE VECTOR RESULTING FROM THE MULTIPLICATION                |
C    NROW1 = THE # ROWS IN THE ARRAY                                     |
C    NCOL1 = THE # OF COLS IN THE ARRAY AND THE # OF ENTRIES IN THE VECTOR |
C                                                                        |
C    THIS SUBROUTINE CALCULATES:                                         |
C          RESULT=ARRAY1*VECTOR                                          |
C-----------------------------------------------------------------------
C
      DO 20 IROW=1,NROW1
C COMPUTE THE INNER PRODUCT OF THE VECTOR AND EACH ROW OF THE ARRAY
      SUM=0.
      DO 10 IENTRY=1,NCOL1
10    SUM=SUM+ARRAY1(IROW,IENTRY)*VECTOR(IENTRY)
20    RESULT(IROW)=SUM
      RETURN
      END
```

```
C UPDATE THE AIRCRAFT PILOT'S VESTIBULAR SYSTEM WITH THE NEW AIRCRAFT
C   LINEAR ACCEL AND ANGULAR VELOCITY
20      CALL STVAR(CONTRL,AAC,BAC,3,2,ACST,DT)
C
C
C REVISE SIMCTL(1) TO THE VALUE ACTUALLY COMMANDED TO THE SIMULATOR
C   AFTER THE LIMITING LOGIC. (I90 ADDED JULY 30,1984)
        SIMCTL(1)=SIMACC
C
C UPDATE THE SIMULATOR PILOT'S VESTIBULAR SYSTEM AND THE SIMULATOR
C   MOTION BASE STATES

        CALL STVAR(SIMCTL,ASIM,BSIM,5,2,SIMST,DT)
C
C LOAD THE 'STATES' VECTOR WITH THE 3 NEW AIRCRAFT VESTIBULAR STATES,
C   THE 3 NEW SIMULATOR VESTIBULAR STATES, THE 2 NEW SIMULATOR MOTION
C   BASE STATES, AND THE 2 NEW STOCHASTIC PROCESS STATES.
        STATES(1)=  ACST(1)
        STATES(2)=  ACST(2)
        STATES(3)=  ACST(3)
        STATES(4)=  SIMST(1)
        STATES(5)=  SIMST(2)
        STATES(6)=  SIMST(3)
        STATES(7)=  SIMST(4)
        STATES(8)=  SIMST(5)
        STATES(9)=  CONTRL(1)
        STATES(10)= CONTRL(2)
C
C MULTIPLY THE FEEDBACK MATRIX BY THE NEWLY DEFINED 'STATES' VECTOR
        CALL PRDUCT(FDBK,2,10,STATES,SIMCTL)
C
C CORRECT THE SIGNS OF THE SIMULATOR CONTROLS
        SIMCTL(1)=-1.*SIMCTL(1)
        SIMCTL(2)=-1.*SIMCTL(2)
C
C*************************************************************************
C DETRANSFORM THE COMMANDED INERTIAL AXIS SIMULATOR CONTROLS TO BODY AXES
C   SUCH THAT THEY ARE CORRECTLY TRANSFORMED BACK INTO BODY AXES IN THE
C   AMES WASHOUT. NOTE THAT THE SIMULATOR PITCH TRANSFORMATION ANGLE IS
C   UPDATED HERE SINCE THE PITCH ANGLE IS UPDATED IN ROTFIL BEFORE THE
C   AXIS TRANSFORMATION IS MADE IN TRANFL.
C.......................I90=0.....................................
        IF (I90.EQ.1) GO TO 30
        AYIN=SIMCTL(1)+ZSDD*(PHIS+SIMCTL(2)*DT)-YDDO
        PDA=SIMCTL(2)-THETR*RDA
        GO TO 40

C.......................I90=1.....................................
30      AXIN=SIMCTL(1)-ZSDD*(THES+SIMCTL(2)*DT)-XDDO
        QDA=SIMCTL(2)+PHIR*RDA
C*************************************************************************

40      RETURN
        END
```

APPENDIX B

PILOT BRIEFING MATERIAL

EXPERIMENTAL PROCEDURE FOR VMS MOTION WASHOUT EXPERIMENTS

This document describes the specific tasks and experimental measurements to be used in the evaluation of the optimal washout system on the Vertical Motion Simulator (VMS).

MOTION WASHOUT SYSTEM CONDITIONS

The two basic washout systems to be used on the VMS are the second order Ames washout and the Optimal washout. Each of the washouts will be presented in three conditions, yielding six washouts to be evaluated. The Ames washout will be presented as nominal, reduced gain, and increased break frequency. The Optimal Washout System (OWS) will be presented as nominal, reduced simulator travel, and high otolith weight.

1. Ames Nominal. This will be the washout system best suited to the particular aircraft dynamics used. The gains and break frequencies will be chosen by Ames personnel aquainted with the second order washout system.

2. Ames Reduced Gain. This will be the Ames Nominal condition with the gain in the pitch-surge axis reduced such that the simulator will travel less for a given acceleration of the aircraft model.

3. Ames Increased Break Frequency. This will be the Ames Nominal condition with the break frequency in the pitch-surge axis increased. This will tend to reduce the transmission of low frequency aircraft model motion to the simulator.

4. OWS Nominal. This will be the washout generated by the optimal control technique with the best estimates of the desired weights on the cost function components. Essentially, it will be the best a priori guess of the desired washout.

5. OWS Reduced Simulator Travel. In this condition, the cost of simulator travel will be increased such that the motion produced by the resulting washout will be of lesser amplitude. This is analogous to the Ames Reduced Gain condition.

6. OWS High Otolith Weight. This condition will be produced by increasing the weight of the otolith errors with respect to those of the semicircular canals. This will increase the amount of "coordination" used to keep the net force vector oriented in the direction consistent with the actual aircraft.

FLIGHT TASKS

The three basic flight tasks are presented below.

Tracking With Target Disturbance. This task will involve flying formation to the rear of the target aircraft. The target aircraft will be disturbed longitudinally with a sum-of-sines disturbance.

Forward Step Maneuver. This task will begin with the aircraft at the beginning of the canyon in a stationary hover at approximately 20 ft altitude. The pilot will be instructed to establish a 5-degree nose-down pitch attitude while maintaining altitude. This 5-degree pitch down will be held as the aircraft accelerates to a steady flight speed. As the aircraft approaches the road through the canyon, the nose will be brought to a pitch up attitude and the aircraft brought to a stationary hover over the road.

Pitching Maneuver. With the aircraft in a stationary hover, the pitch attitude will be oscillated through positive and negative 5-10 degrees with a period of 4, 2, and 1 second.

EXPERIMENTAL MEASUREMENTS

During each trial, the following measurements will be taken:

Pilot Describing Function. The gain and phase of the open-loop pilot/vehicle combination will be calculated using an on-line computer routine and recorded for each trial (this measure will be taken for the longitudinal tracking task only).

Task Performance. The target and vehicle positions will be recorded during each trial. From these, the error in tracking can be computed.

Subjective Ratings of Aircraft Handling Qualities. The Cooper-Harper rating scale will be used by the pilots to estimate the handling qualities of the test aircraft in each trial.

Subjective Ratings of Simulator Motion. A rating scale for simulator motion will be employed to assess the effectiveness and acceptability of the washout system for each trial. Ratings of the motion will be taken during the forward step and pitching maneuver tasks. Pilots will be informed if the simulator encounters limits during this evaluation. They will be told to "disregard the previous maneuver" if that maneuver resulted in a limit encounter.

MOTION RATING SCALES

The motion of the simulator will be rated on the following seven scales:

Attribute	Rating 1	5
SMOOTHNESS:	extremely smooth-comparable with fixed base	extremely jerky limit of tolerance
SENSE:	definitely correct as in aircraft	totally reversed
AMPLITUDE:	no motion experienced	at least twice that expected
PHASE LAG:	none experienced	at least 180°
DISCOMFORT:	none experienced	cannot continue maneuver
DISORIENTATION:	none experienced	cannot perform maneuver
OVERALL:	excellent	extremely poor

Pilots will be asked to rate the motion during the Forward Step and Pitching Maneuvers. If they desire, they may fly the vehicle in the canyon to elucidate any particular attribute of the motion. Their comments will be recorded.

Note: To avoid encounters with the software limits during motion evaluation, pilots will be requested to keep pitch angle excursions within positive or negative 10 degrees.

ORDER OF PRESENTATION

The order of presentation given below is based on 4 subjects. If less than 4 are employed, the order will be truncated at the appropriate subject number. Each experimental session will involve the evaluation of three washout conditions. The washout conditions are numbered as on page one of this document. Each session will begin with the fixed base case as a warm-up. The pilot subject will be asked to perform each task 4 times and then proceed to the next task.

Subject 1

Session 1	Session 2
Fixed Base	Fixed Base
Washout 1	Washout 2
Washout 4	Washout 5
Washout 6	Washout 3

Subject 2

Session 1	Session 2
Fixed Base	Fixed Base
Washout 6	Washout 3
Washout 4	Washout 5
Washout 1	Washout 2

Subject 3

Session 1	Session 2
Fixed Base	Fixed Base
Washout 2	Washout 1
Washout 5	Washout 4
Washout 3	Washout 6

Subject 4

Session 1	Session 2
Fixed Base	Fixed Base
Washout 3	Washout 6
Washout 5	Washout 4
Washout 2	Washout 1

APPENDIX C

RAW DATA

RAW VELOCITY VARIANCES

	PILOT #1	PILOT #2	PILOT #3	PILOT #4
FIXED BASE #1	11.94000	15.83000	44.24000	44.24000
	23.14000	13.65000	18.54000	64.89000
	9.380000	24.50000	26.78000	30.22000
	12.53000	15.45000	25.56000	
FIXED BASE #2	11.10000	32.44000	15.80000	17.68000
	24.18000	25.02000	18.96000	10.97000
	13.38000	21.80000	41.32000	12.33000
	6.460000	12.02000	35.29000	14.80000
AMES NOMINAL	10.60000	14.00000	7.260000	13.50000
	5.890000	8.280000	5.980000	18.47000
	2.760000	6.530000	10.65000	25.03000
	9.060000	4.260000	15.15000	13.56000
AMES DECR GAIN	12.21000	10.31000	15.42000	14.08000
	17.32000	9.560000	7.800000	9.490000
	6.820000	4.470000	11.95000	9.180000
	6.810000	6.710000	7.200000	14.30000
AMES INCR OMEGA	7.700000	11.05000	9.160000	8.090000
	4.850000	14.56000	9.530000	9.280000
	5.800000	12.81000	4.390000	12.28000
	8.300000	9.390000	10.62000	6.820000
OWS NOMINAL	6.210000	0.0000000	16.14000	21.83000
	5.550000	6.510000	21.22000	19.28000
	7.510000	6.180000	9.330000	19.39000
	6.060000	7.810000	8.160000	11.80000
OWS DECR GAIN	7.530000	16.39000	11.64000	15.58000
	5.630000	9.750000	7.640000	11.36000
	11.08000	0.0000000	16.38000	11.95000
	10.76000	12.71000	28.61000	13.34000
OWS HIGH OTOLITH WT	6.450000	11.68000	13.89000	24.85000
	2.610000	8.190000	18.34000	17.53000
	4.480000	8.090000	15.52000	14.45000
	5.430000	8.290000	19.44000	11.42000

RAW BIASES

	PILOT #1	PILOT #2	PILOT #3	PILOT #4
FIXED BASE #1	49.41000	35.00999	61.60001	43.74001
	18.32000	34.30000	-7.050003	43.00000
	-6.830002	33.48000	-9.302002	11.24000
	11.17000	37.28000	-11.12300	
FIXED BASE #2	-20.51500	29.44000	-0.3799973	13.49000
	-6.989998	33.58000	-6.629997	14.41000
	-11.49800	25.64000	-12.20100	18.35000
	-22.22700	21.00999	-2.669998	-0.3799973
AMES NOMINAL	-23.42100	13.21000	-7.580002	18.16000
	-24.79800	20.61000	-9.570999	28.32001
	-22.57700	0.5699997	-7.599998	26.80000
	-27.72600	2.010002	-10.12000	19.47000
AMES DECR GAIN	-7.500000	40.61000	-1.239998	4.449997
	-9.077003	47.84000	-8.084000	-11.19000
	-8.0001831E-02	25.16000	-9.9998474E-02	1.989998
	-14.39900	24.36000	-3.110001	8.879997
AMES INCR OMEGA	-7.540001	46.41000	-9.249001	10.55000
	-20.70600	37.03999	-7.339996	2.489998
	-17.14400	24.08000	-15.67000	5.300003
	-17.35700	32.02000	-7.360001	10.73000
OWS NOMINAL	-14.28600	21.84000	12.65000	24.08000
	-14.11900	13.66000	-2.000000	31.25999
	-26.40700	0.5199966	-17.02900	32.16000
	-11.65100	9.529999	-10.24200	17.70000
OWS DECR GAIN	-2.230003	60.89000	4.959999	24.55000
	-12.26000	33.89000	2.139999	12.10000
	-20.40600	25.12000	8.010002	-3.570000
	-9.069000	31.37000	5.519997	14.33000
OWS HIGH OTOLITH WT	-9.360001	13.50000	-3.699997	30.99001
	-15.64700	14.40000	-2.199997	37.92999
	-17.21400	23.72000	-6.070000	34.16000
	-19.16600	16.67000	4.669998	23.39999

RAW DISPLACEMENT VARIANCES

	PILOT #1	PILOT #2	PILOT #3	PILOT #4
FIXED BASE #1	610.5840	268.9600	1906.196	915.6676
	399.2004	320.0521	499.5225	1301.045
	114.2761	417.3849	238.0849	278.5561
	199.9396	341.1409	250.5889	
FIXED BASE #2	151.7824	512.5696	144.0000	218.4484
	238.6000	470.8900	81.88440	127.4641
	125.6641	329.4225	290.7025	178.2225
	112.1481	165.1225	305.5504	194.3236
AMES NOMINAL	124.5456	152.2756	87.83438	142.8025
	140.1856	141.6100	50.05562	315.4176
	184.6881	77.47520	71.19984	445.2100
	178.4896	40.05624	101.6064	331.6041
AMES DECR GAIN	86.47140	375.1969	148.5961	359.1025
	192.6544	584.6700	75.16890	195.4404
	108.3681	121.2201	116.2084	95.68752
	54.98222	129.7321	65.99937	602.2117
AMES INCR OMEGA	164.6089	400.4001	75.62041	135.0244
	84.05223	379.4704	58.01869	256.6404
	68.85681	199.0921	78.78339	202.7776
	100.6009	228.0100	68.26064	85.28522
OWS NOMINAL	55.90553	133.1200	126.8600	250.2724
	97.59464	71.35180	116.8561	315.4176
	178.2225	50.28228	88.20967	371.3329
	66.63457	104.2441	60.79321	152.0289
OWS DECR GAIN	52.98384		93.02603	364.0464
	109.2025	273.5716	46.32164	239.3209
	130.8736	214.7200	177.6889	147.1369
	55.98032	385.7296	176.0929	214.3296
OWS HIGH OTOLITH WT	57.59293	82.97388	52.37417	438.0649
	92.35210	92.94888	192.0996	416.9764
	54.09602	139.9489	114.7041	347.4496
	77.77477	108.7849	74.92000	176.6241

APPENDIX D

PILOT COMMENTS

Comments of Pilot #1

* Fixed Base:
  -

* Ames Nominal:
(#4) -Fourth washout tried
  -No objectionable motion
  -Looked coordinated
  -One of the better ones - similar to Ames Incr Omega

* Ames Decreased Gain:
(#1) -First washout tried
  -Didn't feel enough motion, did feel coordinated

* Ames Increased Omega:
(#3) -Third washout tried
  -Best washout yet (prior washouts:Ames Decr Gain & MIT Decr Gain)
  -No more surge phasing as compared to MIT Decr Gain
  -Amplitude looked like real world
  -Could be a little more motion

* MIT Nominal:
(#5) -Fifth washout tried
  -Aware of more surge accel
  -Able to use motion to help in tracking (pilot could increase tracking aggressiveness)
  -Not enough surge on large pitchdown steps (surge lag) (not as bad as in MIT Decreased Gain) (lag is acceptable)
  -Good configuration

* MIT Decreased Gain:
(#2) -Second washout tried
  -Slides forward in seat upon pitchdown - longit accel not sufficient to properly coordinate

* MIT High Otolith Weighting:
(#6) -Sixth washout tried
  -Best washout yet

General Comments:
  -Pilot didn't like helicopter collective
  -Vehicle well damped in pitch
  -Tracking task is not that easy

Comments of Pilot #2

* Fixed Base:
  - -A bit disorienting in pitch maneuver
  - -Used the collective quite a bit more the second session during fixed base

* Ames Nominal:
(#6)
  - -Sixth washout tried
  - -Able to stay closer to the F-111 than with previous washout (MIT Nominal Washout)
  - -Better than previous washouts (MIT High Oto and MIT Nominal)
  - -Felt a lot more motion during hover (in a good sense)
  - -Roughness felt in the cab during last run (hardware problem)

* Ames Decreased Gain:
(#3)
  - -Third washout tried
  - -Pilot liked washout (helped him fly closer to F-111)
  - -Too much seat-of-the-pants decel (during steps)
  - -Not too much feeling of accel (during steps)

* Ames Increased Omega:
(#1)
  - -First washout tried
  - -Becoming more aggresive on controls

* MIT Nominal:
(#5)
  - -Fifth washout tried
  - -Better able to predict stopping point during the step accel runs than he was with the MIT High Oto Wt
  - -Seat-of-the-pants good. Motion matched the visuals
  - -Felt less discomfort than with the MIT High Oto Wt washout

* MIT Decreased Gain:
(#2)
  - -More seat-of-the pants accel than expected when pitch up (slightly disorienting)
  - -Slow to catch up with pitch input (probably lagging surge accel) during step maneuvers
  - -More responsive in pitching task than last washout (Ames Incr Omega)

* MIT High Otolith Weighting:
(#4)
  - -Fourth washout tried
  - -During pitchup (during step maneuver), experienced too much decel
  - -Seat-of-the-pants feel is good
  - -Pitch response is not that good at lower frequencies, but is better at higher frequencies

---

General Comments:
  - -Had to increase altitude to keep F-111 in sight
  - -Tracking task is relatively easy
  - -Tended to overcompensate on backup maneuvers during tracking
  - -Due to blending of the F-111's elevator into the fuselage, it was easier to see when the F-111 was pitching forward than when it was pitching back

Comments of Pilot #3

* Fixed Base:
  - -None

* Ames Nominal:
(#3)
  - -Third washout tried
  - -Pilot felt no difference betweem this washout and the MIT Nom WO

* Ames Decreased Gain:
(#6)
  - -Sixth washout tried
  - -Much easier than the previous washout (MIT Decr Gain)
  - -Motion of chase aircraft more closely linked in translation to that of the F-111 - same time delay between pitch attitude and translation - made tracking easier

* Ames Increased Omega:
(#4)
  - -Fourth Washout tried
  - -Tracking improved with motion as compared to the fixed base runs
  - -Motion would be too sluggish for a more aggressive maneuver

* MIT Nominal:
(#2)
  - -Second washout tried
  - -Last tracking task, sufficient pilot learning to give the vehicle a handling qualities rating of 4 (best run of the four)
  - -Slight degradation in the time to generate longitudinal motion as compared to the high otolith weighting
  - -Noticable lag between pitch rate and onset of longitudinal accel

* MIT Decreased Gain:
(#5)
  - -Fifth washout tried
  - -Pitch response is similar to the last washout (Ames Incr Omega), but it takes longer to develop a translational rate - this makes it more difficult to do the tracking task
  - -slightly smoother than the previous washout - didn't notice bumps as much
  - -More noticable phase lag with increasing pitch freq as compared to the Ames Incr Omega washout

* MIT High Otolith Weighting:
(#1)
  - -First washout tried
  - -Takes too long to develop the longitudinal accel cues
  - -Motion "chugging" keeps this washout from being excellent

---

General Comments:
  - -Had to lean forward in cockpit during large nose down attitudes in order to keep F-111 in sight
  - -CGI not continuous (adds scenery as you go down the canyon) - causes a feeling of "chugging" some of which is in the motion though
  - -Short period of time between F-111 pitching motions makes it much more difficult to evaluate the response of the chase aircraft
  - -White flashes in the CGI starting with washout #4 (second session)
  - -Pilot thought he was doing poorer tracking job second session, possibly since he just got through flying an OH-58
  - -Attitude of F-111 drives tracking task, not really its position
  - -Difficult to judge the amplitudes of motion since didn't have a real aircraft to compare to

Comments of Pilot #4

* Fixed Base:
  - -Amazing sensations of motion due to visuals
  - -Found that when both he and the F-111 were nose high, and then the F-111 pitched down, he felt as if he was pitching up

* Ames Nominal:
(#1)
  - -First Washout tried
  - -Pitch response good
  - -Didn't see too much that was interesting
  - -Pitch maneuver good
  - -Nothing erratic
  - -Lag is perceptible (less than 90)

* Ames Decreased Gain:
(#4)
  - -Fourth Washout tried
  - -Best washout yet
  - -Easier to track F-111
  - -Pitch Maneuvers good (but blurred visuals)

* Ames Increased Omega:
(#6)
  - -Sixth Washout tried
  - -Best maneuvering config, on same par as Ames Decr Gain washout
  - -Good hover handling qualities
  - -Pitch maneuver doesn't feel too good - motion matches controls, but possibly some overshoot

* MIT Nominal:
(#2)
  - -Second Washout tried
  - -Tracking task harder to fly than in Ames Nominal
  - -More of a bang-bang control (result of uncomfortable lags)
  - -Harder to hold attitude and hover
  - -Get desired input sooner but causes overshoot
  - -After dash, pull nose up, and push back down to hover, produces "tide of motion" in surge forward

* MIT Decreased Gain:
(#5)
  - -Fifth Washout tried
  - -Feels phase lag, overshoot, follow-on time constant with motion
  - -Easy to get out of phase with motion
  - -"Not one of your star configurations"
  - -Borders on disorienting
  - -Severe lags in onset cues (in large pitch motions, motion initially lags and then rushes in and overwhelms you [in large nose up or nose down attitudes)
  - -Still not as sickening as MIT High Otolith Wt Washout
  - -Difficulty in holding hover (X-Y pos)
  - -Aircraft pitch response more than expected
  - -Pitching control out of phase and causes overshoots
  - -Pitch maneuvers - motion out of phase
  - -Motion overtravels visuals
  - -Worst configuration yet

* MIT High Otolith Weighting:
(#3)
  - -Third Washout tried
  - -Thought performance improved in this washout from that in Ames Nom and MIT Nom
  - -Motion overshoots in pitch more prevalent after large maneuvers than in Ames Nom and MIT Nom
  - -Small pitch oscillations made him sick

General Comments:
  - -Tracking task requires little collective
  - -Found it easy to end up far away from the F-111 (initial fixed base)
  - -Sinusoid pitch oscillations: inputs more step response to make the aircraft respond with a sinusoidal pitch maneuver
  - -Chase aircraft performance not sufficient to really tightly track the lead aircraft
  - -Hard to nail down many items in our rating scale